VERIFICATION OF POTENTIAL PROTEIN BIOMARKERS FOR DETECTION OF ENDOMETRIAL CANCER BY TARGETED MASS SPECTROMETRY-BASED APPROACH

A THESIS SUBMITTED TO
THE GRADUATE SCHOOL OF NATURAL AND APPLIED SCIENCES
OF
MIDDLE EAST TECHNICAL UNIVERSITY

BY

ÖYKÜ SU YILDIRIM

IN PARTIAL FULFILLMENT OF THE REQUIREMENTS
FOR
THE DEGREE OF MASTER OF SCIENCE
IN
BIOCHEMISTRY

AUGUST 2025

Approval of the thesis:

VERIFICATION OF POTENTIAL PROTEIN BIOMARKERS FOR DETECTION OF ENDOMETRIAL CANCER BY TARGETED MASS SPECTROMETRY-BASED APPROACH

submitted by **ÖYKÜ SU YILDIRIM** in partial fulfillment of the requirements for the degree of **Master of Science** i**n Biochemistry, Middle East Technical University** by,

Prof. Dr. Naci Emre Altun
Dean, **Graduate School of Natural and Applied Sciences** _____

Prof. Dr. Çağdaş Devrim Son
Head of the Department, **Biochemistry, METU** _____

Assoc. Prof. Dr. Süreyya Özcan Kabasakal
Supervisor, **Biochemistry, METU** _____

Prof. Dr. Abdullah Kararer
Co-Advisor, **Obstetrics & Gynecology, İnönü University** _____

Examining Committee Members:

Prof. Dr. Çağdaş Devrim Son
Biological Sciences, METU _____

Assoc. Prof. Dr. Süreyya Özcan Kabasakal
Chemistry, METU _____

Prof. Dr. Abdullah Kararer
Obstetrics & Gynecology, İnönü University _____

Prof. Dr. Özgül Persil Çetinkol
Chemistry, METU _____

Assoc. Prof. Dr. Basri Gülbakan
Pediatric Basic Sciences, Hacettepe University _____

Date: 19.08.2025

I hereby declare that all information in this document has been obtained and presented in accordance with academic rules and ethical conduct. I also declare that, as required by these rules and conduct, I have fully cited and referenced all material and results that are not original to this work.

Name Last name : Öykü Su Yıldırım

Signature :

ABSTRACT

VERIFICATION OF POTENTIAL PROTEIN BIOMARKERS FOR DETECTION OF ENDOMETRIAL CANCER BY TARGETED MASS SPECTROMETRY-BASED APPROACH

Yıldırım, Öykü Su
Master of Science, Biochemistry
Supervisor: Assoc. Prof. Dr. Süreyya Özcan Kabasakal
Co-Advisor: Prof. Dr. Abdullah Karaer

August 2025, 122 pages

Endometrial cancer (EC) is one of the most common gynecologic malignancies, with 420.242 new cases and 97.704 deaths reported worldwide in 2022. EC comprises two major subtypes, endometrioid (EEC) and non-endometrioid (NEC), which differ in prognosis and therapeutic response. Thus, subtype-specific biomarkers are crucial for precise diagnosis, prognosis, and treatment stratification.

This study aims to verify previously reported potential biomarkers for EC as an essential phase in the biomarker development pipeline and to evaluate their potential diagnostic and prognostic value. For this purpose, multiple-reaction-monitoring (MRM) method specific to nine proteins, namely transgelin (Q01995), peptidyl-prolyl cis-transisomerase (Q00688), cyclophilin A (P62937), macrophage capping protein (P40121), pyruvate kinase M1/M2 (P14618), glutathione S-transferase P (P09211), manganese-superoxide dismutase (P04179), cytosol aminopeptidase (P28838), and complement component C4A (P0C0L4), was developed with stable-isotopic-labeled (SIL) peptides. Method performance was evaluated through linearity, limit-of-detection, instrument stability, and reprodubility of sample preparation by following European Medicines Agency guideline.

Unique peptides of nine proteins were monitored in tissue samples from EEC, NEC, and healthy groups following protein extraction and proteolytic digestion. Seven proteins displayed significant dysregulation. Down-regulation of Q01995 is a recurring event in malignancies, serving as a potential biomarker of cancer progression. Conversely, P14618, P40121, Q00688, P28838 were up-regulated, reflecting hallmarks of cancer. However, down-regulation of P0C0L4 and up-regulation of P09211 are not typically observed across cancers. Importantly, P09211 was the only protein showing subtype-specific elevation in EEC compared to NEC, highlighting its prognostic value. Further studies are needed for the verified proteins to be translated into clinical practice.

Keywords: Biomarker, Endometrial cancer, Mass spectrometry, Multiple reaction monitoring (MRM), Targeted proteomics

ÖZ

ENDOMETRİYUM KANSERİ TESPİTİ İÇİN HEDEFLİ KÜTLE SPEKTROMETRESİ TEMELLİ YAKLAŞIMLA POTANSİYEL PROTEİN BİYOBELİRTEÇLERİNİN DOĞRULANMASI

Yıldırım, Öykü Su
Yüksek Lisans, Biyokimya
Tez Yöneticisi: Doç. Dr. Süreyya Özcan Kabasakal
Ortak Tez Yöneticisi: Prof. Dr. Abdullah Karaer

Ağustos 2025, 122 sayfa

Endometriyum kanseri (EC), 2022 yılında dünya genelinde 420.242 yeni vaka ve 97.704 ölüm ile en yaygın jinekolojik malignitelerden biridir. EC, prognoz ve tedavi yanıtı açısından farklılık gösteren iki ana alt tipe ayrılır: endometrioid (EEC) ve non-endometrioid (NEC). Bu nedenle, alt tip-spesifik biyobelirteçler doğru tanı, prognoz ve tedavi sınıflandırması için kritik öneme sahiptir.

Bu çalışma, EC için daha önce bildirilen potansiyel biyobelirteçleri, biyobelirteç geliştirme sürecinin temel bir aşaması olarak doğrulamayı ve onların tanısal ve prognostik açıdan değerlendirmeyi amaçlamaktadır. Bu amaçla, transgelin (Q01995), peptidil-prolil cis-trans izomeraz (Q00688), siklofilin A (P62937), makrofaj kapping proteini (P40121), pirüvat kinaz M1/M2 (P14618), glutatyon S-transferaz P (P09211), manganez-süperoksit dismutaz (P04179), sitozolik aminopeptidaz (P28838) ve kompleman komponenti C4A (P0C0L4) olmak üzere dokuz proteine özgü çoklu reaksiyon izleme (MRM) yöntemi, stabil izotopik etiketli peptitler kullanılarak geliştirilmiştir. Yöntemin performansı, Avrupa İlaç Ajansı

kılavuzuna uygun olarak doğrusallık, tespit limiti, cihaz stabilitesi ve örnek hazırlama tekrarlanabilirliği üzerinden değerlendirilmiştir.

EEC, NEC ve sağlıklı gruplara ait doku örneklerinin protein ekstraksiyonu ve proteolitik sindirimi sonrasında dokuz proteinin özgün peptitleri izlenmiştir. Yedi proteinde anlamlı regülasyon göstermiştir. Q01995'in aşağı regülasyonu, malignitelerde tekrarlayan bir olaydır ve kanser sürecinin potansiyel biyobelirteci olabileceğini göstermektedir. Buna karşılık, P14618, P40121, Q00688 ve P28838 yukarı regülasyon göstermiştir ve kanserin karakteristik özelliklerini yansıtmaktadır. Ancak, P0C0L4'ün aşağı regülasyonu ve P09211'in yukarı regülasyonu kanserlerde genellikle gözlenmemektedir. Ek olarak, yalnızca P09211 EEC'de NEC'e kıyasla alt tip-spesifik artış göstermiş ve prognostik değerini ortaya koymuştur. Doğrulanan proteinlerin klinik uygulamaya taşınabilmesi için ileri çalışmalara ihtiyaç vardır.

Anahtar Kelimeler: Biyobelirteç, Endometriyum kanseri, Kütle spektrometresi, Çoklu reaksiyon izleme (MRM), Hedefli proteomik

To my family, my love, my friends, and my lovely children filling my life with joy

Bal, Zeytin, Peynir, Anne Kahvaltı, Süt, Falafel, Huci…

ACKNOWLEDGMENTS

I would like to express my appreciation to my advisor, Assoc. Prof. Dr. Süreyya Özcan Kabasakal, for making mass spectrometry a part of my life. I am grateful for her patience and generosity with her time and expertise throughout my learning and research process.

Special thanks to Assoc. Prof Dr. Berat Doğan for his valuable support in providing meaningful insights from the data. I am thankful to Prof. Dr. Abdullah Karaer for helping to shape this research project.

It is impossible to express gratitude to members of Q-OmicS Lab. My heartfelt thanks to Elif Akmermer for sleepless nights we shared in lab and companionship during experimental work. I wish to offer my deepest thanks to Esin Şahin for her key role in the statistical analysis. I am grateful to Ceren Kul for standing by my side throughout the entire process of learning use of mass spectrometer.

I wish to express my heartfelt thanks to my family for their encouragement, and love. I am thankful to my mother for giving me freedom to make mistakes, and for always supporting me. Thank you for embracing me in my most difficult moments.

To my dearest friend Barkın Kutrup, I could not have completed this work without your support. Your belief in me gave me strength when I needed it most. Thank you for being my place of comfort and calm during challenging moments.

Many thanks to my friends Damla Bozkurt and Ayşen Bakıcı, for their constant motivation (CV<15%), and humor.

This work was funded by the TUBITAK 2519 The European Cooperation in Science and Technology (COST) (Project No: 122S951). I would like to acknowledge Shimadzu Middle East & Africa for providing LC-MS 8060, which greatly contributed to this study.

TABLE OF CONTENTS

ABSTRACT v

ÖZ vii

ACKNOWLEDGMENTS x

TABLE OF CONTENTS xi

LIST OF TABLES xiii

LIST OF FIGURES xiv

LIST OF ABBREVIATIONS xvii

LIST OF SYMBOLS xix

CHAPTER 1 1

INTRODUCTION 1

1.1 Endometrial Cancer 1

1.2 Protein-based Cancer Biomarkers 3

1.3 Biomarker Pipeline 7

1.3.1 Discovery Phase 8

1.3.2 Current Protein Biomarker Candidates for Endometrial Cancer 11

1.3.3 Verification Phase 13

1.3.4 Validation Phase 18

1.4 Design of MRM Assay with SIL Peptides for Biomarker Verification 18

1.4.1 Selection and Randomization of Clinical Samples 19

1.4.2 Preparation of Clinical Samples for MS-Based Proteomics 19

1.4.3 Development of MRM Method 20

1.5 Statistical Analysis for Biomarker Performance 30

1.6 Motivation 31
CHAPTER 2 33
MATERIALS & METHODS 33
2.1 Materials 33
2.1.1 Clinical Samples 33
2.1.2 Quality Control (QC) Samples 34
2.1.3 Reagents for Protein Extraction and Proteolytic Digestion 34
2.1.4 Chemicals and Standards for LC-MRM-MS Analysis 35
2.2 Methods 35
2.2.1 Development of MRM Method 35
2.2.2 Preparation of Clinical Samples 59
2.2.3 Data Processing and Statistical Analysis 63
CHAPTER 3 65
RESULTS & DISCUSSION 65
3.1 Results 65
3.2 Discussion 77
CHAPTER 4 83
CONCLUSION 83
REFERENCES 85
APPENDICES 117
A. HPLC-MS Results of SIL Peptides for the Determination of Purity 117
B. Ethical Committee Approval 121

LIST OF TABLES

Table 1.1 Bokhman's dualistic classification for EC 2
Table 1.2 Types of biomarkers in terms of clinical applications 4
Table 1.3 Ideal features of cancer biomarkers 5
Table 1.4 List of biomarkers approved by FDA 6
Table 1.5 List of candidate biomarkers for EC by different discovery studies..... 11
Table 1.6 Nine candidate protein markers reported for the detection of EC and PCOS 12
Table 1.7 Comparison of MRM to ELISA..... 14
Table 1.8 The m/z values of LISWYDNEFGYSNR peptides 25
Table 2.1 Tryptic peptides of transgelin protein by Expasy PeptideCutter..... 36
Table 2.2 Unique peptides representing transgelin protein. 38
Table 2.3 The list of twenty-three stable isotopic label (SIL) peptides 39
Table 2.4 Hydrophobicity of the selected peptides 41
Table 2.5 The retention times of the selected peptides 45
Table 2.6 The optimized parameters of ESI-MS..... 47
Table 2.7 The selected precursor ions per the selected peptide 49
Table 2.8 The parameters of the developed MRM method..... 51
Table 2.9 The representative peptides of the candidate proteins from the finalized MRM method..... 56
Table 2.10 The values of LOD, and R^2 calculated by Skyline..... 58
Table 2.11 Total protein concentration (µg/µL) of the homogenized tissue samples of healthy group (N=26) 60
Table 2.12 Total protein concentration (µg/µL) of the homogenized tissue samples of EEC group (N=23)..... 60
Table 2.13 Total protein concentration (µg/µL) of the homogenized tissue samples of NEC group (N=20) 60

LIST OF FIGURES

Figure 1.1 Illustration of stage IA EC an stage IB EC 1
Figure 1.2 Classification of biomarkers by FDA-NIH Biomarker Working Group 3
Figure 1.3 Biomarker pipeline from laboratory to clinical use 7
Figure 1.4 Phases of biomarker pipeline 8
Figure 1.5 The representation of proteolytic digestion..... 9
Figure 1.6 The workflows of discovery proteomics..... 10
Figure 1.7 The workflow of biomarker verification using MRM-MS 17
Figure 1.8 Tryptic digestion of a representative protein in silico..... 21
Figure 1.9 (a) Endegenous peptide with C-terminal natural arginine 24
Figure 1.9 (b) SIL peptide with C-terminal heavy isotopic Arginine ($^{13}C_6$, $^{15}N_4$) 24
Figure 1.9 (c) Representation for co-elution of endogeneous peptide from sample and SIL peptide..... 24
Figure 1.10 Relative intensity of ions in different charge states with different voltage potential 26
Figure 1.11 Fragmentation of peptide backbone to obtain y- and b- ions..... 27
Figure 1.12 Dynamic concentration range of targeted proteins in human plasma detected by MS 29
Figure 2.1 The protein sequence of transgelin protein (Q01995)..... 36
Figure 2.2 The chromatogram of LVNSLYPDGSKPVK, TDMFQTVDLFEGK, TLMALGSLAVTK, DHLVTAYNHLFETK and LEIEPEWAYGK peptides..... 43
Figure 2.3 The chromatogram of QAALQVAEGFISR, VSDATGQMNLTK, YQEGGVESAFHK, FEDENFILK and EGMNIVEAMER peptides 43
Figure 2.4 The chromatogram of AAGIDEQENWHEGK, TLIEFLLR, ETLNISGPPLK, LNFSHGTHEYHAETIK, DPVQEAWAEDVDLR and IYVDDGLISLQVK peptides 44
Figure 2.5 The chromatogram of HHAAYVNNLNVTEEK, MLLADQGQSWK, AIWNVINWENVTER and AFLASPEYVNLPINGNGK peptides 44

Figure 2.6 The chromatogram of VLSLAQEQVGGSPEK, LVNGQSHISLSK and DSSTWLTAFVLK peptides 45
Figure 2.7 The signal intensities of the m/z values of (a) 606.86 and (b) 404.91 corresponding to (+2) and (+3) charges states of TLMALGSLAVTK* peptide in MRM mode, respectively 48
Figure 2.8 MRM transitions of TLMALGSLAVTK* peptide with (+2) charge state (a) before filtering (b) after filtering 50
Figure 2.9 MRM transitions of (a) endogenous TLMALGSLAVTK peptide (b) SIL TLMALGSLAVTK* peptide in EC-QC1. 54
Figure 2.10 Confirmation of co-elution of interference-free MRM transitions representing (a) endogeneous and (b) SIL peptides in EC-QC1 55
Figure 2.11 The instrument stability of MS-QC using the ratio (L/H) normalization 57
Figure 2.12 The instrument stability calculated by CV% for each peptide 57
Figure 2.13 The matrix-matched calibration curve of FEDENFILK peptide generated by Skyline 58
Figure 2.14 The localization of endometrioid endometrial cancer samples (purple) in a 96-well plate. All samples were placed from A1 to G8 61
Figure 2.15 The sample preparation stability between EC-QC samples using the ratio (L/H) normalization 62
Figure 2.16 The reproducibility of sample preparation calculated by CV% for each peptide 63
Figure 3.1 Representative MSstat input of transgelin protein exported using Skyline 66
Figure 3.2 Relationship between raw log2(light/heavy) ratios and MSstats normalized log2 intensities after global standard normalization. 67
Figure 3.3 Heatmap analysis of nine targeted proteins among healthy, EEC and NEC groups. 68
Figure 3.4 (a) The volcano graphs showing the regulations of candidate biomarkers between EEC and healthy groups. 69

Figure 3.4 (b) p-values and box plots for each protein, comparing the protein levels between EEC and healthy groups 70
Figure 3.5 (a) The volcano graphs showing the regulations of candidate biomarkers between NEC and healthy groups. 71
Figure 3.5 (b) p-values and box plots for each protein, comparing the protein levels between NEC and healthy groups 72
Figure 3.6 (a) The volcano graphs showing the regulations of candidate biomarkers between EEC and NEC groups..... 73
Figure 3.6 (b) p-values and box plots for each protein, comparing the protein levels between EEC and NEC groups..... 73
Figure 3.7 ROCs and AUC values for each protein, indicating the classification performance between EEC and healthy groups..... 74
Figure 3.8 ROCs and AUC values for each protein, indicating the classification performance between NEC and healthy groups 75
Figure 3.9 ROCs and AUC values for each protein, indicating the classification performance between EEC and NEC groups 76

LIST OF ABBREVIATIONS

ABBREVIATIONS

AA	Amino acid
ACN	Acetonitrile
AUC	Area under curve
BCA	Bicinchoninic acid
CE	Collision energy
CID	Collision-induced dissociation
CV	Coefficient of variation
Da	Daltons (g/mol)
DTT	Dithiothreitol
EC	Endometrial cancer
EEC	Endometroid endometrial cancer
ELISA	Enzyme-linked immunosorbent assay
EMA	European Medicines Agency
ESI	Electrospray ionization
FDA	The U.S. Food and Drug Administration
FPR	False positive result
HPLC	High-pressure liquid chromatography
IAA	Iodoacetamide
iTRAQ	Isobaric tag for relative and absolute quantitation
LC	Liquid chromatography

LIT	Linear ion trap
LOD	Limit of detection
LLOQ	Lower limit of quantification
m/z	Mass-to-charge-ratio
MALDI	Matrix-assisted laser desorption/ionization
MRM	Multiple reaction monitoring
MS	Mass spectrometer
MS/MS	Tandem mass spectrometer
NEC	Non-endometrioid endometrial cancer
NIH	National Institutes of Health
Q	Quadrupole
QC	Quality control
QQQ	Triple quadrupole
ROC	Receiver operating characteristic
RT	Retention time
SDC	Sodium deoxycholate
SIL	Stable isotopic labeled
TFA	Trifluoroacetic acid
TMT	Tandem mass tag
TOF	Time-of-flight mass spectrometry
TPR	True positive result
Tris	Tris(hydroxymethyl)aminomethane

LIST OF SYMBOLS

SYMBOLS

K*	[$^{13}C_6$, $^{15}N_2$]-lysine
R*	[$^{13}C_6$, $^{15}N_4$]-ariginine

CHAPTER 1

INTRODUCTION

1.1 Endometrial Cancer

Endometrial cancer (EC) is a gynecological cancer that arises in the inner lining of the uterus, known as the endometrium (Figure 1.1)[1]. Global cancer statistics presented that EC was diagnosed by 420.242 women and 97.704 deaths were reported worldwide in 2022[2]. According to American Cancer Society, nearly 70.000 women will be diagnosed with EC in the United States by the end of 2025[3]. The incidence of EC is increasing more in high-income countries than low-/middle-income countries. This trend causes a critical challenge for healthcare systems[4].

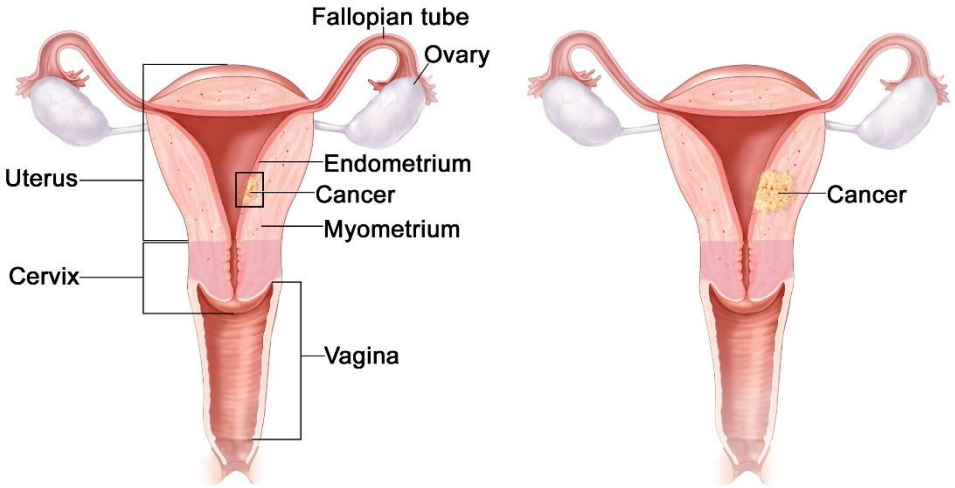

Figure 1.1 *Illustration of stage IA endometrial cancer (left) and stage IB endometrial cancer (right). Retrieved from https://www.cancer.gov/types/uterine/hp/endometrial-treatment-pdq#section_3.4*

EC has different histological subtypes, including endometrioid endometrial cancer (EEC), serous, clear-cell, undifferentiated carcinomas, and carcinosarcomas[5]. EC has been broadly divided into two subtypes according to their histological and clinical features, grade and prognosis: type I and type II. Type I is the most commonly occurring subtype, also known EEC. It is oestrogen driven, consists of low-grade cells with a good prognosis. Type II is also called as non-endometrioid endometrial cancer (NEC), which is less common and has a poor prognosis. According to Bokhman's dualistic classification, the clinical characteristics, histology, grade, and prognosis of both types were compared in Table 1.1[4].

Table 1.1 *Bokhman's dualistic classification for EC[4].*

	Type I (EEC)	**Type II (NEC)**
Clinical characteristics	Oestrogen dependent	Non-oestrogen dependent
Histology	Endometrioid	Non-endometrioid (serous, clear-cell, undifferentiated carcinomas, and carcinosarcomas)
Grade	Low	High
Prognosis	Good	Poor

Although the majority of EC cases belong to type I, which is associated with obesity and metabolic diseases[6], type II is clinically more aggressive than type I and this subtype has relatively poor survival rates compared to type I[4].

The most common symptom of EC is abnormal uterine bleeding, and over 90% of EC cases have this symptom. However, this symptom is not specific to EC[7]; only 5–10% of women with abnormal uterine bleeding are eventually diagnosed with EC[8].

Endometrial biopsy is based on histopathological analysis. It is a gold standard for the detection of EC[9] even though histopathology is not sufficient for the identification of molecular character of tumor[10]. Hence, in early-stage EC, the presence of aggressive or metastatic disease cannot generally be reliably assessed[10].

Considering the rise in the prevalence and complexity of EC, there has been a growing need for early detection and effective treatment. To differentiate the sub-types of EC, and improve the early diagnosis and prognosis, biomarkers are required[11].

1.2 Protein-based Cancer Biomarkers

In 2016, Food and Drug Administration (FDA)-National Institutes of Health (NIH) Biomarker Working Groups identified the term of "biomarker" as a feature that can be used as an indicator of the processes which are biologically normal and pathogenic[12].

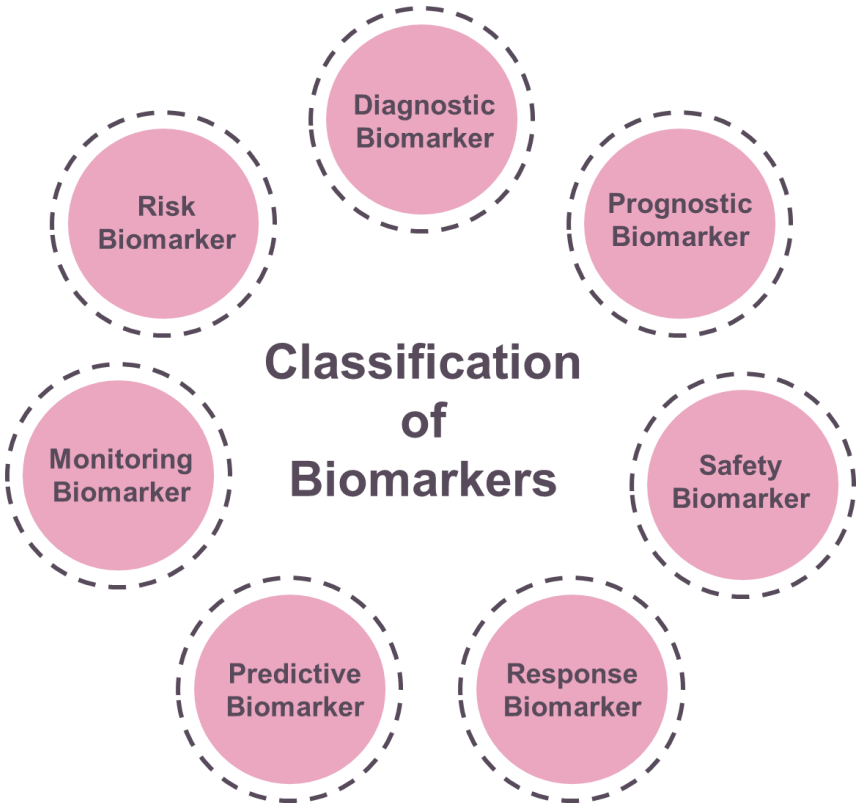

Figure 1.2 *Classification of biomarkers by FDA-NIH Biomarker Working Groups*[12]

In addition, the classification of biomarkers by clinical application broadened the scope of their definitions as specified in Figure 1.2[12].

A “diagnostic biomarker” facilitates the detection of disease/condition as well as to identify people with a particular sub-type of the disease. In medical practice, diagnostic biomarkers are vital for the determination of a patient’s medical condition, followed by the clinical intervention[12]. In Table 1.2, the roles of other types of biomarker were described[12].

Table 1.2 *Types of biomarkers in terms of clinical applications*[12]

Types of Biomarker	Definition	Example(s)
Prognostic biomarker	A biomarker predicting the risk of disease progression/outcome independent of any treatment.	C-reactive protein (CRP) for identification of unstable angina
Safety biomarker	A biomarker predicting the risk of side effects/harm of a medicinal product or indicating early toxicity.	Hepatic aminotransferases and bilirubin for evaluating potential hepatotoxicity
Response biomarker	A biomarker which direct indicator of biological response to an intervention.	Circulating B lymphocyte for evaluating systemic lupus erythematosus
Predictive biomarker	A biomarker predicting the likelihood of better benefit or greater harm from a given treatment/agent exposure.	BReast CAncer genes 1 and 2 (BRCA1/2) mutations for the evaluation of platinum-sensitive ovarian cancer
Monitoring biomarker	A biomarker evaluating the status of disease by measuring repeatedly.	B-type natriuretic peptide for pulmonary hypertension
Risk biomarker	A biomarker identifying people with an increased likelihood of developing a disease.	Apolipoprotein E (APOE) gene variations for identifying people develop Alzheimer’s disease

The use of biomarkers is crucial for the diagnosis, prognosis, and treatment of cancer. Cancer biomarkers have multiple clinical applications, including assessing cancer predisposition, screening, predicting recurrence, evaluating treatment outcomes, determining patient prognosis, enabling early detection, and differentiating the sub-types of cancer[13,14].

The desired characteristics of a biomarker vary depending on its clinical purpose. For instance, diagnostic and prognostic biomarkers prioritize the accuracy even if they are invasive or costly; on the other hand, screening and predictive biomarkers must be easy to perform, have low cost, be noninvasive, and accurate (Table 1.3)[14].

Table 1.3 *Ideal features of cancer biomarkers*[14]

Clinical Use	Simple to Perform	Noninvasive Body Source	Accuracy[§]	Low Cost
Early diagnosis	**	**	***	**
Prognosis	*	*	**	*
Screening	***	***	***	***
Predisposition	***	***	***	***

Degree of importance: * < ** < ***
[§]Low rate of false-negative results

The molecular changes in a cancer cell that occurs at the DNA, RNA, protein, or metabolite level can be a cancer biomarker[15]. Those molecular changes such as genetic variants, transcriptional alterations, epigenetic and proteomic signatures should be quantifiable and specific[14,15]. They can be detected in the biological sources obtained from a patient's tissue sample through tumor biopsy or from blood, urine, saliva, and other body fluids[15].

Several cancer biomarkers have been discovered and are mainly categorized based on the presence of proteins serving as hormones, enzymes, antigens, and receptors[13]. In 1847, the Bence-Jones protein in urine was reported as the first identified protein biomarker for cancer[15,16]. The discovery of carcinoembryonic antigen in 1971 was another milestone in the advancement of cancer biomarker research[15]. Nowadays, both tests of Bence-Jones protein and carcinoembryonic antigen are used for the prognosis and diagnosis of multiple myeloma and colorectal cancer, respectively[17-

[20]. Additionally, there are several protein cancer markers approved by FDA in the current clinical applications as specified in Table 1.4[21].

The release or secretion of proteins by tumor cells provides information about the presence or absence of the proteins in cells at healthy and cancer conditions using clinical samples[15,22]. Those certain proteins (such as proteins in Table 1.4) are potential biomarkers for a specific cancer type[23].

Table 1.4 *List of some biomarkers approved by FDA[21]*

Biomarker	**Clinical Application**	**Type of Cancer**	**Body Source**
ROMA (HE4+CA-125)	Prediction of malignancy	Ovarian	Serum
HE4	Monitoring recurrence or progression of disease	Ovarian	Serum
Circulating Tumor Cells (EpCAM, CD45, cytokeratins 8, 18+, 19+)	Prediction of cancer progression and survival	Breast	Whole blood
Estrogen receptor (ER)	Prognosis, response to therapy	Breast	FFPE tissue
Nuclear Mitotic Apparatus protein (NuMA, NMP22)	Diagnosis and monitoring of disease (professional and home use)	Bladder	Urine
Pro2PSA	Discriminating cancer from benign disease	Prostate	Serum

1.3 Biomarker Pipeline

The development of protein biomarkers is a process including multiple phases (Figure 1.3). Once a specific clinical question has been defined, the biomarker pipeline for the identification of protein biomarkers has to be followed[24]. The biomarker pipeline contains biomarker discovery, verification, and validation phases[25,26]. In this pipeline, the discovery phase focuses on protein identification and biomarker candidate selection, and in phase II, these candidates are verified in an independent sample cohort[24,25]. In the validation phase, biomarker performance is assessed in both analytical and clinical terms[25]. Analytical validation confirms the technical performance of the assay whereas clinical validation establishes the association between the biomarker and the clinical condition[27]. Finally, the developed clinical assay is needed to be approved by the health agencies such as the U.S. Food and Drug Administration (FDA) or the European Medicines Agency (EMA). The process from discovery to clinical use may last for several years[24]. For instance, the discovery of HE4 protein occurred in 2000[28]; however, the approval of its clinical assay was given in 2008[29].

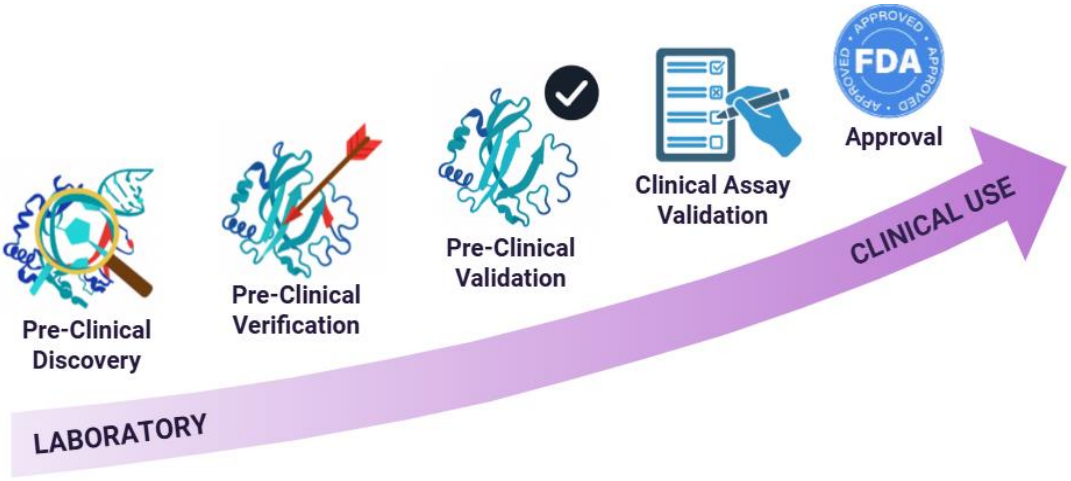

Figure 1.3 *Biomarker pipeline from laboratory to clinical use*[24-27]

Each phases aims to achieve different outcomes during the biomarker development. Hence, the required sample size and analyte size differ from phase to phase (Figure 1.4)[25,26].

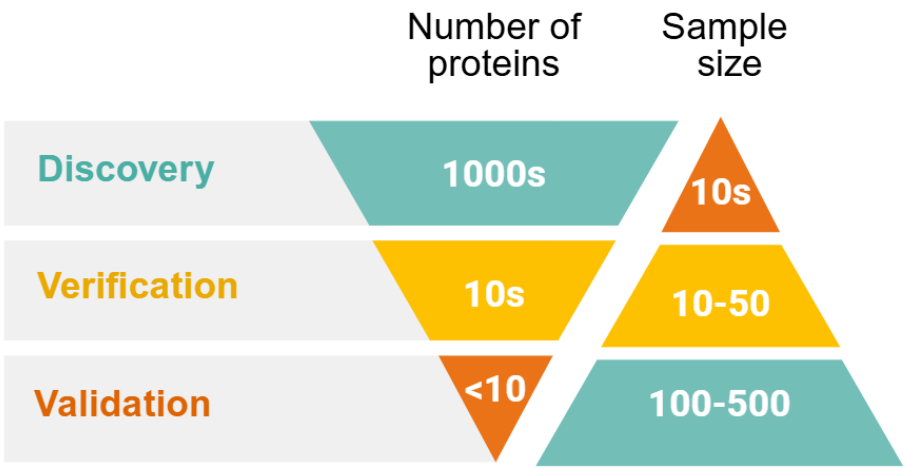

Figure 1.4 *Phases of biomarker pipeline with the comparison of number of proteins and sample size*[25,26]

1.3.1 Discovery Phase

The initial phase of biomarker pipeline is "discovery", which is the unbiased and semi-quantitative step[27]. The aim of the discovery phase is to enable large-scale screening of proteins by identifying thousands of proteins, and determine the candidate biomarkers. A relatively small cohort of samples (10s) are analyzed due to relatively low throughput of discovery proteomics, long run times, and complex data analysis[25-27].

The analysis method of discovery phase is primarily focused on in-depth and untargeted proteomics using bottom-up (shotgun) approach to detect the proteins with high coverage[25]. This approach measures the proteins indirectly through the analysis of the peptides rather than the intact proteins[30]. The proteins undergo to proteolytic digestion, which breaks down the proteins down into the peptides (Figure

1.5) and then, those peptides are subjected to liquid chromatography tandem mass spectrometer (LC-MS/MS)[30].

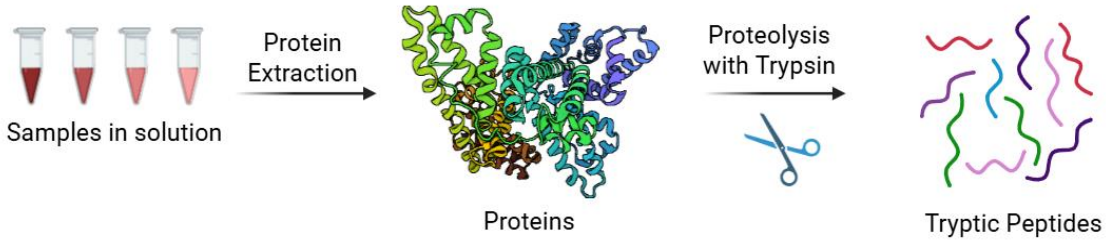

Figure 1.5 *The representation of proteolytic digestion*[30]

In the discovery phase, it is important to identify as many proteins as possible in LC-MS/MS. Thus, increasing the chances of detecting low-abundance proteins is required. In order to broaden of protein coverage, the depletion of abundant proteins and peptide pre-fractionation can be performed depending on the complexity of biological sample[25]. Another factor enhancing the proteome coverage is to use mass spectrometers with high resolution such as quadrupole time-of-flight (Q-TOF), Q-orbitrap, and linear ion trap (LIT)–orbitrap, as presented in Figure 1.6(a)[31].

The tandem mass spectrometer fragments the peptides by applying collision energy. The peptide fragmentation gives tandem mass spectra (Figure 1.6(b)), and the peptide characterization is achieved by the comparison of the obtained spectra with the theoretical tandem mass spectra produced from in-silico digestion of a protein database. This method is especially appropriate for the studies involving the proteome from organisms lacking existing experimental spectral data[30]. Another characterization method is the use of publicly available spectral libraries, which are experimental MS/MS spectra previously obtained and stored in a database. It facilitates a standard data analysis and reduced false-positive identifications since it offers more specific search and direct comparison with the data obtained[24], as presented in Figure 1.6(c).

Untargeted proteomics facilitates protein identification using relative quantification approach, which enables the results with up/down-regulation, or fold changes[26,32]. The techniques for the relative quantitation includes label-free techniques, and also some isotopic labeling techniques such as isobaric tagging (e.g., iTRAQ or TMT) or non-isobaric tagging (e.g., mTRAQ, or acetylation)[32,33]. Additionally, isobaric tagging for peptide labeling can be preferred to decrease the variation between measurements by multiplexing the samples in a single experiment[24].

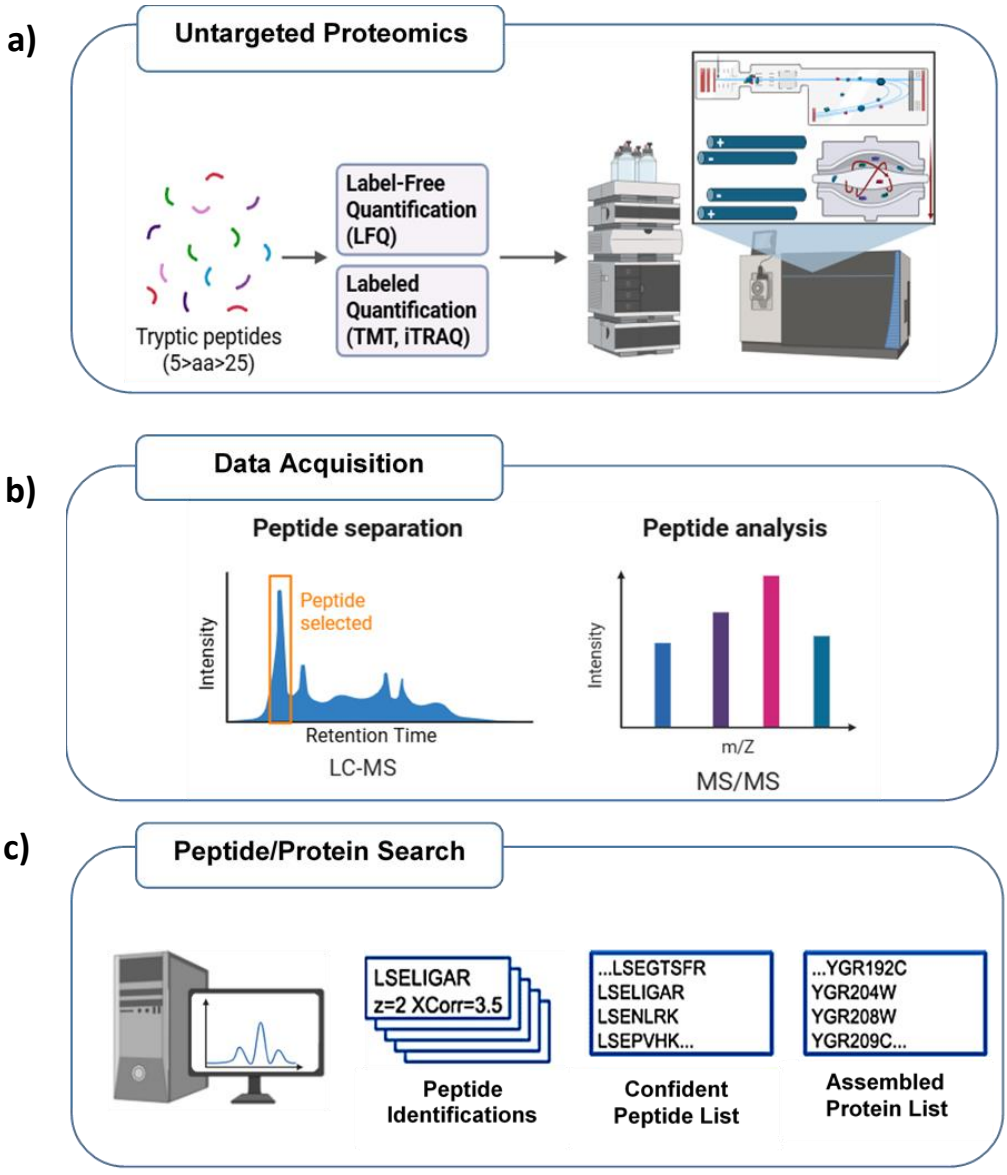

Figure 1.6 *The workflow of discovery proteomics*[31-33]

1.3.2 Current Protein Biomarker Candidates for Endometrial Cancer

Many biomarker discovery studies for EC have been conducted to improve its diagnostic and prognostic outcomes. From 2014 to 2024, the use of MS-based untargeted proteomics on diverse biological sources such as blood, tissue, urine, and other body fluids resulted in the identification of 263 candidate biomarkers for EC.[11] There are some protein biomarkers that have been commonly identified as candidates in the different studies, as specified in Table 1.5[11].

Table 1.5 *List of candidate biomarkers for EC by different discovery studies*[11]

Protein Name	**UniProt ID**	**MS-based Technique**	**Biological Source**
Alpha-2-macroglobulin	P01023	SWATH-MS[34] 2D-DIGE-MALDI-TOF MS[35]	Blood[34,35]
Apolipoprotein A-I	P02647	SWATH-MS[34] LTQ-Orbitrap MS[36]	Blood[34,36]
Apolipoprotein E	P02649	SWATH-MS[34] LTQ-Orbitrap MS[36]	Blood[34,36]
Complement C3	P01024	2D-DIGE-MALDI-TOF MS[37] MALDI-TOF MS[38]	Blood[37,38]
Complement factor B	P00751	SWATH-MS[34] LTQ-Orbitrap MS[39]	Blood[34,39]
Galectin-3-binding protein	Q08380	SWATH-MS[34] Q-Orbitrap MS[40]	Blood[34,40]
Catenin beta-1	P35222	MALDI-TOF MS[41] LTQ-Orbitrap MS[42] MALDI-TOF/TOF MS[42]	Cervical fluid[41] Uterine aspirate[42]
Annexin A2	P07355	SWATH-MS[43] 2D-DIGE-MALDI-TOF MS[44] LTQ-Orbitrap MS[45] MALDI-TOF MS[46] LC-QTOF MS[47] MALDI MSI[50]	Tissue[43,44,45,46,47]
Calcyphosin (Calcyphosine)	Q13938	Q-TOF MS[49] SWATH-MS[51]	Tissue[49,51]

Table 1.5 *Continued*

Creatine kinase B-type	P12277	2D-DIGE-LTQ-Orbitrap MS[52] LTQ-Orbitrap MS[53]	Tissue[52,53]
SRSF protein kinase 1	Q96SB4	MALDI-TOF MS[54] Q-Orbitrap MS[55]	Tissue[54,55]

Among these different biological samples, tissue has been the most extensively studied source in the MS-based biomarker discovery studies for EC, and 111 out 263 biomarkers were discovered using tissue samples. Although 111 of biomarkers have been discovered, only 4 of them have advanced to the verification phase, which is critical step in biomarker development pipeline[11].

The proteomic biomarker studies for EC in the literature have also examined for the explanation its relationship with other diseases such hyperplasia[37,44], diabetes[35], polycystic ovary syndrome (PCOS)[53] etc. The study[53] which combined data from the proteomic studies of EC[54-57] and PCOS[58-60] identified a panel of nine candidate biomarkers of EC in women with PCOS, as presented in Table 1.6. These proteins have been identified in various EC studies[54-63] but have not been verified in large sample size. If validated in EC, these proteins could subsequently be validated in PCOS to clarify the relationship between the two conditions[53].

Table 1.6 *Nine candidate protein markers reported for the detection of EC and PCOS*

Protein Name	**UniProt ID**	**MS-based Technique**	**Biological Source**
Transgelin	Q01995	iTRAQ LC-MS/MS[54]	Endometrial tissue[54]
Pyruvate Kinase M1/M2	P14618	iTRAQ LC-MS/MS[54]	Endometrial tissue[54]
Peptidyl-Prolyl Cis-Transisomerase (FKBP3)	Q00688	MALDI-MS[55]	Endometrial tissue[55]

Table 1.6 *Continued*

Cyclophilin A	P62937	MALDI-Q-TOF-MS/MS[56]	Endometrial tissue[56]
Glutathione S-Transferase P	P09211	MALDI-Q-TOF-MS/MS[56]	Endometrial tissue[56]
Complement Component C4A	P0C0L4	LC-MS/MS[57] iTRAQ LC-MS/MS[61]	Serum[57] Endometrial tissue[61]
Macrophage Capping Protein (Gelsolin-like Capping Protein)	P40121	iTRAQ LC-MS/MS[61] 2D-LC-MS/MS[62]	Endometrial tissue[61,62]
Cytosol Aminopeptidase (Leucine Aminopeptidase)	P28838	LC-MS/MS[63]	Endometrial tissue[63]
Manganese-Superoxide Dismutase*	P04179*	-	-

*****Galazis et al.[53] presented that manganese-superoxide dismutase helps protect cells against reactive oxygen species–induced death, which is linked to cancer and insulin resistance—both important concerns in women with PCOS.

The verification and validation phases are important since the proteins are identified in a putative and semi-quantitative way in the discovery phase. Therefore, the candidate proteins are required to quantitavely verify using the same or similar clinical samples[25].

1.3.3 Verification Phase

Biomarker verification is a critical step to determine whether the levels of candidate biomarkers differ significantly between case and control groups[24,25]. In this phase, sample size (10-100) increases to encompass a wide range of cases and controls

while the number of proteins (10s) decreases to confirm the sensitivity of candidate biomarkers, and assess their specificity. Unlike discovery phase, verification phase enables the analysis of large cohort since the methods used offers much faster analysis per sample, and tends to improve reproducibility[25-27].

Enzyme-linked immunosorbent assays (ELISA) and selected or multiple reaction monitoring (SRM or MRM) are most commonly used assays for the verification phase, which measure the protein abundances[24-27].

ELISA is one of the most sensitive immunoassays, and offers the detection and quantitation of disease biomarkers in a simple and rapid way[64]. The working principle of ELISAs relies on two specific antibodies detecting targeted proteins accurately[65-68]. MRM is a targeted MS technique used to quantify specific molecules (e.g. peptides) in complex biological samples. It measures the specific peptide mass (precursor ion) and its fragment ions using stable isotope-labeled (SIL) peptide standards[35].

Table 1.7 *Comparison of MRM to ELISA*[75]

	MRM	**ELISA**
Detection method	Mass spectrometry	Absorbance, fluorescence, luminescence
Principle	Detection of targeted peptides using stable isotope-labeled peptide standards	Antibody–antigen binding
Development time	3-4 weeks	3-6 months
Multiplexing	High	Limited, due to antibody cross reactivity
Batch-to-batch variation	Low, highly reproducible with spiking equimolar stable isotope-labeled peptide standards	High, due to antibody lot differences

Table 1.7 *Continued*

Sensitivity	ng/mL	pg/mL
Specificity	High, detection of precursor/fragment ions	Depending on the antibody and the protein epitope
Widely used for	Biomarker verification/ validation, multiplex protein quantification	Routine diagnostics, clinical tests

Table 1.7 shows the comparison of MRM-MS and ELISA techniques[75]. In the development and validation of an ELISA kit, it is necessary to test each antibody combination for interferences due to the possibility of cross-reactivity[26,67], causing reduced sensitivity and specificity. Furthermore, it limits the ability to multiplex multiple proteins in a single experiment with high precision. MRM has high multiplexing capability, for instance, 142 high-to-moderate abundance proteins (from 31 mg/mL to 44 ng/mL) were measured in undepleted and non-enriched human plasma in a single run with a wide dynamic range[70]. Additionally, ELISA exhibits batch-to-batch variation primarily due to differences in reagent and plate manufacturing, antigen coating, calibrators, and control adjustments between production runs[71]. In MRM-MS, batch-to-batch variation is minimal since the spiking equimolar SIL peptide standards into the biological samples, correcting for sample preparation and instrument fluctuations across runs. While ELISA is widely used for clinical diagnostics, MRM is more appropriate for biomarker verification, and multiplexed protein measurements[71-73].

MRM is performed using triple quadrupole (QQQ) mass spectrometers, which has a unique capability to act as mass filters and to selectively analyze targeted analyte ions[72,73]. Two quadrupoles (Q1 and Q3) in QQQ are responsible for mass filtering. The ionized peptide (representing the target protein) reaches the first quadrupole, which is the first mass filter. Q1 selects the precursor ion defined by the m/z of the

peptide. The selected precursor ion is fragmented at the peptide bonds using collision-induced dissociation in Q2. Third quadrupole acts as the second mass filter, which selects the fragment (product) ions derived from the precursor ion of the targeted peptide. Then, the fragment ions reach the detector[72-74]. The precursor/fragment (Q1/Q3) ion pair is called as "MRM transition"[32]. The combination of both mass filters, Q1 and Q3, facilitates highly sensitive and selective detection of the peptide in a reproducible way, and the accurate quantification of targeted peptides (Figure 1.7(a))[74].

Furthermore, the SIL peptides (analogs of endogeneous peptides) are utilized to provide confident detection and quantification of the endogeneous peptides in the samples from a living organism[25]. The SIL peptides offer highly selective detection of the candidate protein markers since the SIL ([^{13}C,^{15}N]-labeled forms) and endogeneous peptides co-elute and have a similar ionization efficiency, and MS/MS fragment pattern, as presented in Figure 1.7(b)[27,75]. MRM with SIL peptides serves as the "gold standard" of the quantification in MS-based proteomics[75].

MRM data analysis involves detection and integration of chromatographic peaks in the raw data, normalization using SIL peptides as internal standards, quantification via calibration curves, and statistical evaluation of differences between case-control or case-case groups, as specified in Figure 1.7(c)[71,75].

The quantification strategies consist of "relative" and "absolute" quantifications. Relative quantification refers to the comparative measurement of protein abundance between different conditions, providing fold-change rather than exact concentrations[74]. In contrast, absolute quantification uses SIL peptides of precisely known concentrations as internal standards. SIL peptides allow for direct calculation of the absolute concentrations of the target peptides in the sample. Both types can be used to confirm the abundances of the candidate biomarkers[76].

In addition to the confirmation, the results of the quantification also help to estimate the required sample size in order to differentiate between the targeted clinical groups for the validation phase[29]. Furthermore, these findings can be applied to a second,

independent clinical cohort in which verification is carried out using a more sensitive and reliable analytical approach. This approach enhances the validity of the results across different patient populations[25,29].

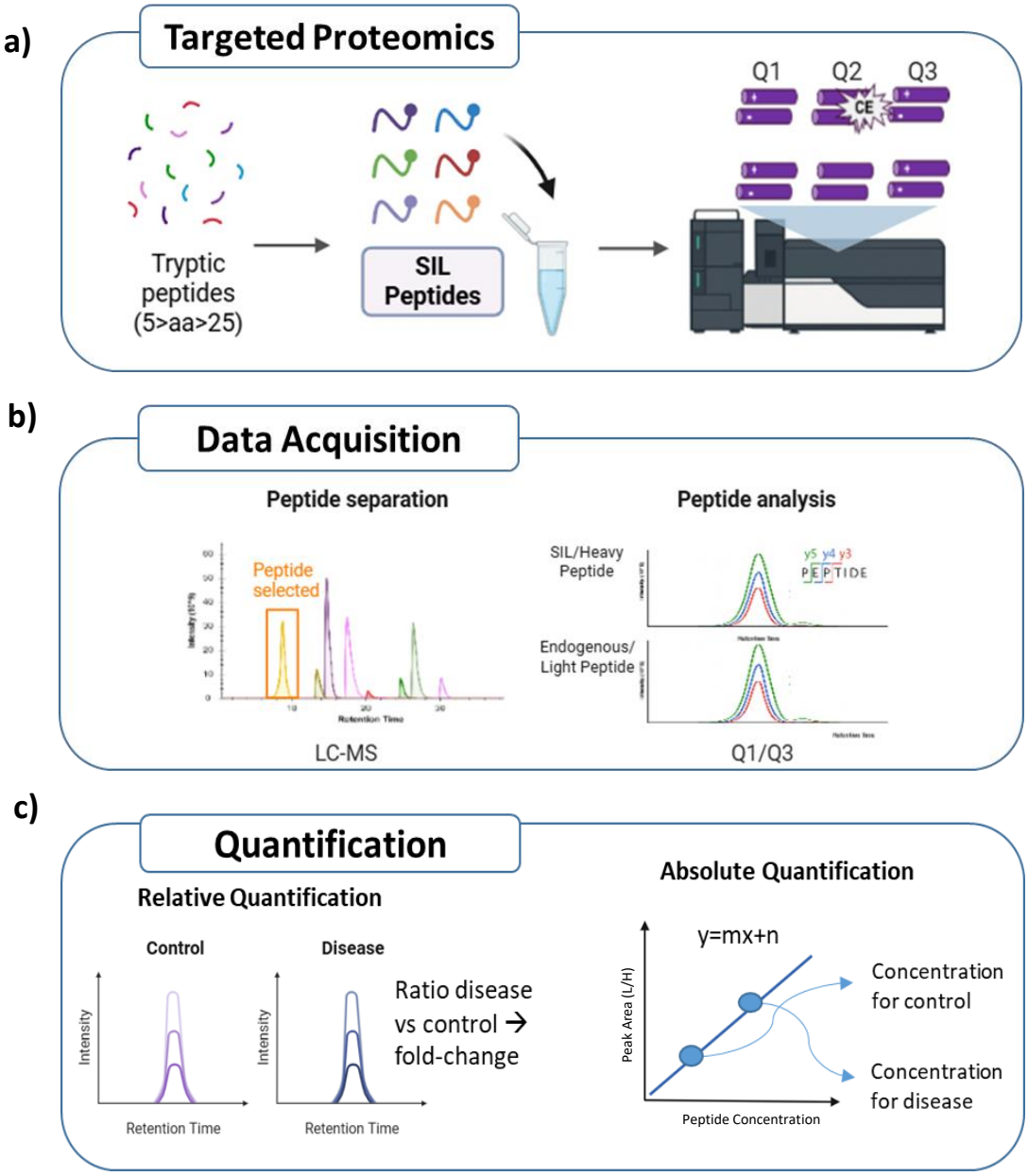

Figure 1.7 *The workflow of biomarker verification using MRM-MS*[74-76]

1.3.4 Validation Phase

The third phase is a preclinical assessment determining the analytical and clinical performance of the candidate protein markers to achieve the study objective[26]. In this phase, only a few number of the best biomarker candidates (3-10) are tested on 100-500 samples[25,26.] The actual clinical validation is performed by measuring final biomarker candidates using 1000s of the samples during a period of >24 months[26,27,32].

This step is conducted by either ELISA, or MRM-MS assays in cases where particular antibodies are not accessible. If MRM-MS assays are utilized for both the verification and analytical validation phases, these phases will share the identical design and experimental parameters[25].

The results are evaluated in two ways where the analytical performance considers accuracy and precision of protein assays, and the clinical performance focuses on sensitivity, specificity, and clinical utility indication[77].

The combination of the most promising proteins serves as the biomarker panel, which will be utilized in the prospective study phases[78]. If the performance characteristics of the biomarker panel meet the defined clinical objective, then the panel shows sufficient promise to warrant clinical evaluation[79].

1.4 Design of MRM Assay with SIL Peptides for Biomarker Verification

A biomarker verification study requires to be meticulously designed, and cannot be regarded as a straightforward analysis of additional samples utilized in the discovery phase[80]. For a robust and representative assessment of the potential biomarker concentration ranges, the study population should include both males and females, a broad age range, diverse racial and ethnic backgrounds[80]. In addition, for patients with EC, it is essential to collect detailed demographic information such as age at

diagnosis, pre- and post-menopausal status, parity, gravida, history of abortions, and dilatation and curettage procedures[4,5].

1.4.1 Selection and Randomization of Clinical Samples

The same or similar biological samples are used to verify the initial biomarker candidates identified in the biomarker discovery phase[25]. These biological samples are collected from subjects with disease (case) and non-disease (control). The collected case samples may represent different subtypes of the disease (e.g. endometrioid and non-endometrioid type). The individuals from case group with different subtypes and control group should have similar characteristics such as age, sex, race, body mass index, or pre-existing conditions which are affecting some diseases. Thus, they can be matched, and case-control as well as distinct subtypes of cases were compared appropriately[81]. The comparison of subtypes leads to improve patient outcomes and reveal different disease progression patterns[81].

Randomization is important to prevent human bias during preparation and analysis. The randomization of sample groups can be performed across the plate or chip locations[25]. It can help to minimize batch effect if the number of samples is over the assay batch size[82].

1.4.2 Preparation of Clinical Samples for MS-Based Proteomics

In peptide-centric approach, the identification and quantification of proteins are performed by the analysis of unique peptides representing proteins rather intact proteins[83]. Therefore, the main goal of sample preparation is the conversion of proteins to peptides[84].

The first step is to isolate protein mixture from clinical samples[84,85]. The workflow of protein isolation may differ depending on the type of biological samples and include homogenization of sample, protein extraction, precipitation with organic

solvents, or etc. For instance, while tissue samples need to be homogenized, urine samples are subjected to protein extraction using solvent precipitation[85].

The other step is the quantification of protein concentration in the biological samples. Colorimetric or fluorescent dye methods might be used to determine the protein concentration before the proteolytic digestion. Both methods are based on the protein-dye binding[85]. The measurement of total protein concentration enables calculation of the protein-to-enzyme ratio used in the digestion step and facilitates normalization of total protein levels in the clinical samples[75].

The workflow from proteins to peptides consists of protein denaturation, reduction, alkylation, and enzymatic digestion steps[84-86]. To begin with, three-dimensional structure of proteins is denatured using some reagents such as urea, and sodium deoxycholate (SDC). Then, intra- and intermolecular disulfide bonds between cysteine (C) amino acid residues are reduced using the reduction agents such as dithiothreitol (DTT) or tris(2-carboxyethyl)phosphine (TCEP)[85,87]. This step is followed by alkylation step, which alkylates the free sulfhydryl groups with iodoacetamide (IAA) to avoid the reformation of disulfide bonds[86]. Final step is the protein digestion with trypsin enzyme. Trypsin enzyme is gold standard in proteomics studies since it offers high specificity to cleave off the C-terminal ariginine (R) and lysine (K) residues[75].

Prior to LC-MS analysis, the digested samples must be cleaned by removing salts, detergents, and buffer solutions used during sample preparation[85]. Reversed phase solid-phase extraction (SPE) is a purification technique which can be used for desalting the peptides. C18 SPE cartridge trapes the peptides and removes the contaminants by washing them. Subsequently, the peptides are eluted and dried[88].

1.4.3 Development of MRM Method

MRM-MS in combination with SIL peptide standards has been used as a tool for biomarker verification using QQQ-MS system[71,75]. MRM is useful to perform

targeted proteomics which analyzes the target peptides representing the protein biomarkers. In order to analyze the targeted peptides in a reliable way, it is needed to develop an analytical MRM method. Mass spectrometer is programmed with an MRM method for the targeted analysis[89]. The SIL peptides representing the targeted protein biomarkers provides the specificity and accuracy of MRM quantification[90].

- **Selection of Targeted Proteins and Peptides**

The selection of the proteins may be based on the prior experiments or the other scientific publications. Moreover, several online resources can assist in identifying the target proteins, such as gene and protein expression data, protein-protein interaction data, or protein information obtained from KEGG and gene ontology database. As a result, each study determines the targeted proteins depending on its purpose therefore, the selection of the targeted proteins is subjective[74]. However, the selection of the peptides representing the targeted proteins is crucial to achieve a successful MRM experiment[74]. Each targeted proteins produce the yield of 10-100 of tryptic peptides during the enzymatic digestion with trypsin[91]. Each targeted proteins produce the yield of 10-100 of tryptic peptides during the enzymatic digestion with trypsin,[91] as specified in Figure 1.5 and 1.7[92]. Trypsin offers high

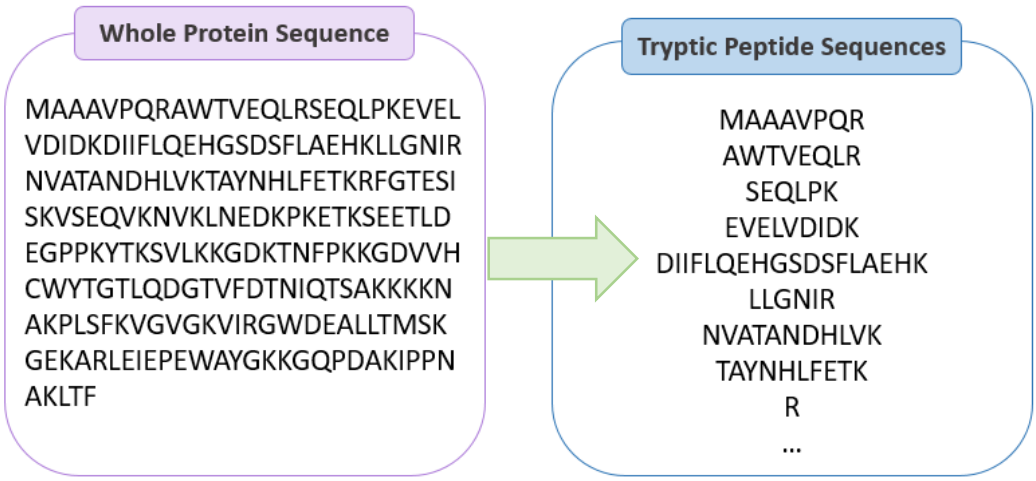

Figure 1.8 *Tryptic digestion of a representative protein in silico*

efficiency and specificity, and generates the peptides with optimal charge and length characteristics for MS/MS sequencing[93].

In order to infer the presence of a protein in a clinical sample and to quantify it, only a few representative peptides per protein are required. So, there are helpful empirical rules for the selection of the targeted peptides[74]. The peptides following the rules are called as "proteotypic" peptides:[74,94]

- The amino acid sequence of the targeted peptide must be *entirely unique to the targeted protein* within the biological system (in this case, human) in order to achieve the highest selectivity[95,96]. A BLASTp analysis is the most reliable way to confirm if a sequence is unique or shared with the other proteins[76,95].

- The characteristics of the targeted peptide must provide *good response in the MS* to achieve the highest sensitivity. The use of databases such as PeptideAtlas, spectral libraries or preliminary experimental results are helpful for the evaluation of signal intensity[94,96].

- Only peptides with complete tryptic cleavage should be selected, meaning internal lysine (K) or arginine (R) residues (miscleavege) are absent within the sequence. Additionally, they must not contain ragged ends, which are KK, RR, KR or RK[97]. These result in the generation of various forms of the same peptides due to the variations in digestion efficiency[95].

- The length of the selected peptides should be between 5-25 AAs to increase specificity and synthesis efficiency. Furthermore, the signals of the protonated small peptides (<5 AAs) might be overlapped by the solvent used in LC-MRM-MS analyses while long peptides (>25 AAs) might not have good ionization efficiency and fragmentation in MS/MS[95].

- Peptide sequences should not have the AA residues causing chemical modifications. For example, methionine (M) and tryptophan (W) has a tendency to oxidation while N-terminal glutamine (Q) is susceptible to cyclization to form pyroglutamate. In addition, the disulfide bonds form between cysteine (C) residues, which lead to generate insoluble aggregates in peptides[95,96].

- Peptides carrying post translational modifications (PTMs) should not be selected[96].

Following the selection rules above if it is feasible, at least two proteotypic peptides should be selected per protein to ensure robust quantification[97,98] SIL peptides analogous to the proteotypic peptides can be synthesized or purchased to be used in method development, optimization, and quantification[95].

- **SIL Peptides**

In general, SIL peptides are preferred as [^{13}C,^{15}N]-labeled peptides, and not [^{2}D]-labeled ones since the deuterated and non-deuterated peptides cannot co-elute in reversed phase liquid chromatography[95]. The [^{13}C,^{15}N]-labeled SIL peptides and endogeneous peptides co-elute and have a similar ionization efficiency, and MS/MS fragment pattern[27,75]. In targeted proteomics studies, the C-terminus K or R amino acid residues are labeled with ^{13}C and ^{15}N isotopes while the remaining AAs are in the natural forms due to providing consistent mass shift (Figure 1.9)[99-102].

The commercial SIL peptides can be produced according to the need of relative/absolute quantitative data[103]. In relative quantification, the abundance of proteins/peptides is defined as a relative term such as a fold change of peptide abundance in a diseased state compared to healthy state[75,104]. The absolute amount is unknown in relative quantification; however, absolute quantification determines the exact amount of proteins/peptides in the sample of interest[75,104]. For the absolute quantification, purified peptide standards with known concentration are used and

cost the range of €300-500 per peptide[99,105]. Unpurified peptides might be preferred for relative quantification, which costs the range of €10-50 per peptide[105]. Also, the use of unpurified peptides is optimal for the early-stage MRM method development since they are cheaper, faster to obtain, and sufficient for method optimization. Once the conditions are set, purified peptides are used for absolute quantification[105].

Additionally, spiking equimolar SIL peptide mixture into all samples within a batch, which improves precision and reproducibility, monitoring the instrument performance.[95].

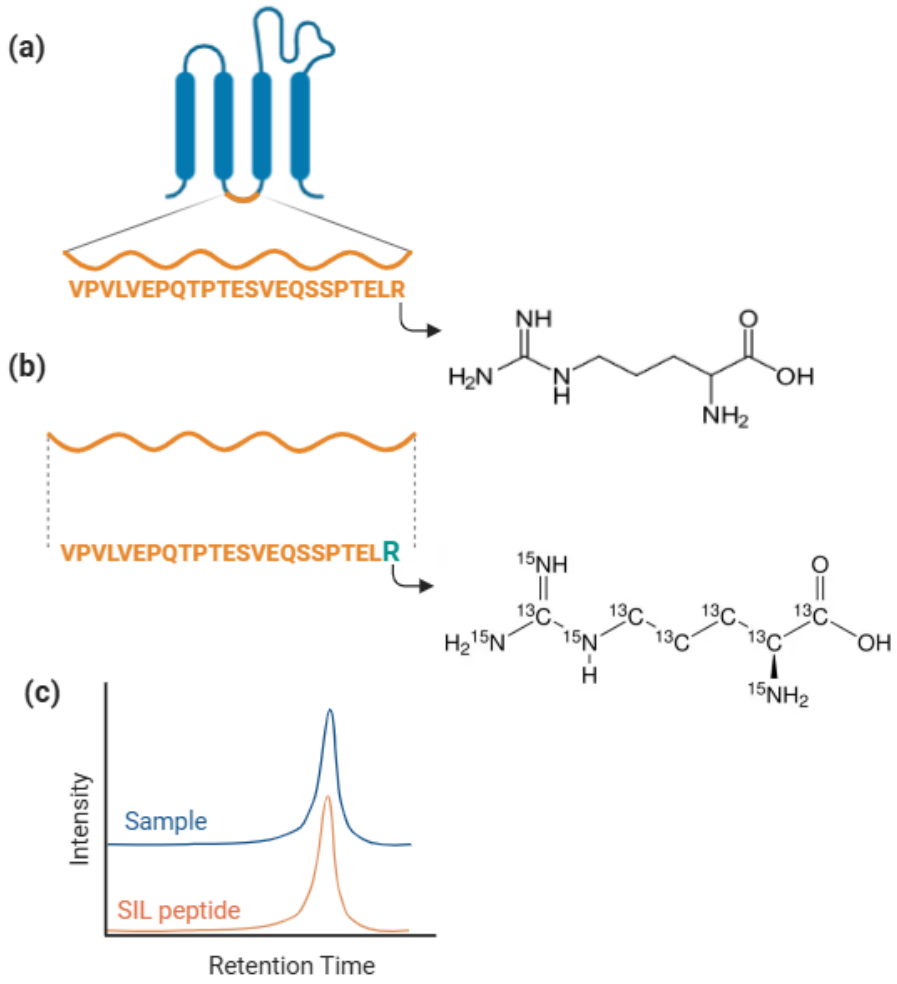

Figure 1.9 (a) *Endogenous peptide with C-terminal natural (light) Arginine* ***(b)*** *SIL peptide with C-terminal heavy Arginine with* $^{13}C_6$, $^{15}N_4$ ***(c)*** *Representation for co-elution of endogeneous peptide from sample and SIL peptide. Modified in BioRender.*

- **Selection of Precursor and Fragment Ions**

There are two factors affecting the MRM signal intensity: ionization and fragmentation conditions[74]. While ionization conditions are related to "precursor charge state" and "parameters of ESI", "fragment ion type" and "collision energy" is associated with fragmentation conditions[74].

ESI-MS analyses are performed in the positive ionization mode and peptides can exist in multiple charged forms during ionization[106], which are called as "precursor ions (or parent ions)":[107]

$$M + nH^+ \rightarrow (M + nH)^{n+}$$

(M=Peptide)

The first quadrupole isolates the specific precursor ion in accordance with its m/z setting[74]. The equation calculating the value of m/z as follows:

$$m/z = \frac{M_w + nH}{n}$$

(M_w=Molecular weight of peptide, H=1.00784 u)

An example is given for the precursor ions of "LISWYDNEFGYSNR" peptide in the Table 1.8 below.

Table 1.8 *The m/z values of LISWYDNEFGYSNR peptide in different charge states.*

Charged forms	**m/z values**
[M]	1762.7951
$[M+H]^+$	1763.8029
$[M+2H]^{2+}$	882.054
$[M+3H]^{3+}$	588.6062

It is an important step to determine the dominant precursor ion charge state of a peptide and the precursor ion giving the highest signal intensity should be selected to achieve the highest sensitivity[96].

The ionization process is supported by a voltage potential of ESI, which is needed to be optimized for the selection of optimum precursor charge state as shown in Figure 1.10[74,95]. If the voltage potential is too high, peptide fragmentation occurs in the source[74].

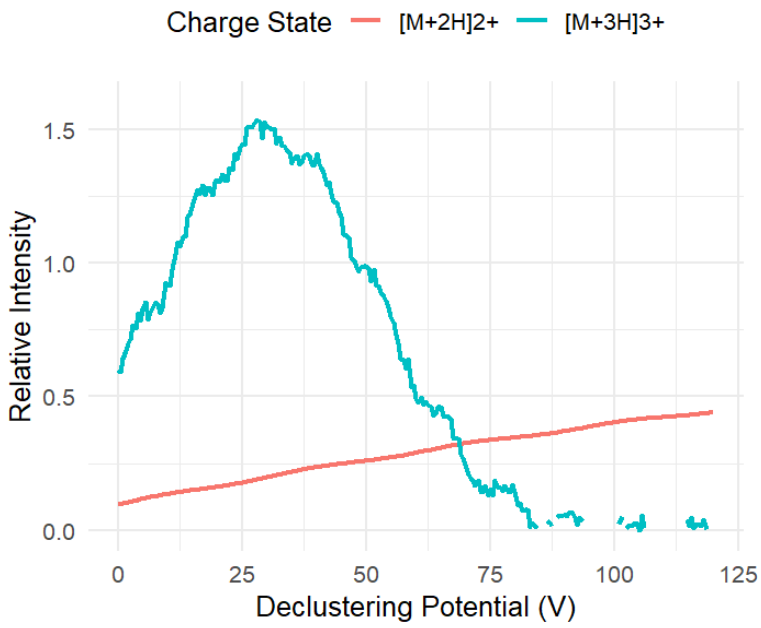

Figure 1.10 *Relative intensity of ions in different charge states with different voltage potential. Modified from Kuzyk, M. A.et al.*[95]

After the isolation of optimal precursor ion in the first quadrupole (Q1), fragmentation is performed in Q2[74] through collision-induced dissociation (CID) as following:[107]

$$(M + nH)^{n+} + N(gas) \rightarrow (M + nH)^{n+*} + N^{*} \rightarrow \text{fragments}$$

Several types of fragment ions of a peptide might arise during the fragmentation of the peptide bonds. The amino-terminal fragments (N→C) consist of a_n, b_n, and c_n ions, while carboxyl-terminal fragment ions (C→N) include x_n, y_n, and z_n[108]. The

primarily produced fragments are b_n and y_n ions due to the charge-driven mechanism[109].

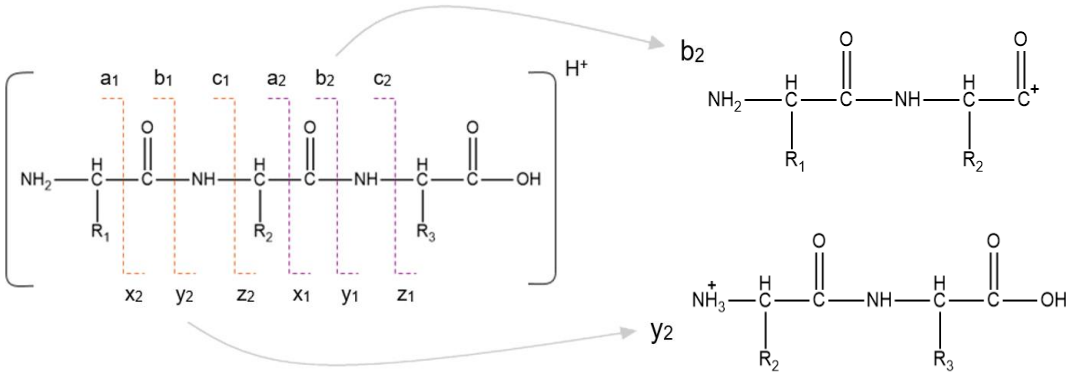

Figure 1.11 *Fragmentation of peptide backbone to obtain y- and b- ions. Modified from Amoresano, A., Carpentieri, A., Giangrande, C., Palmese, A., Chiappetta, G., Marino, G., & Pucci, P. (2009). Technical advances in proteomics mass spectrometry: Identification of post-translational modifications.*

Multiple y- and b- fragments can be derived by one precursor ion of a peptide and their intensities can be different from each other. In this case, it is important to select the most intense fragment ion to obtain a high sensitive MRM method[74,96]. The specific fragment ions are isolated by third quadrupole (Q3)[74].

The number of MRM transition, precursor/fragment (Q1/Q3) ion pair,[32] is limited per LC-MS run to be analyzed since the analysis of all transitions causes the analysis of limited number of peptides. Therefore, the number of fragment ions selected should be limited to 3 or 4[74].

The signal intensity of transitions is related to the collision energy (CE) voltage applied to the collision cell during CID in MS. Over- or under-fragmentation results in the decrease of signal intensity[110]. If the CE is lower than optimum value, fragmentation cannot occur;[111] however, the elevated value of CE causes over-fragmentation. So, there is a need to optimize CE values per transition[110].

Q1 and Q3 offers two stages of mass discrimination, which makes MRM transitions highly specific to the targeted peptides[112]. In addition to the mass filters, co-elution of SIL and endogeneous peptides contributes to achieve a high sensitive and specific analysis[95]. During co-elution of ion pairs derived from SIL and endogeneous peptides, it is essential to determine if they are interference-free for reliable quantitation. Spiking SIL peptide standards into digested sample, co-elution and presence of interference can be monitored in LC-MRM-MS analysis[75,95].

For the quantitative analysis of endogeneous peptides coming from biological sample, at least three and interference-free MRM transitions can be selected[113,114]. While MRM transition with the highest intensity (containing interference-free y fragment ion) is used for the quantitation, the other two transitions are used as "qualifier"[95,97]. The qualifier transitions provide the identification of biological sample if it contains a co-eluting interference. The final MRM assay involves three-four, interference-free transitions per a proteotypic peptide[95].

- **MRM Method Performance and Data Analysis**

The validation of bioanalytical methods, e.g. MRM, are performed according to some analytical guidelines such EMA[115] and FDA[116]. Those guidelines suggest that quality control (QC) samples must be involved during the analysis of bioanalytical methods. The QC samples facilitate the monitoring of method performance and validity of the results of unknown clinical samples[115,116]. In addition to method performance, proteolytic digestion efficiency can be monitored by the QC samples[117].

The determination of lower limit of quantification (LLOQ) and upper limit of quantification values represents a critical aspect of method development[115]. Accordingly, the construction of a calibration curve that spans the dynamic range of

the target protein is essential to enable accurate quantification in the clinical samples[115,116].

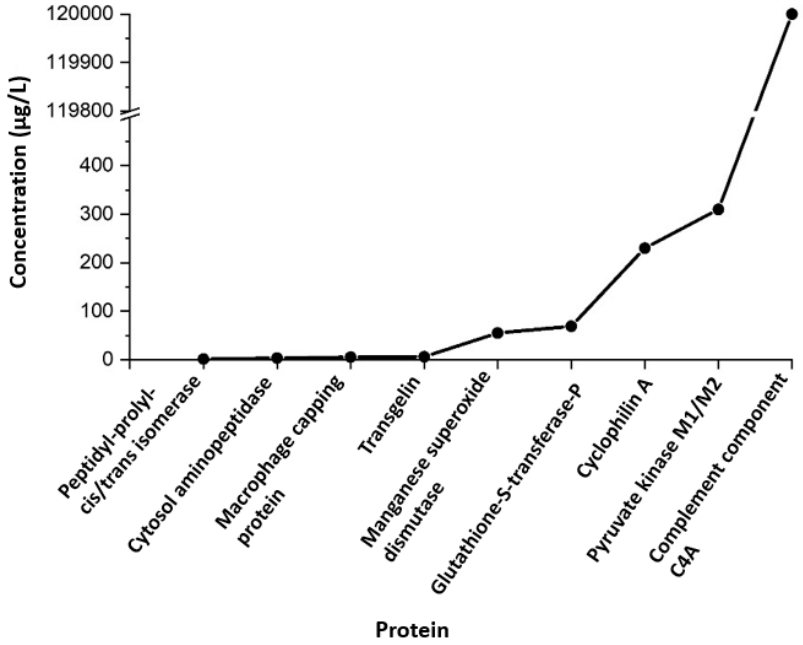

Figure 1.12 *Dynamic concentration range of targeted proteins in human plasma detected by MS. Retrieved and modified from proteinatlas.org.*

In Figure 1.12, the concentration of the targeted proteins in human plasma was illustrated, ranging from very low levels (e.g., peptidyl-prolyl-cis/trans isomerase at 1.3 µg/L) to extremely high levels (complement component C4A at 120,000 µg/L). This wide dynamic range highlights the importance of selecting appropriate concentration windows tailored to each targeted protein, especially when using multiplexed methods like MRM. Since different proteins exist in vastly different abundance levels within biological samples, each peptide/protein often requires separate optimization to ensure accurate quantification[115,116].

The chromatogram of each MRM transition per peptide is obtained as the output of LC-MRM-MS analyses. The data analysis comprises the integration of the interference-free precursor/fragment ion pair, and determination of peak area of the quantifier ion[95]. The integration of the peaks and extraction of peak area can be

carried out using available software from each vendor of QQQ-MS[95], or Skyline which is an open source and user-friendly software used for MRM data analyses[120]. The peaks can be integrated automatically; however, it is recommended to inspect the peaks manually in order to ensure if the correct one is integrated by software[121,122].

1.5 Statistical Analysis for Biomarker Performance

During LC-MRM-MS analyses, variability can occur due to the fluctuations in instrument signal, differences between injections, and inconsistencies in analyte recovery during sample preparation. The normalization of these variations is achieved by the ratio of peak area of endogeneous peptide to that of SIL peptide spiked in equal amount to the samples as internal standard[123]. The relative abundances of each protein/peptide across the clinical samples were compared using the normalized peak areas of endogenous peptides[100].

The statistical models visualize the comparison of the relative abundances between the conditions such as case-control or case-case with the Student's t-test.[121] A significant p-value given by the Student's t-test indicates if there is a statistically significant difference between the conditions. If the p-value is less than 0.05, the change in two conditions is statistically significant[124].

The receiver operating characteristic (ROC) curve is used to evaluate the diagnostic performance of a biomarker, which offers the values of sensitivity and 1-specificity. The ability to confirm the presence of the disease in a patient is known as "sensitivity (or true-positive results, TPR)" while "1-specificity (or false-positive result, FPR)" is the ability to confirm the absence of the disease in a patient[125]. The area under curve (AUC) of ROC is a measure for the performance of discrimination. The value of 0.5 for AUC give a diagonal line on ROC curve, which means that there is no discriminative property[125]. If the value of AUC is higher than 0.75, the performance of discrimination for biomarkers is good. Higher value of AUC than 0.90 is

considered as excellent discrimination[125,126]. The statistical outputs can be obtained using R software.

1.6 Motivation

Endometrial cancer is one of the most common gynecologic cancers with increasing incidence and mortality among women. Early detection and accurate risk stratification are critical to improve patient outcomes[1-3]. Proteomics offers a promising approach for the discovery of novel biomarkers that can aid in early detection of disease. MS-based proteomics provides robust analytical capabilities and in-depth understanding of protein changes. Among MS techniques, MRM-MS has emerged as a powerful tool for the biomarker verification. It effectively meets the need for a high-throughput, selective and reliable method to verify candidate biomarkers identified in discovery studies[25-27].

Nine proteins, namely transgelin (Q01995), peptidyl-prolyl cis-transisomerase (Q00688), cyclophilin A (P62937), macrophage capping protein (P40121), pyruvate kinase M1/M2 (P14618), glutathione S-transferase P (P09211), manganese-superoxide dismutase (P04179), cytosol aminopeptidase (P28838), and complement component C4A (P0C0L4), were selected as candidate biomarkers based on their potential relevance in PCOS and female malignancies such as ovary and breast cancer[53]. The motivation for this research originates from the need for the development of robust, reproducible, and sensitive methodology to verify these candidate protein biomarkers for EC. The verification of the candidate proteins confirms the molecular differences between sub-types of EC, and provides understanding of their distinct biological behaviors. Focusing on a significant panel of candidate proteins, this study aims to offer a clinically relevant path toward the clinical validation.

CHAPTER 2

MATERIALS & METHODS

2.1 Materials

2.1.1 Clinical Samples

This study was approved by Atatürk University, Faculty of Medicine, Clinical Research Ethics Committee (Approval No: B.30.2 .AT A.0.0 l .00/2.). All procedures involving human participants were conducted in accordance with the ethical standards of the institutional and/or national research committee and with the 1964 Helsinki Declaration and its later amendments.

The total of 69 fresh-frozen tissue samples (26 healthy-control, 23 EEC, and 20 NEC EC) were collected in the Ankara Memorial Hospital (Ankara, Turkiye). The diagnosis was confirmed under the microscope during routine frozen examination and the samples were included to the study after this examination. The demographic information such as age, smoking, hemoglobin, white blood cells, glucose was collected. In the study, control and cancer groups were matched according to menopausal status. A premenopausal patient with EC was matched to a premenopausal control whereas a postmenopausal patient with EC was matched to a postmenopausal control. Exclusion criteria were the use of antibiotics within last six-month, chemotherapy or radiotherapy, and steroid. In addition, pregnant women were not included.

2.1.2 Quality Control (QC) Samples

A total of 4 different QC samples were prepared by pooling all homogenized tissue samples, and which were then subjected to protein extraction and digestion. Then, equal amount of the mixture of SIL peptides described in Table 2.1 were spiked into QC samples.

a) 1 QC sample, called as MS-QC, was used to monitor possible errors and deviations that may occur during LC-MS analysis and to observe the performance of the MRM method. It was injected in every 30 runs corresponding to 1 day, which is total of four injections.

b) 3 different QC samples, called as EC-QC1, EC-QC2, EC-QC3, were used to monitor reproducibility of sample preparation. They were placed in a 96 well plate among the clinical samples, and injected once. EC-QC1 was also used for the screening of interferences.

2.1.3 Reagents for Protein Extraction and Proteolytic Digestion

Tris(hydroxymethyl)aminomethane (Tris), Sodium deoxycholate (SDC), Dithiothreitol (DTT) ve iodoacetamide (IAA) were obtained from Sigma-Aldrich (St. Louis, MO USA). Trypsin/Lys-C enzyme mixture was purchased from Promega (Madison, WI USA). Silent Crusher S Homogenizer was used to homogenize tissue samples and obtained from Heidolph Instruments (Schwabach, Germany). Bicinchoninic acid (BCA) assay was purchased from ThermoScientific Pierce (Waltham, MA, USA) to measure protein concentrations of tissue samples. The UV-Vis Spectrophotometer used for BCA assay was the Thermo Scientific Multiskan Skyhigh Microplate Spectrophotometer. Disposable scalpels and tweezers were used during the homogenization step. Clinical tissue samples and QC samples were transferred to 96-well plate. C18 SPE cartidges (Discovery® DSC-18 SPE Tube) were purchased from Merck (Darmstadt, Germany).

2.1.4 Chemicals and Standards for LC-MRM-MS Analysis

The development of the MRM method and analysis of clinical samples were performed by a Shimadzu LC-40 HPLC system coupled to a Shimadzu LCMS-8060 triple quad (QQQ) LC-MS/MS system (Kyoto, Japan). Data acquisition and processing were conducted by LabSolutions (v5.3). LC-MS grade water, acetonitrile, and formic acid were obtained from Merck (Darmstadt, Germany). Agilent AdvanceBio Peptide Mapping Column (2.1 x 150 mm, 2.7 microns) reversed-phase column was purchased from Agilent (Santa Clara, CA). Heavy [$^{13}C_6$, $^{15}N_2$]-lysine (K*) or [$^{13}C_6$, $^{15}N_4$]-arginine (R*) labeled peptides (SpikeTides_L) were obtained from JPT Peptide Technologies (Berlin, Germany) in the lyophilized form.

2.2 Methods

2.2.1 Development of MRM Method

In this study, the previously discovered nine proteins in the litearure[53] were selected for the verification phase.

- **Peptide Selection for Target Proteins**

Unique peptides corresponding to the nine target proteins, transgelin (Q01995), peptidyl-prolyl cis-transisomerase (Q00688), cyclophilin A (P62937), macrophage capping protein (P40121), pyruvate kinase M1/M2 (P14618), glutathione S-transferase P (P09211), manganese-superoxide dismutase (P04179), cytosol aminopeptidase (P28838), and complement component C4A (P0C0L4) were selected as described below. Stable isotopic labeled (SIL) peptides were purchased for use in method development and the semi-quantitative comparison of clinical samples.

To illustrate the peptide selection procedure, one representative protein, transgelin (Q01995) was selected. The same procedure was then applied to all other target proteins. First, the protein sequences were obtained from UniProt as FASTA files (Figure 2.1).

```
        10         20         30         40         50         60
MANKGPSYGM SREVQSKIEK KYDEELEERL VEWIIVQCGP DVGRPDRGRL GFQVWLKNGV

        70         80         90        100        110        120
ILSKLVNSLY PDGSKPVKVP ENPPSMVFKQ MEQVAQFLKA AEDYGVIKTD MFQTVDLFEG

       130        140        150        160        170        180
KDMAAVQRTL MALGSLAVTK NDGHYRGDPN WFMKKAQEHK REFTESQLQE GKHVIGLQMG

       190        200
SNRGASQAGM TGYGRPRQII S
```

Figure 2.1 *The protein sequence of transgelin (Q01995)*

Then, the protein sequence was subjected to in-silico tryptic digestion, cleaving the C-terminal lysine (K) and arginine (R) residues using Trypsin/LyC enzyme using Expasy PeptideCutter, as specified in Table 2.2.

Table 2.1 *Tryptic peptides of transgelin protein by Expasy PeptideCutter*

Transgelin (Q01995)			
Position of cleavage site	**Resulting peptide sequence**	**Peptide length [AA]**	**Peptide mass [Da]**
4	MANK	4	462.565
12	GPSYGMSR	8	853.948
17	EVQSK	5	589.646
20	IEK	3	388.464
21	K	1	146.189
29	YDEELEER	8	1082.089
47	LVEWIIVQCGPDVGRPDR	18	2052.379
49	GR	2	231.255
57	LGFQVWLK	8	990.213

Table 2.1 *Contiuned*

64	NGVILSK	7	729.875
78	LVNSLYPDGSKPVK	14	1516.758
89	VPENPPSMVFK	11	1244.471
99	QMEQVAQFLK	10	1221.437
108	AAEDYGVIK	9	965.071
121	TDMFQTVDLFEGK	13	1530.713
128	DMAAVQR	7	789.905
140	TLMALGSLAVTK	12	1204.491
146	NDGHYR	6	760.764
154	GDPNWFMK	8	994.133
155	K	1	146.189
160	AQEHK	5	611.655
161	R	1	174.203
172	EFTESQLQEGK	11	1295.368
183	HVIGLQMGSNR	11	1211.404
197	GASQAGMTGYGRPR	14	1408.555
201	QIIS	4	459.543

After determining the tryptic peptides, the rules given in Chapter 1.5.3 are followed for the selection. The tryptic peptides with <5 and >25 AAs were eliminated among them. The uniqueness of the remaining tryptic peptides was analyzed using BLASTp with the default parameters. The peptides which are not shared with the other human proteins were marked, as given in Table 2.2.

Among all unique peptides, the peptides with reactive amino acids (such as cysteine and methionine), known PTMs, and miscleavage were not prioritized; however, some were not excluded. Since the selection criteria contains the peptides providing good and high response, public data repositories such as PeptideAtlas were reviewed. In addition, preliminary orbitrap MS data were utilized to support peptide selection. One EEC and one healthy tissue sample were analyzed using orbitrap MS. Among

the unique peptides, those exhibiting the highest signal intensities were selected. Even though TDMFQTVDLFEGK and TLMALGSLAVTK peptides have methionine, and LVNSLYPDGSKPVK peptide has miscleavage, they prove intense signals.

Table 2.2 *Unique peptides representing transgelin protein*

Unique peptide sequence	Peptide length [AA]	Orbitrap MS data signal (in Healthy Tissue)	Orbitrap MS data signal (in EEC Tissue)
YDEELEER	8	8.732.100	69.595.000
LVEWIIVQCGPDVGRPDR	18	not found	not found
LGFQVWLK	8	21.137.000	0
LVNSLYPDGSKPVK	14	134.419.000	15.569.000
VPENPPSMVFK	11	not found	27.235.000
QMEQVAQFLK	10	21.139.000	not found
AAEDYGVIK	9	0	0
TDMFQTVDLFEGK	13	134.913.000	60.270.000
TLMALGSLAVTK	12	128.435.000	not found
GDPNWFMK	8	not found	not found
EFTESQLQEGK	11	68.761.000	59.763.000
HVIGLQMGSNR	11	not found	not found
GASQAGMTGYGRPR	14	not found	10.308.000

As a result, two or three proteotypic peptides per protein were selected following the steps above, and total of twenty-three peptides were determined for the MRM analyses, as presented in Table 2.3.

Table 2.3 *The list of twenty-three SIL peptides*

Proteins	UniProt ID	Peptide Sequence	C-term	Mw (average, Da)	Purity by HPLC-MS
Transgelin	Q01995	LVNSLYPDGSKPVK	K*	1524.67957	48.7%
		TDMFQTVDLFEGK	K*	1538.63987	-
		TLMALGSLAVTK	K*	1212.42253	-
Peptidyl-Prolyl Cis-Transisomerase	Q00688	DHLVTAYNHLFETK	K*	1695.79201	-
		LEIEPEWAYGK	K*	1342.41509	-
Cyclophilin A	P62937	FEDENFILK	K*	1162.21131	-
		EGMNIVEAMER	R*	1288.38514	-
Macrophage Capping Protein	P40121	YQEGGVESAFHK	K*	1359.36279	-
		VSDATGQMNLTK	K*	1272.34861	-
		QAALQVAEGFISR	R*	1399.48546	-
Pyruvate Kinase M1/M2	P14618	LNFSHGTHEYHAETIK	K*	1891.95543	-
		DPVQEAWAEDVDLR	R*	1652.65054	-
		IYVDDGLISLQVK	K*	1470.62889	-
Glutathione S-Transferase P	P09211	MLLADQGQSWK	K*	1284.40391	58.1%
		AFLASPEYVNLPINGNGK	K*	1912.06941	-
Manganese-Superoxide Dismutase	P04179	AIWNVINWENVTER	R*	1753.84538	-
		HHAAYVNNLNVTEEK	K*	1746.79745	-
Complement Component C4A	P0C0L4	VLSLAQEQVGGSPEK	K*	1549.64443	-
		LVNGQSHISLSK	K*	1290.38865	-
		DSSTWLTAFVLK	K*	1375.48807	66.9%
Cytosol Aminopeptidase	P28838	ETLNISGPPLK	K*	1176,28271	65.1%
		AAGIDEQENWHEGK	K*	1591.55677	-
		TLIEFLLR	R*	1014.15280	-

- **Preparation of SIL Peptides**

The proteotypic peptides were purchased as their C-terminal amino acids labeled ([$^{13}C_6$, $^{15}N_2$]-lysine or [$^{13}C_6$, $^{15}N_4$]-arginine) as the lyophilized form in a 96-well plate, and stored at -20^{o}C. Those peptides were dissolved according to the protocol of JPT Peptide Technologies.

The peptides in a 96-well plate were stored at +4 ^{o}C for 1 hour before the process. A solution containing 80% (v/v) of 0.1 M ammonium bicarbonate and 20% (v/v) of acetonitrile (ACN) was prepared to solubilize them. Then, 220 µL of the prepared solution was added for each peptide. The plate was incubated at 60 rpm for 30 minutes at room temperature. After the incubation, it was centrifuged at 4000 rpm.

Each peptide was aliquoted as individual peptides and as a mixture containing equimolar 23 of SIL peptides. In the certificate of the peptides, their targeted amount was specified as 11 nmol/well with the purity of the range in 48.7% - 66.9%. Their stock concentration was determined as $5.0x10^{-5}$ µmol/µL (11 nmol/220 µL).

A mixture containing equimolar 23 SIL peptides was prepared in the concentration of $2.0x10^{-6}$ µmol/µL in order to develop an MRM method, and spiked into clinical tissue samples as internal standard after the proteolytic digestion.

- **Matrix-Matched Calibration Curve**

Matrix-matched calibration standards were prepared by spiking a mixture containing equimolar 23 SIL peptides into the matrix of endogeneous peptides to yield five levels ($1.0x10^{-8}$ – $2.0x10^{-7}$ µmol/µL).

- **Optimization of LC Conditions**

The reversed-phase C18 column (Agilent AdvanceBio Peptide Mapping Column (2.1 x 150 mm, 2.7 microns)) was incubated during the analysis in the oven at 40 ºC

in Shimadzu LC-40 HPLC system. The gradient elution was carried out to elute the peptides at the different times by using two mobile phases, which are aqueous phase (mobile phase A) and organic phase (mobile phase B). Mobile phase A was 0.1% formic acid in LC-MS grade water and mobile phase B was 0.1% formic acid in LC-MS grade ACN.

Since there are peptides having similar hydrophobicity calculated by Peptide Analyzing Tool of ThermoFisher Scientific, the optimization of LC conditions is important to reduce the overlapping, improving peak selectivity.

Table 2.4 *Hydrophobicity of the selected peptides*

Selected Peptides	**Hydrophobicity**
LVNSLYPDGSKPVK	24.77
TDMFQTVDLFEGK	37.77
TLMALGSLAVTK	33.10
DHLVTAYNHLFETK	34.04
LEIEPEWAYGK	28.72
FEDENFILK	30.04
EGMNIVEAMER	26.28
YQEGGVESAFHK	19.22
VSDATGQMNLTK	16.67
QAALQVAEGFISR	32.21
LNFSHGTHEYHAETIK	24.24
DPVQEAWAEDVDLR	34.10
IYVDDGLISLQVK	35.70
MLLADQGQSWK	26.77
AFLASPEYVNLPINGNGK	36.06
AIWNVINWENVTER	41.24
HHAAYVNNLNVTEEK	23.34

Table 2.4 *Contiuned*

VLSLAQEQVGGSPEK	23.37
LVNGQSHISLSK	19.49
DSSTWLTAFVLK	43.75
ETLNISGPPLK	25.29
AAGIDEQENWHEGK	18.20
TLIEFLLR	39.46

Considering the hydrophobicity of the peptides, the first gradient was adjusted as following:

(1) 0-20 min: %5 B to %40 B

(2) 20-30 min: %40 B to %50 B

(3) 30.0-30.1 min: %50 B to %5

(4) 30.1-40 min: %5 B

Their retention times were observed in the five different chromatograms (Figure 2.2-2.6) by creating five different MRM methods. Since many of the peptides eluted in a 7-11-minute window during the run, the final gradient was optimized as: (1) 0-4 min: %5 B to %15, (2) 4-9 min: %15 B, (3) 9-20 min: %15 B to %25 B, (4) 20-25 min: %25 B, (5) 25-30 min: %25 B to %55, (6) 30-35 min: %55 B, (7) 35-35.1 min: %55 B to %80 B, (8) 35.1-40 min: %80 B, (9) 40-40.1 min: %80 B to %5 B, and 10) 40.1-50 min: %5 B. A mixture of equimolar SIL peptides in the concentration of $2.0x10^{-5}$ µmol/µL was injected at the volume of 20 µL. The chromatograms were visualized from Figure 2.2 to Figure 2.6.

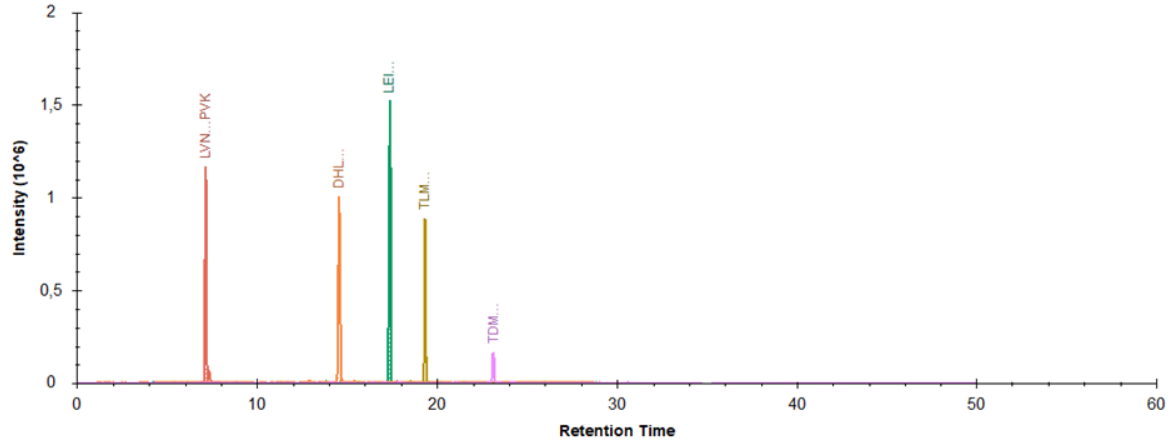

Figure 2.2 *The chromatogram of LVNSLYPDGSKPVK*, TDMFQTVDLFEGK*, TLMALGSLAVTK*, DHLVTAYNHLFETK* and LEIEPEWAYGK* peptides.*

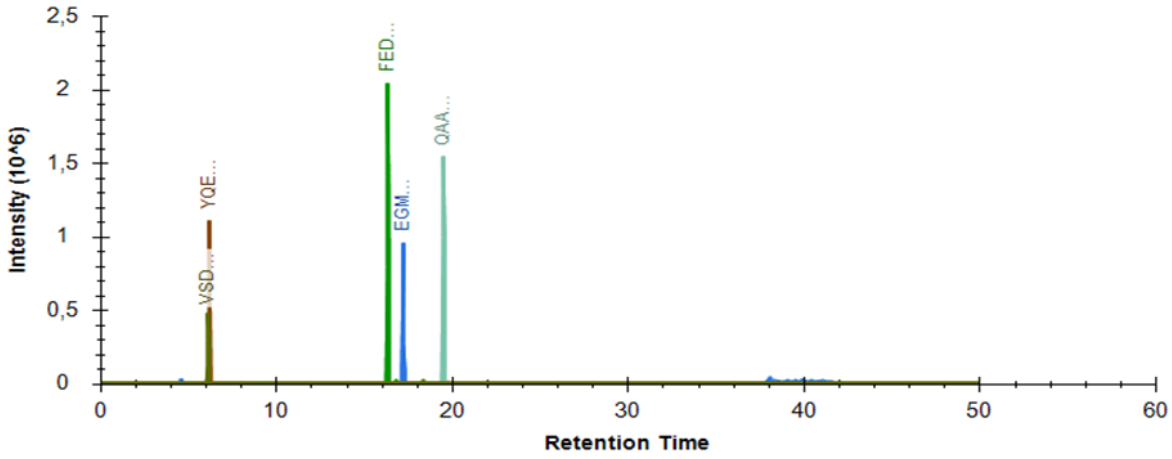

Figure 2.3 *The chromatogram of QAALQVAEGFISR*, VSDATGQMNLTK*, YQEGGVESAFHK*, FEDENFILK* and EGMNIVEAMER* peptides*

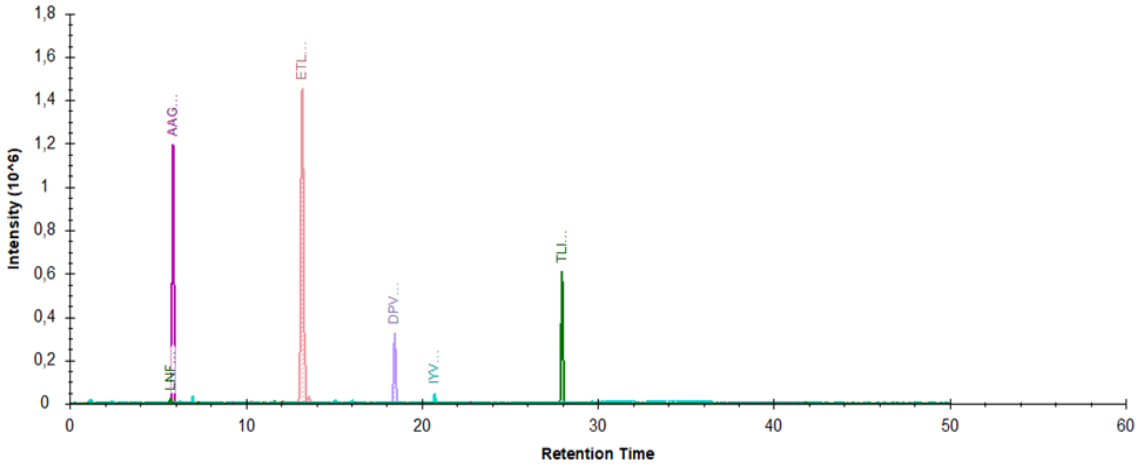

Figure 2.4 *The chromatogram of AAGIDEQENWHEGK*, TLIEFLLR*, ETLNISGPPLK*, LNFSHGTHEYHAETIK*, DPVQEAWAEDVDLR* and IYVDDGLISLQVK* peptides*

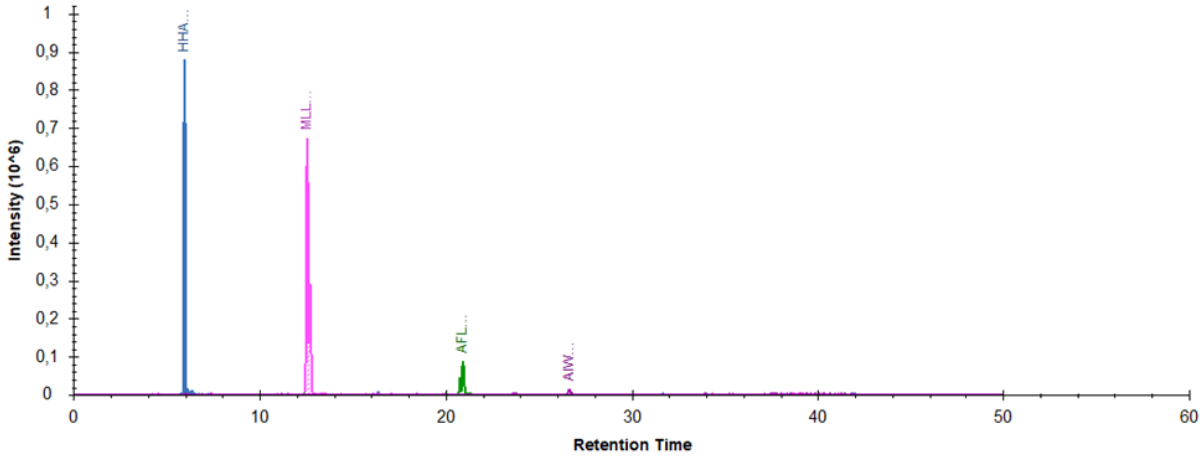

Figure 2.5 *The chromatogram of HHAAYVNNLNVTEEK*, MLLADQGQSWK*, AIWNVINWENVTER* and AFLASPEYVNLPINGNGK* peptides*

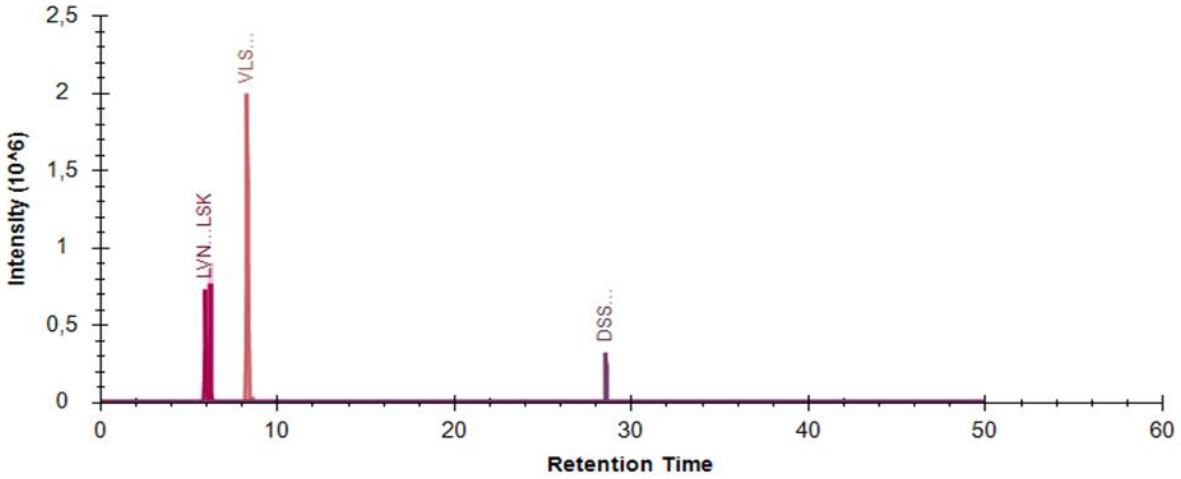

Figure 2.6 *The chromatogram of VLSLAQEQVGGSPEK*, LVNGQSHISLSK* and DSSTWLTAFVLK* peptides*

Once the retention time for each peptide was determined, as presented in Table 2.5, and an MRM method was developed including all peptides to enable simultaneous monitoring during sample analysis.

Table 2.5 *The retention times of the selected peptides*

Proteotypic Peptide Sequences	**Retention Time (min)**
LVNSLYPDGSKPVK	6.9
TDMFQTVDLFEGK	22.4
TLMALGSLAVTK	18.8
LNFSHGTHEYHAETIK	5.7
DPVQEAWAEDVDLR	17.9
IYVDDGLISLQVK	20.2
QAALQVAEGFISR	19.0
VSDATGQMNLTK	6.0
YQEGGVESAFHK	6.1

Table 2.5 *Contiuned*

MLLADQGQSWK	11.2
AFLASPEYVNLPINGNGK	20.4
AAGIDEQENWHEGK	5.8
TLIEFLLR	26.6
ETLNISGPPLK	12.0
DHLVTAYNHLFETK	13.8
LEIEPEWAYGK	16.8
FEDENFILK	15.8
EGMNIVEAMER	16.6
VLSLAQEQVGGSPEK	7.9
LVNGQSHISLSK	5.9
DSSTWLTAFVLK	28.4
HHAAYVNNLNVTEEK	5.9
AIWNVINWENVTER	24.9

- **Optimization of ESI-MS Conditions**

After the separation of the proteotypic peptides in the LC system, those are introduced to ESI, followed by the QQQ-MS system. ESI was adjusted to positive (+) mode and MS was set to MRM mode. Each peptide was analyzed in 1-min RT window at a unit resolution. MS parameters were tested for the high sensitive and selective analysis and, final MS parameters were determined below (Table 2.6).

Table 2.6 *The optimized parameter of ESI-MS*

Temperature of Interface (°C)	300
Temperature of Desolvation Line (°C)	260
Temperature of Heater Block (°C)	400
Flow Rate of Nebulizing Gas (L/min)	3.0
Flow Rate of Heating Gas (L/min)	10
Flow Rate of Drying Gas (L/min)	10
Collision Energy (V)	442.3 - 1337.7

Q1 and Q3 were programmed for the selection of MRM transitions (precursor/fragment ion pair) per peptide.

- **Selection of Precursor Ions**

ESI-MS in the positive ionization mode enables to exist in the formation of multiple charged species, which are called as precursor ions[106,107] since peptides contain multiple proton-accepting (basic) sites such as the side chains of L, R, and histidine (H)[127].

The precursor ions with high signal intensity should be selected for the development of a highly sensitive MRM method. Skyline software (v.2.1.1.0) helps in visualizing and filtering precursor/fragment pair of peptides[95].

For example, TLMALGSLAVTK* peptide is one of the proteotypic peptides representing transgelin protein. Its m/z values with (+2) and (+3) charge states calculated are 606.86 and 404.91, respectively. In full windows scan of MRM mode, it was observed that the signal intensity of m/z value of 606.86 value was nearly 100 times higher than that of 404.91 value, as presented in Figure 2.7.

a)

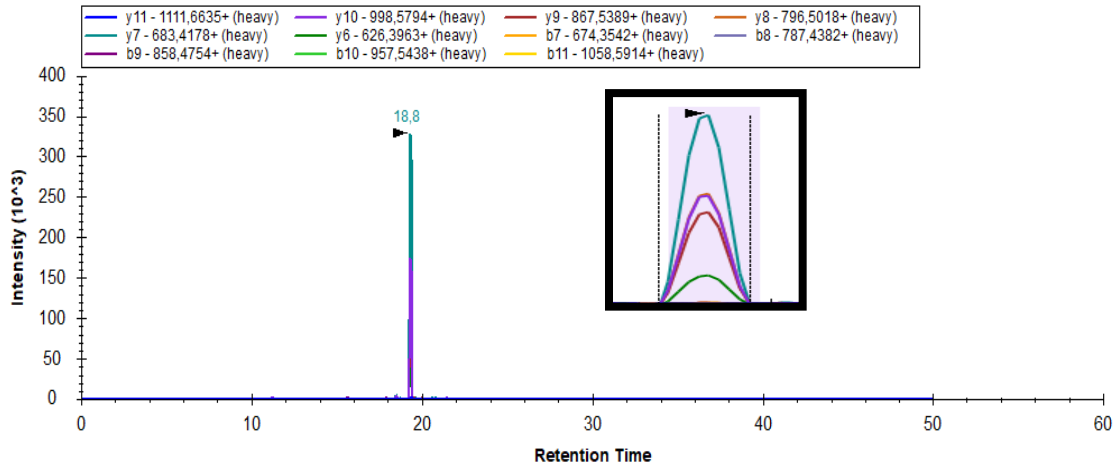

b)

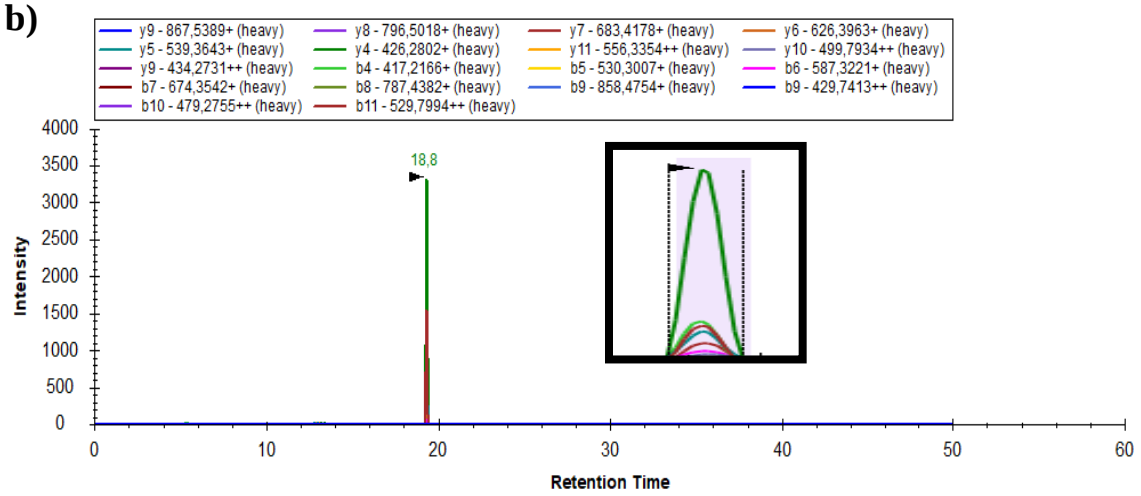

Figure 2.7 *The signal intensities of the m/z values of (a) 606.86 and (b) 404.91 corresponding to (+2) and (+3) charges states of TLMALGSLAVTK* peptide in MRM mode, respectively. Injected sample was the mixture of equimolar SIL peptides in the concentration of* $2.0x10^{-5}$ *µmol/µL. Injection volume was 20 µL.*

As a result, the precursor ion with (+2) charge state was selected for TLMALGSLAVTK* peptide. The precursor ions for each peptide were determined following the same steps (Table 2.7).

Table 2.7 *The selected precursor ions per the selected peptide*

Peptide Sequence	Precursor Ion for SIL peptides (m/z)	Charge State
LVNSLYPDGSKPVK*	508.96	+3
TDMFQTVDLFEGK*	769.87	+2
TLMALGSLAVTK*	606.86	+2
LNFSHGTHEYHAETIK*	631.31	+3
DPVQEAWAEDVDLR*	551.60	+3
IYVDDGLISLQVK*	735.92	+2
QAALQVAEGFISR*	700.38	+2
VSDATGQMNLTK*	636.82	+2
YQEGGVESAFHK*	453.89	+3
MLLADQGQSWK*	642.83	+2
AFLASPEYVNLPINGNGK*	638.01	+3
AAGIDEQENWHEGK*	531.24	+3
TLIEFLLR*	507.81	+2
ETLNISGPPLK*	588.84	+2
DHLVTAYNHLFETK*	565.96	+3
LEIEPEWAYGK*	671.84	+2
FEDENFILK*	581.80	+2
EGMNIVEAMER*	644.80	+2
VLSLAQEQVGGSPEK*	775.42	+2
LVNGQSHISLSK*	430.91	+2
DSSTWLTAFVLK*	688.37	+2
HHAAYVNNLNVTEEK*	582.96	+3
AIWNVINWENVTER*	585.30	+3

- **Selection of Fragment Ions**

Since y- and b- fragment ions are commonly used in proteomics studies, the selection of transitions was carried out among y- and b- ions. The recommendation is to determine at least three and interference-free transitions[113,114].

The most intense fragment ions of TLMALGSLAVTK* peptide with (+2) charge state were selected for the quantitative analysis. The most intense peaks were filtered, which are y7, y10 and y9 in descending order, as presented in Figure 2.8. Because the most intense peak was y7, it was determined as "quantifier". The other peaks were called as "qualifier", which ensures the specificity.

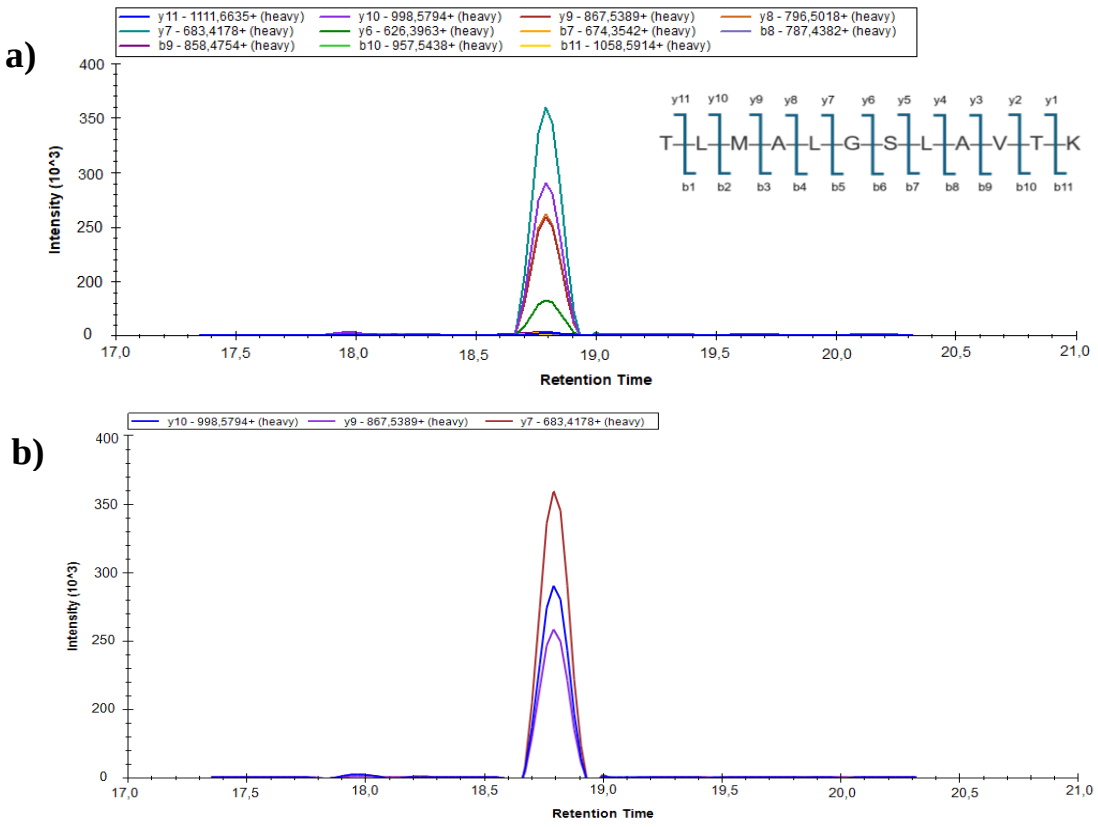

Figure 2.8 *MRM transitions of TLMALGSLAVTK* peptide with (+2) charge state (a) before filtering (b) after filtering. Injected sample was the mixture of equimolar SIL peptides in the concentration of 2.0x10^{-5} µmol/µL. Injection volume was 20 µL.*

The selected ions were isolated in both Q1 and Q3 using unit resolution. The fragmentation of the selected peptides was performed in Q2 using peptide specific collision energies as specified in Table 2.8.

Table 2.8 *The parameters of the developed MRM method. In fragment ions, (+) and (++) denote the ion's electrical charge, specifically how many positive charges it carries.*

Peptide Sequence	**Precursor Ion (m/z)**	**Fragment Ion (y, b)**	**Fragment Ion (m/z)**	**Collision energy (V)**
LVNSLYPDGSKPVK*	508.96	y8 y12 y11	835.4763+ 656.8530++ 599.8315++	17.9
TDMFQTVDLFEGK*	769.87	y10 y9 y8 y7	1191.6136+ 1044.5452+ 916.4866+ 815.4389+	30.1
TLMALGSLAVTK*	606.86	y7 y10 y9	683.4178+ 998.5794+ 867.5389+	23.6
LNFSHGTHEYHAETIK*	631.31	y15 y14 y13 y12	889.9204++ 832.8990++ 759.3648++ 715.8488++	22.4
DPVQEAWAEDVDLR*	551.60	y7 y6 y5 b6	827.4133+ 756.3762+ 627.3336+ 640.2937+	19.4
IYVDDGLISLQVK*	735.92	y11 y10 y9 y8	1194.6820+ 1095.6136+ 980.5866+ 865.5597+	28.8

Table 2.8 *Contiuned*

QAALQVAEGFISR*	700.38	y9 y8 y7 y6	1016.5399+ 888.4813+ 789.4129+ 718.3758+	27.3
VSDATGQMNLTK*	636.82	y11 y10 y8 y7	1173.5660+ 1086.5339+ 900.4699+ 799.4222+	24.8
YQEGGVESAFHK*	453.89	y5 y10 b5 b10	597.3235+ 534.7636++ 535.2147+ 534.7353++	15.9
MLLADQGQSWK*	642.83	y9 y8 y7 y6	1040.5251+ 927.4410+ 856.4039+ 741.3770+	25.0
AFLASPEYVNLPINGNGK*	638.01	y13 b7 b8 b10	11.8770++ 716.3614+ 879.4247+ 1092.5360+	22.7
AAGIDEQENWHEGK*	531.24	y13 y12 y10 y9	760.8464++ 725.3279++ 640.2751++ 582.7616++	18.7
TLIEFLLR*	507.81	y6 y5 y4	800.4904+ 687.4064+ 558.3638+	19.6

Table 2.8 *Contiuned*

ETLNISGPPLK*	588.84	y8 y7 y6	833.4971+ 719.4542+ 606.3701+	22.9
DHLVTAYNHLFETK*	565.96	y5 y12 y11 b12	645.3698+ 722.3897++ 665.8477++ 720.8490++	20.0
LEIEPEWAYGK*	671.84	y9 y8 y7	1100.5502+ 987.4662+ 858.4236+	26.2
FEDENFILK*	581.80	y8 y7 y6 y5	1015.5186+ 886.4760+ 771.4491+ 642.4065+	22.6
EGMNIVEAMER*	644.80	y8 y7 y6	971.4854+ 857.4425+ 744.3584+	25.1
VLSLAQEQVGGSPEK*	775.42	y13 y11 y10 y9	1337.6787+ 1137.5626+ 1066.5255+ 938.4669+	30.3
LVNGQSHISLSK*	430.91	y4 y10 y9	442.2751+ 539.7902++ 482.7687++	15.0
DSSTWLTAFVLK*	688.37	y10 y9 y8 y7	1173.6758+ 1086.6437+ 985.5961+ 799.5168+	26.9

Table 2.8 *Contiuned*

HHAAYVNNLNVTEEK*	582.96	y7 y6 b6 b7	840.4553+ 727.3712+ 679.3311+ 793.3740+	20.6
AIWNVINWENVTER*	585.30	y6 y5 b5 b6	757.3714+ 628.3288+ 584.3191+ 697.4032+	20.7

- **Interference Screening**

Prior to finalizing the method, it is essential to assess the co-elution of SIL and endogeneous peptides, and potential interferences. EC-QC1 sample, including endogeneous and SIL peptides as described in 2.2, was analyzed by the developed MRM method for the screening of interferences.

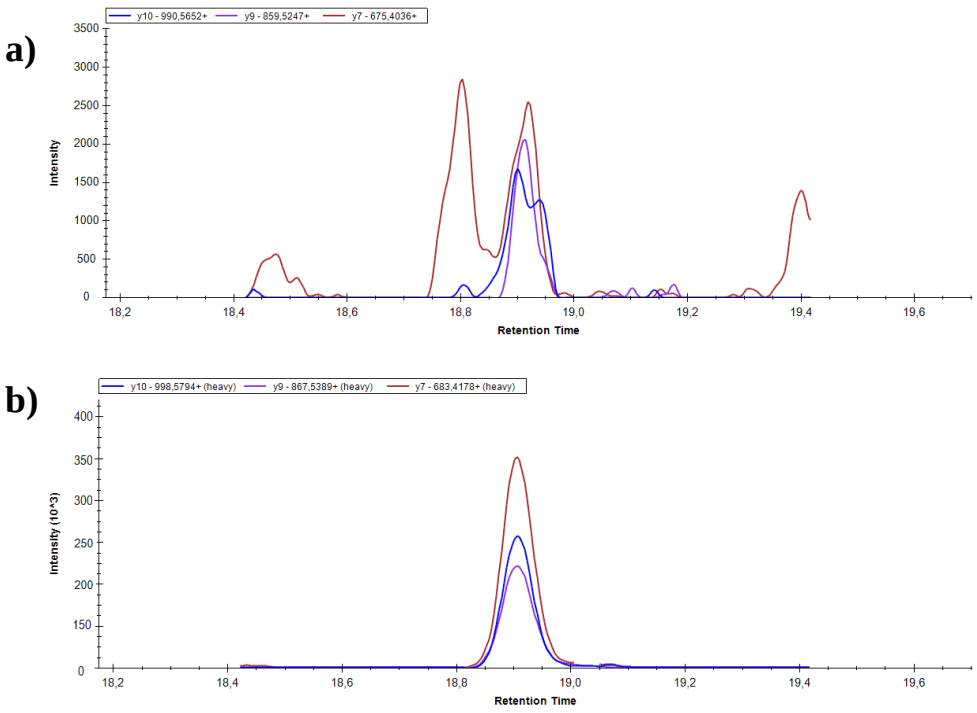

Figure 2.9 *MRM transitions of (a) endogenous TLMALGSLAVTK peptide (b) SIL TLMALGSLAVTK* peptide in EC-QC1 samples. Injection volume was 20 µL.*

The SIL and endogeneous forms of TLMALGSLAVTK peptides were co-eluted; however, the signal intensity of endogeneous was lower than that of SIL peptide and its quality of peak shape was poor, as presented in Figure 2.9.

For the other proteotypic peptide of transgelin protein, LVNSLYPDGSKPVK, both forms were co-eluted and their transitions were interference-free, as shown in Figure 2.10. Therefore, LVNSLYPDGSKPVK peptide was determined as representing peptide for transgelin protein to achieve high sensitive and specific quantification.

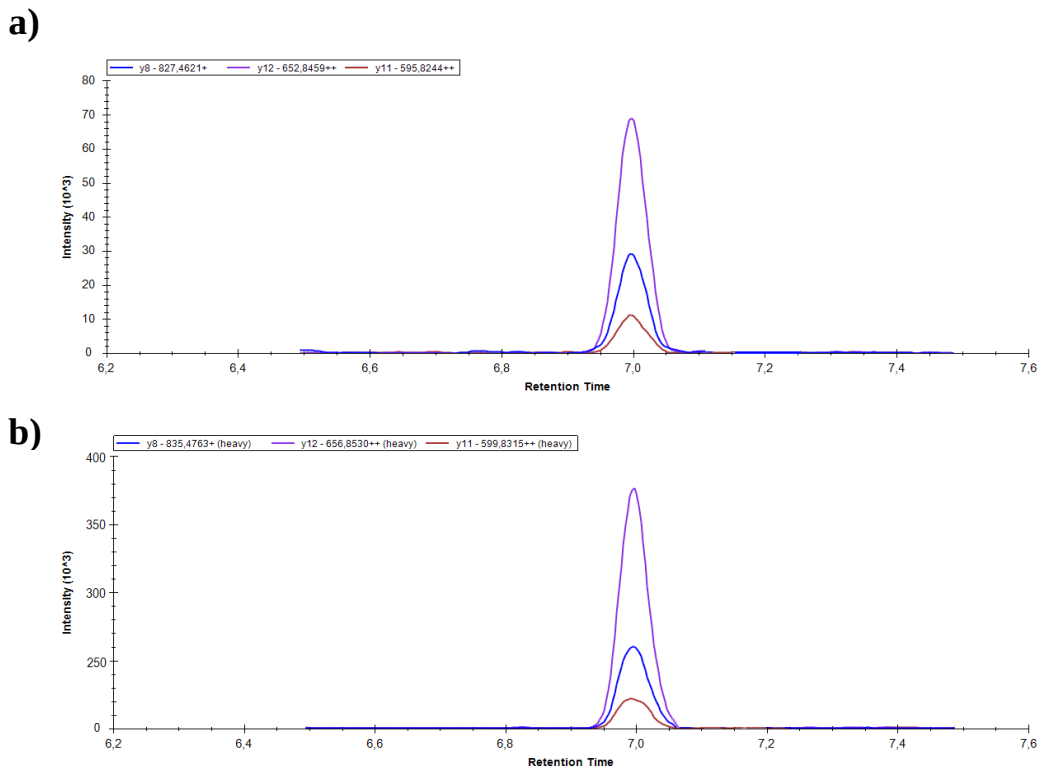

Figure 2.10 *Confirmation of co-elution and interference-free MRM transitions representing (a) endogeneous and (b) SIL of LVNSLYPDGSKPVK peptide representing transgelin protein in EC-QC1 sample. The injection volume was 20 µL.*

Finally, a single peptide exhibiting interference-free and highly sensitive transitions was selected for each protein and presented in Table 2.9.

Table 2.9 *The representative peptides of the candidate proteins from the finalized MRM method*

Candidate Proteins	Representative Peptides
Transgelin	LVNSLYPDGSKPVK
Pyruvate Kinase M1/M2	IYVDDGLISLQVK
Macrophage Capping Protein	QAALQVAEGFISR
Glutathione-S-Transferase-P	MLLADQGQSWK
Leucine Aminopeptidase	AAGIDEQENWHEGK
Peptidyl-prolyl-cis/transisomerase	LEIEPEWAYGK
Cyclophilin A	FEDENFILK
Complement Component C4A	DSSTWLTAFVLK
Mangenese Superoxide Dismutase	HHAAYVNNLNVTEEK

- **Assessment of MRM Method**

MS-QC was used to monitor the deviations in the signal intensities, which includes the endogeneous peptides of pooled all clinical samples and SIL peptides mixture. MS-QC sample was injected in the same volume once in 30 runs. During the analysis, MS-QC was in the autosampler at +4 °C. The instrument stability was evaluated using the ratio of endogeneous/SIL (L/H) peptide as presented in Figure 2.11. The instrument stability was calculated by the percentage of coefficient of variation (CV%). The instrument stability (CV%: 0.3% - 17.7%) was in accordance with the criteria in the EMA guideline[115] as shown in Figure 2.12. QAALQVAEGFISR peptide presented the lowest variation while AAGIDEQENWHEGK peptide showed the highest variation.

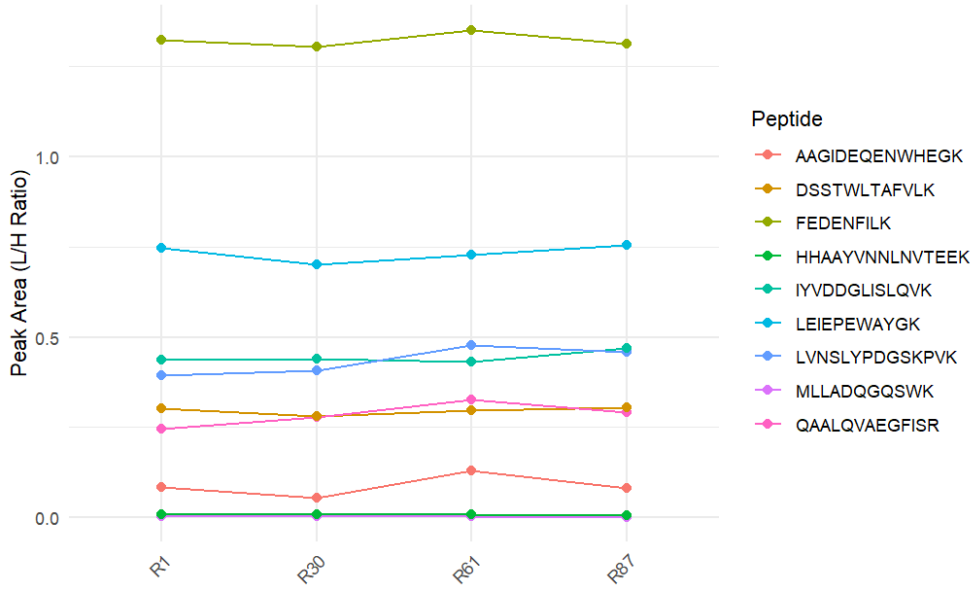

Figure 2.11 *The instrument stability of MS-QC using the ratio (L/H) normalization. MS-QC was injected once every 30 runs (N=4). Each batch of 30 runs corresponds to 1-day of analysis.*

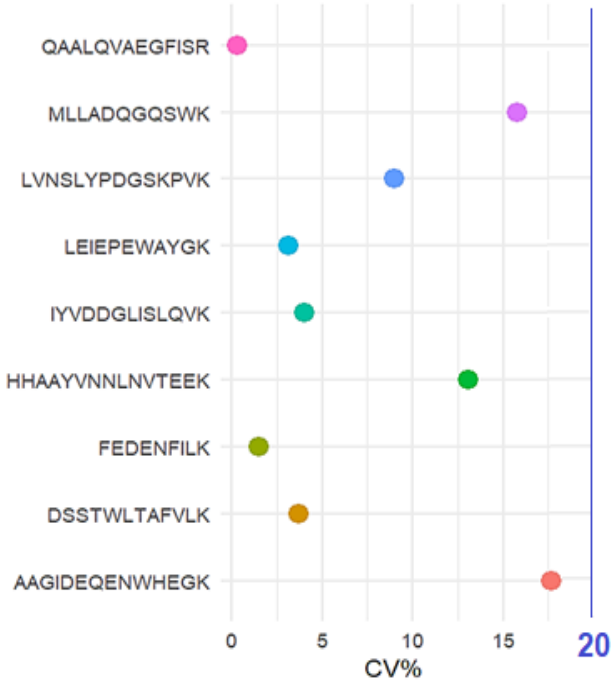

Figure 2.12 *The instrument stability calculated by CV% for each peptide (CV% = 0.3–15.8%).*

Matrix-matched calibration curves for each peptide were prepared in the matrix of endogeneous peptides. Each calibrator was analyzed in single replicate to save run time (50 min per run) and sample volume by following EMA bioanalytical method guideline[115]. The calibration curves and LOD values were generated by Skyline, as presented in Figure 2.13. The LOD value was calculated by adding 3 times the standard deviation of the signal obtained from blank samples to the mean of the blank samples' signals:

$$S_m = S_{blank} + 3 \times s_{blank}$$

S_m: minimum detectable signal, S_{blank}: average of blank signals,

s_{blank}: standard deviation of blank signals

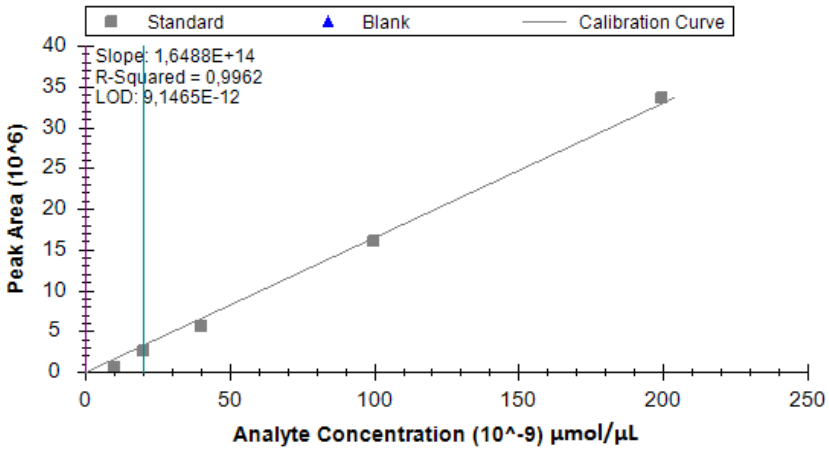

Figure 2.13 *The matrix-matched calibration curve of FEDENFILK peptide generated by Skyline*

As a result, LOD values and linearity were determined for each peptide, as presented in Table 2.10.

Table 2.10 *The values of LOD and R^2 calculated by Skyline*

Proteotypic Peptide	**LOD (µmol/µL)**	**Linearity (R^2)**
LVNSLYPDGSKPVK	3.6×10^{-10}	0.9992

Table 2.10 *Contiuned*

IYVDDGLISLQVK	1.5×10^{-9}	0.9796
QAALQVAEGFISR	6.3×10^{-11}	0.9958
MLLADQGQSWK	2.0×10^{-10}	0.9981
AAGIDEQENWHEGK	6.7×10^{-10}	0.9965
LEIEPEWAYGK	9.1×10^{-12}	0.9962
FEDENFILK	5.1×10^{-10}	0.9978
DSSTWLTAFVLK	3.0×10^{-9}	0.9972
HHAAYVNNLNVTEEK	5.0×10^{-10}	0.9985

2.2.2 Preparation of Clinical Samples

- **Protein Extraction and Tryptic Digestion**

Sample preparation was adapted from the Filter-Aided Sample Preparation (FASP) protocol[128]. Frozen tissue samples were thawed at +4 ºC for 2-3 hours in 1.5 mL of microcentrifuge tubes. The blood-contaminated tissue samples were cleaned with saline (NaCl 0.9%). The tissue sample was finely minced using a scalpel on a glass plate placed on dry ice. A 800 µL of 100 mM Tris-HCl (pH 7.6) was added into the tube and homogenized with a Silent Crusher S Homogenizer (Heidolph). Total protein concentrations of all homogenized tissue samples were analyzed by Pierce BCA Protein Assay Kit (MAN0011430), as presented in Table 2.11-2.13.

Table 2.11 *Total protein concentration (µg/µL) of the homogenized tissue samples of healthy group (N=26) (T: Tissue).*

T3	1.4	**T24**	2.1	**T46**	0.8	**T62**	3.4
T7	1.2	**T26**	0.7	**T49**	3.7	**T66**	2.1
T10	2.5	**T28**	3.1	**T51**	1.7	**T71**	1.9
T12	2.4	**T30**	0.8	**T54**	3.0	**T73**	1.7
T14	1.4	**T34**	0.9	**T56**	2.7	**T76**	1.7
T16	1.0	**T36**	1.4	**T58**	1.9		
T21	1.0	**T40**	1.4	**T59**	1.2		

Table 2.12 *Total protein concentration (µg/µL) of the homogenized tissue samples of EEC group (N=23) (T: Tissue)*

T2	2.6	**T22**	1.7	**T50**	1.1	**T79**	2.5
T5	1.8	**T32**	1.2	**T53**	3.3	**T80**	1.3
T6	1.9	**T37**	3.5	**T65**	1.8		
T8	3.8	**T39**	1.4	**T68**	2.0		
T15	1.6	**T42**	2.0	**T72**	2.7		
T17	2.6	**T44**	1.5	**T74**	1.9		
T20	1.1	**T47**	1.7	**T77**	2.4		

Table 2.13 *Total protein concentration (µg/µL) of the homogenized tissue samples of NEC group (N=20) (T: Tissue)*

T4	2.1	**T33**	3.7	**T61**	2.9
T11	3.5	**T35**	2.5	**T63**	1.9
T13	2.9	**T41**	2.4	**T64**	0.9
T19	1.9	**T45**	2.4	**T67**	2.4
T23	0.9	**T48**	2.7	**T70**	1.7
T27	1.1	**T52**	2.1	**T75**	3.7
T31	1.9	**T55**	3.5		

The total protein amount of all homogenized tissue samples is normalized to 250 µg and transferred to a 96-well plate. A 50 µL of 4% SDC and 1 M DTT were added to all samples and incubated at 95 ^{o}C for 3 minutes. IAA was added to achieve a final concentration of 500 mM, followed by incubation for 30 min at room temperature in the dark. A 5 µL of Trypsin/LysC enzyme was added and incubated at 37 ^{o}C for 18 hours. A 3 µL of formic acid was added to stop the enzymatic reaction.

- **Desalting**

Prior to LC-MS analysis, the digested samples were cleaned by using C18 SPE cartridges for desalting. The use of C18 SPE cartridge includes condition, equilibration, sample loading, washing, and elution steps[85,88]. For the conditioning step, 2.0 mL of ACN with 0.1% trifluoroacetic acid (TFA) was added to the cartridge three times followed by adding 2.0 mL of water with 0.1% TFA three times, which is equilibration step. Then, the sample was added by completing its volume to 1.5 mL. The sample was washed with 2 mL of water with 0.1% TFA three times. Subsequently, the sample was eluted with 2 mL of 80% ACN with 0.1% TFA in a new clean tube, and dried using the vacuum centrifuge concentrator. The dried samples were reconstituted with the mixture of SIL peptide solution, and transferred to 96-well plate, as presented in Figure 2.14.

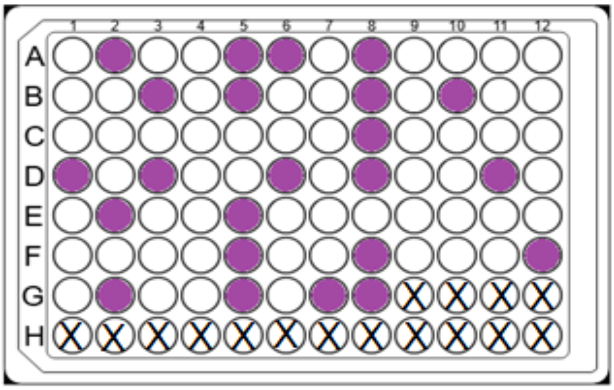

Figure 2.14 *The localization of endometrioid endometrial cancer samples (purple) in a 96-well plate. All samples were placed from A1 to G8.*

- **Reproducibility of Sample Preparation**

Three different QC samples (EC-QC1, EC-QC2, EC-QC3) were prepared to monitor the reproducibility of sample preparation. During the preparation of clinical samples, QC samples were also prepared by pooling all homogenized tissue samples following the steps of protein extraction and digestion. The reproducibility of sample preparation was evaluated using the ratio of endogeneous/SIL (L/H) peptide (Figure 2.15). The lowest variation was presented by MLLADQGQSWK peptide, and the highest variation was monitored by HHAAYVNNLNVTEEK peptide with 10.4% of CV value, which met the acceptance criteria of EMA guideline, as presented in Figure 2.16[115].

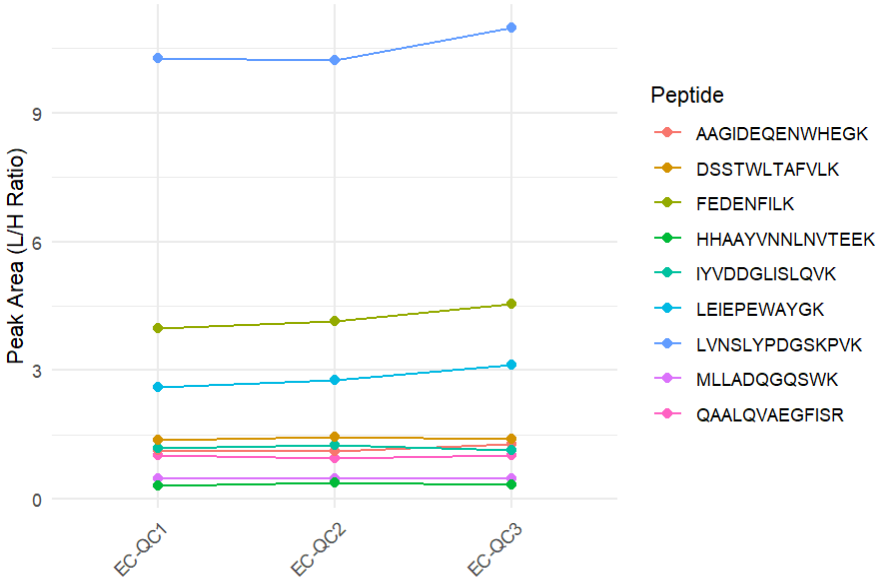

Figure 2.15 *The sample preparation stability between EC-QC samples (N=3) using the ratio (L/H) normalization.*

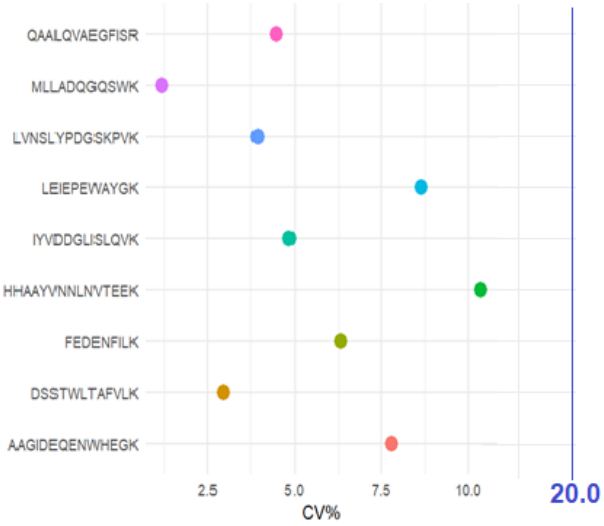

Figure 2.16 *The reproducibility of sample preparation calculated by CV% for each peptide (CV% = 1.2–10.4%).*

2.2.3 Data Processing and Statistical Analysis

Raw MS data were collected in .lcd format from LabSolutions (v5.3) software. The data were imported to Skyline in which the transitions were manually integrated. The peak areas of quantifier ions were exported to .csv file, and also ProteinName, PeptideSequence, PrecursorCharge, FragmentIon, ProductCharge, IsotopeLabelType, Condition, BioReplicate, Run, and Intensity were involved in .csv file.

ProteinName column enables information about each Protein ID of nine biomarkers. PeptideSequence, PrecursorCharge, FragmentIon, and ProductCharge columns define the features of the proteins. IsotopeLabelType is for specifying endogenous (L) and SIL (H) peptides. Condition indicates the groups of interest. BioReplicate represents a unique identifier for each biological replicate. For this study, each clinical sample collected from each patient is a biological replicate. Run is the identifier of a MS run, and Intensity is the peak are of quantifier ion.

All data were pre-processed using the normalization of log2(L/H). The statistical analyses were carried out using R statistical language (v4.4.2) with MSstats package, and applied to the normalized data.

The differences in the protein levels between control-cancer groups, and sub-types visualized using Student's t –test with fold change cutoff of 1.5. p-values were adjusted for pair-wise comparisons using the Benjamini–Hochberg false discovery rate method, with an adjusted p-value threshold of 0.05[121]. Therefore, if p-value is less than 0.05, the change in two conditions is statistically significant[124].

The classification performance for each candidate biomarker was assessed considering the 1-specificity and sensitivity of the biomarkers given by ROC curves. In order to confirm the presence of the disease in a patient "sensitivity (or true-positive results, TPR)" was assessed. "1-specificity (or false-positive result, FPR)" confirms the absence of the disease in a patient[125].

The AUC values were estimated to evaluate the diagnostic performance for each individual biomarker. The value of 0.5 for AUC give a diagonal line on ROC curve, which means that there is no discriminative property[125]. If the value of AUC is higher than 0.75, the performance of discrimination for biomarkers is good. Higher value of AUC than 0.90 is considered as excellent discrimination[125,126].

CHAPTER 3

RESULTS & DISCUSSION

3.1 Results

- **MRM Analysis of Clinical Samples**

A robust and sensitive MRM method was developed for nine candidate proteins, and successfully implemented for the analysis of the clinical samples collected from the patients with endometrioid EC, non-endometrioid EC, and healthy groups. The reproducibility of sample preparation was confirmed by three different QC samples (EC-QC1, EC-QC2, EC-QC3) by showing consistent results with the CV% values of 1.2% - 10.4%. Method performance was evaluated through analytical parameters, including linearity with high correlation coefficients (R^2: 0.9796 - 0.9992), and LOD values. Also, MS-QC sample was used to assess instrument stability throughout the runs, and indicated consistent results with the CV% values of 0.3% - 15.8%. According to the bioanalytical method validation guideline of EMA[115], the results were sufficient for acceptance criteria. These results confirmed that the developed MRM method is suitable for the verification of nine candidate biomarkers in clinical tissue samples.

- **Preparing the Data for MSstats Input**

For each protein, we selected their proteotypic peptides and their representative precursor/fragment ion pairs in Skyline. Three to four MRM transitions were selected based on their MRM intensity. The most intense transition was called as “quantifier”, and their peaks were manually integrated in Skyline.

Statistical analysis was performed in R (v4.4.2) using MSstats package, which is a tool for quantitative proteomics[129]. It enables the detection of the changes in protein abundance between conditions with high sensitivity and specificity[130].

Following peak integration in Skyline, the results were exported as a .csv file including the following variables: ProteinName, PeptideSequence, PrecursorCharge, FragmentIon, ProductCharge, IsotopeLabelType, Condition, BioReplicate, Run, and Intensity. Using Skyline's annotation feature, the analysis was set up as a "GroupComparison" to compare the protein abundances between conditions[121]. Firstly, the study conditions were defined as follows: control (n = 26), endometrioid EC (n = 23), and non-endometrioid EC (n = 20). Each biological replicate in the analysis was assigned a unique identifier labeled as "BioReplicate." The intensity value was taken as the peak area of "quantifier" ion. The complete MSstats input for this analysis was presented in Figure 3.1.

ProteinName	PeptideSequence	PrecursorCharge	FragmentIon	ProductCharge	IsotopeLabelType	Condition	BioReplicate	Run	Intensity
sp|Q01995|TAGL_HUMAN	LVNSLYPDGSKPVK	3	y12	2	L	Healthy	R3	R3	6934428
sp|Q01995|TAGL_HUMAN	LVNSLYPDGSKPVK	3	y12	2	L	Healthy	R7	R7	6845590
sp|Q01995|TAGL_HUMAN	LVNSLYPDGSKPVK	3	y12	2	L	Healthy	R10	R10	6852447
sp|Q01995|TAGL_HUMAN	LVNSLYPDGSKPVK	3	y12	2	H	Healthy	R3	R3	404766
sp|Q01995|TAGL_HUMAN	LVNSLYPDGSKPVK	3	y12	2	H	Healthy	R7	R7	382001
sp|Q01995|TAGL_HUMAN	LVNSLYPDGSKPVK	3	y12	2	H	Healthy	R10	R10	399618

Figure 3.1 *Representative MSstat input of transgelin protein exported using Skyline. In IsotopeLabelType, L represents light peptide i.e. endogeneous peptide, and H represents heavy peptide i.e. SIL peptide. BioReplicates and Runs were assigned based on their run (R) order. Intensity represents peak area of quantifier ions.*

The data were imported into R Studio and necessary libraries were installed such as "library(MSstats) and library(ggplot2)". Then, the data were pre-processed by applying global standard normalization.

- **Data Normalization**

Before the analysis, peptides labeled as “heavy”, which is SIL peptides, in the dataset were relabeled as “Global Standard” to enable global standard normalization in the MSstats package. Next, the run identifiers (Run) for each condition were combined with the condition name to create unique identifiers for every run, ensuring that run numbers repeated across conditions could be distinguished.

Following these preprocessing steps, the dataset was imported into the “dataProcess” function of MSstats. At this stage, the normalization method was set to use log2(L/H). During the normalization, MSstats added a μ (mean) value to the log2(light/heavy) ratios in order to correct systematic biases between measurements, and reduce the variations caused by instrument or experimental conditions. In figure 3.2, the plots of nine proteins shows MSstats log2 intensities are related to the calculated log2(light) – log2(heavy) values, i.e., the log2(L/H) ratios. While x-axis shows the log2(L/H) ratios before the global standard normalization shift is applied, y-axis indicates the normalized intensity after MSstats applies the μ (mean) offset. Each point represents protein-level data.

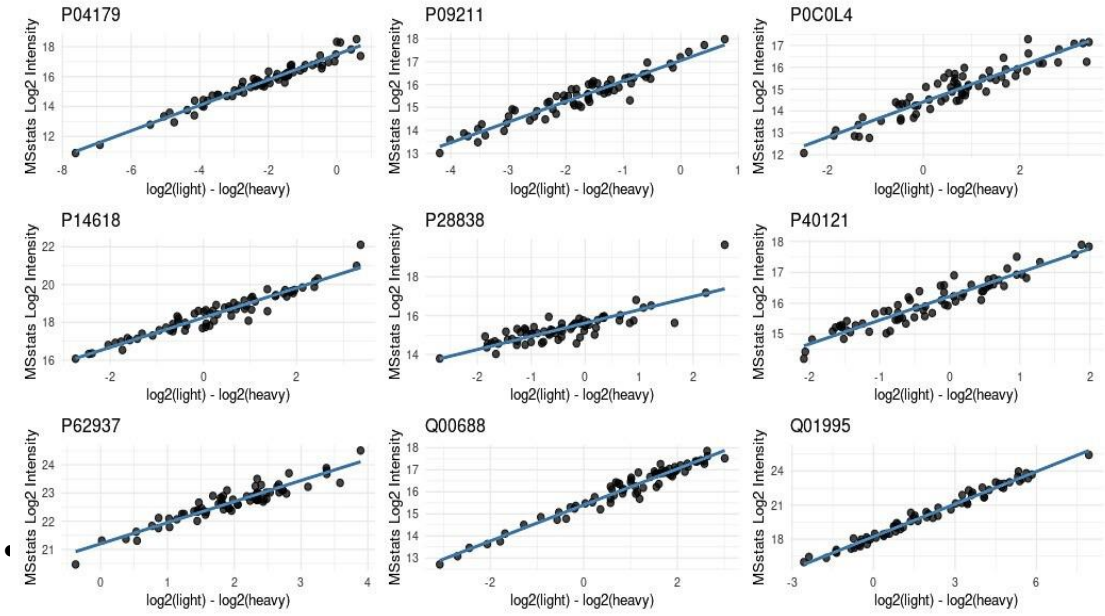

Figure 3.2 *Relationship between raw log2(light/heavy) ratios and MSstats normalized log2 intensities after global standard normalization.*

A heat map is a statistical visualization method that uses “color key” to represent the magnitude of the variables (i.e. protein levels) across samples. Blue color indicates lower expression levels while red color indicates higher expression levels. In the heat map generated in Figure 3.3, hierarchical clustering was used to group the conditions based on their similarity in protein levels. Hence, the most similar pairs were grouped first. Then, the other clusters were formed until all proteins were connected in a tree-like structure, which is called a dendrogram. So, the heat map rows were rearranged and appeared next to each other based on the length of the branch in the dendrogram.

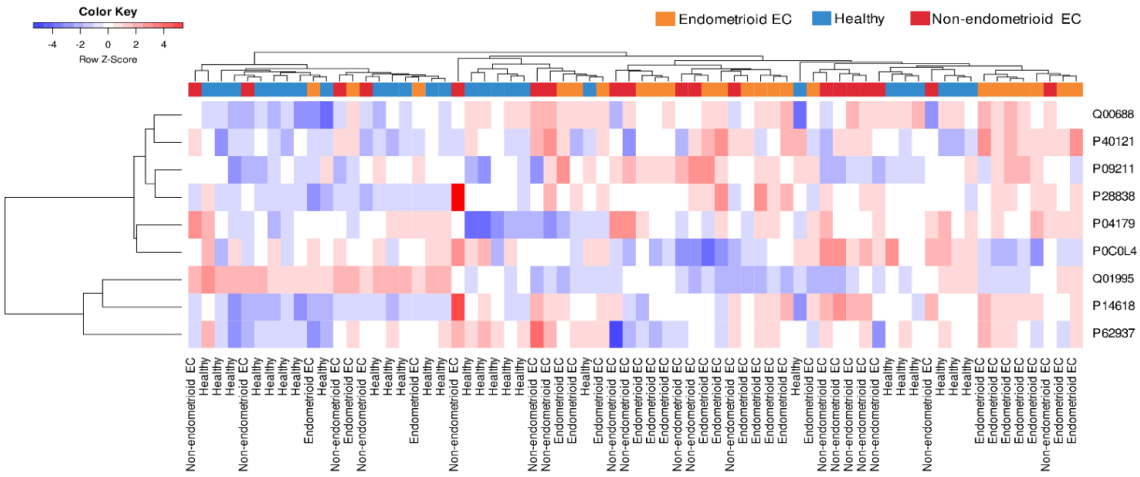

Figure 3.3 *Heat map analysis of nine targeted proteins among healthy, EEC and NEC groups.*

Considering the length of branches, a pair of Q001995 and P14618 proteins had greater distance, and lower similarity. Both proteins showed different abundances in the healthy group: Q001995 was at high abundance while P14618 protein was low abundant in healthy group. A pair of Q00688 and P40121 proteins and a pair of P09211 and P28838 had shorter branch length, meaning more similar clusters. Like P14618 protein, they were at low abundance in healthy group. Those proteins have potential utility for the discrimination of healthy and cancer groups. However, their further discriminative performance for the sub-types should be assessed due to the absence of a distinct separation between the sub-types.

The volcano plot was used to visualize the relationship between fold change and statistical significance, providing the identification of proteins with high differential expression. The differential protein levels were identified using p-values which are estimated based on the distribution of Student's t-test, and the pairwise comparison between the conditions was visualized. Lower p-value than 0.05 was considered statistically significant[124].

In Figure 3.4 (a), the volcano plot shows the relationship between log2 fold change (x-axis) and –log10(p-value) (y-axis) for the candidate proteins, comparing the EEC and healthy groups. Proteins located in the upper right (red) and upper left (blue) points correspond to significantly upregulated and downregulated proteins, respectively, exceeding both the fold change threshold of 1.5 and statistical significance ($p < 0.05$). The horizontal and vertical dashed lines represents the significance (p-value) and fold change cutoffs, respectively[121,124]. This volcano plot indicated that seven proteins above both thresholds represented significantly up-regulated or down-regulated features.

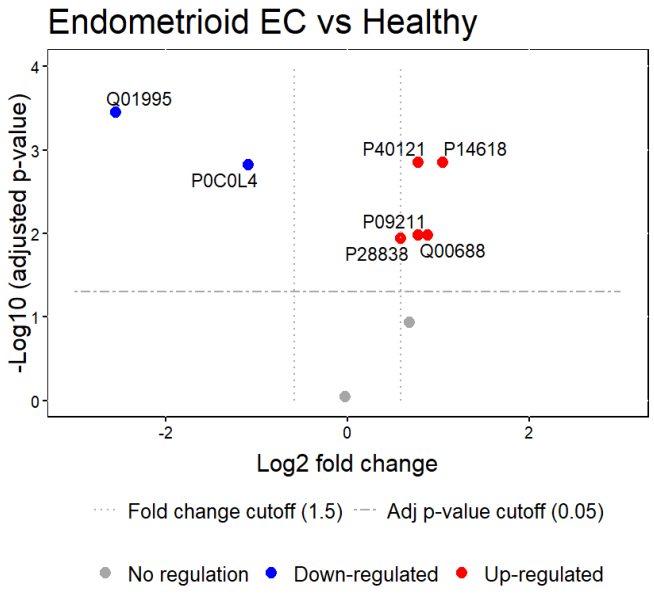

Figure 3.4 *(a) The volcano graphs showing the regulations of candidate biomarkers between EEC and healthy groups.*

P40121, Q00688, P14618, P28838, P09211 proteins were up-regulated, whereas Q01995 and P0C0L4 proteins were down-regulated in EEC group compared to the healthy group. In Figure 3.4 (b), the protein levels were compared between EEC and healthy groups individually and p-values were calculated. P14618, P28838, Q00688, P0C0L4, P40121 and Q001995 were identified as statistically significant proteins with $p<0.05$. The proteins which are significantly up- and down-regulated demonstrated that they are at high and low abundance at EEC compared to healthy group. Furthermore, their abundance difference between the conditions is unlikely to be the result of random variation. Their diagnostic performance should be assessed by the area under ROC.

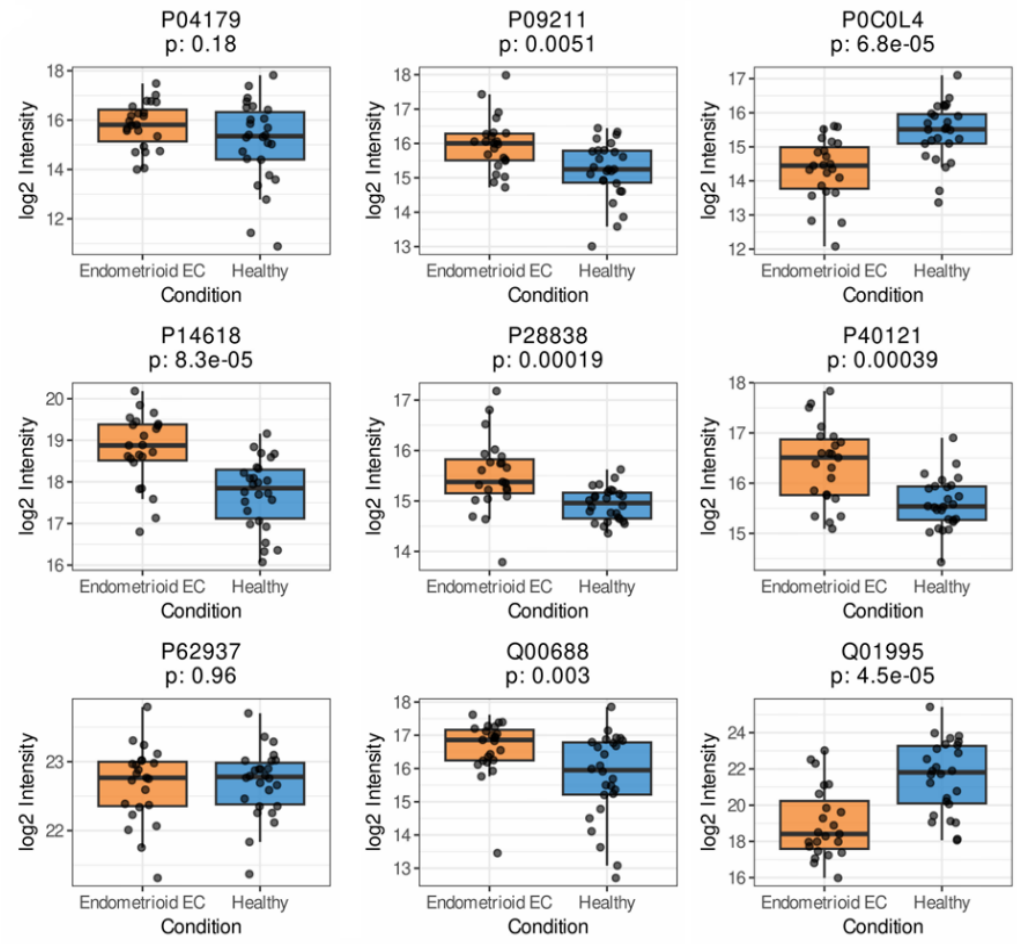

Figure 3.4 *(b) p-values and box plots for each protein, comparing the protein levels between EEC and healthy groups*

Figure 3.5 (a) visualized the significantly differentially expressed proteins between NEC and healthy group. In this volcano plot there were three proteins, P14618, P28838 and Q01995, above both thresholds.[121] In the NEC group, Q01995 protein represented significantly down-regulated feature while P14618 and P28838 proteins showed an up-regulation.

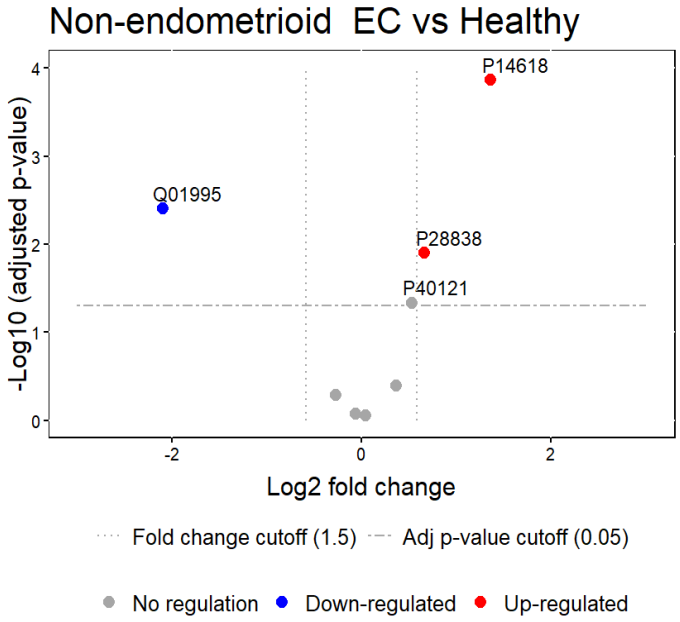

Figure 3.5 *(a) The volcano graphs showing the regulations of candidate biomarkers between NEC and healthy groups.*

The fourth protein, P40121, remained close to the fold change cutoff, and considering Figure 3.5 (b) four proteins, including P40121, showed statistically significant results. The box plot of P40121 protein indicated there was an up-regulation in the NEC group. Proteins below the thresholds, P04179, P09211, P0C0L4, P62937, and Q00688, were considered non-significant with $p>0.05$. Statistically significant results confirmed that Q01995 protein was at low abundance whereas P14618, P28838 and P40121 proteins were at high abundance in non-endometrioid EC compared to healthy group. Those were not random variations and their diagnostic performance should be evaluated.

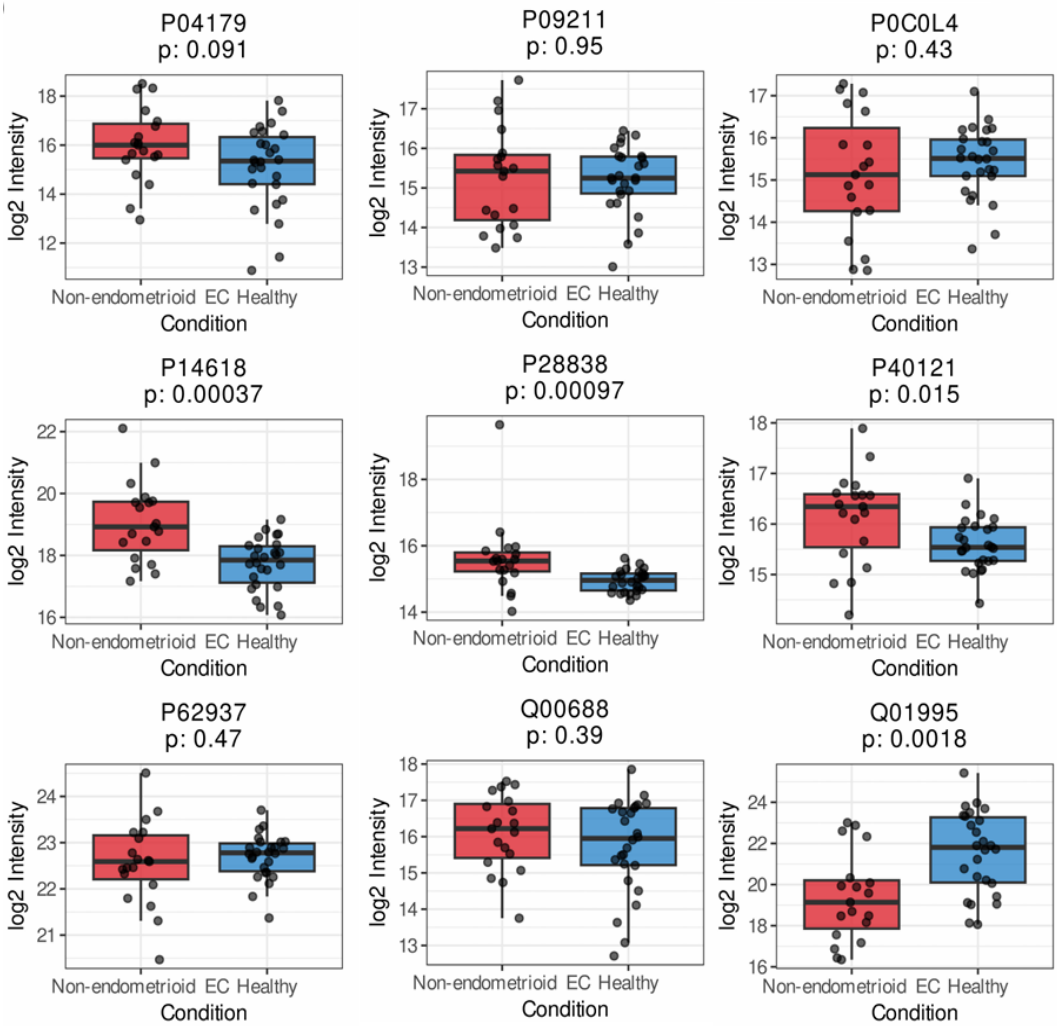

Figure 3.5 *(b) p-values and box plots for each protein, comparing the protein levels between NEC and healthy groups*

Figure 3.6 (a) indicated that the proteins did not exceed the defined threshold in the comparison of EEC and NEC groups. Based on the results of box plots in Figure 3.6(b), only P09211 protein was statistically significant ($p<0.05$) and the level of P09211 protein increased in the EEC group compared to the NEC group. P09211 was high abundant in EEC compared to NEC, and its discriminative performance should be assessed.

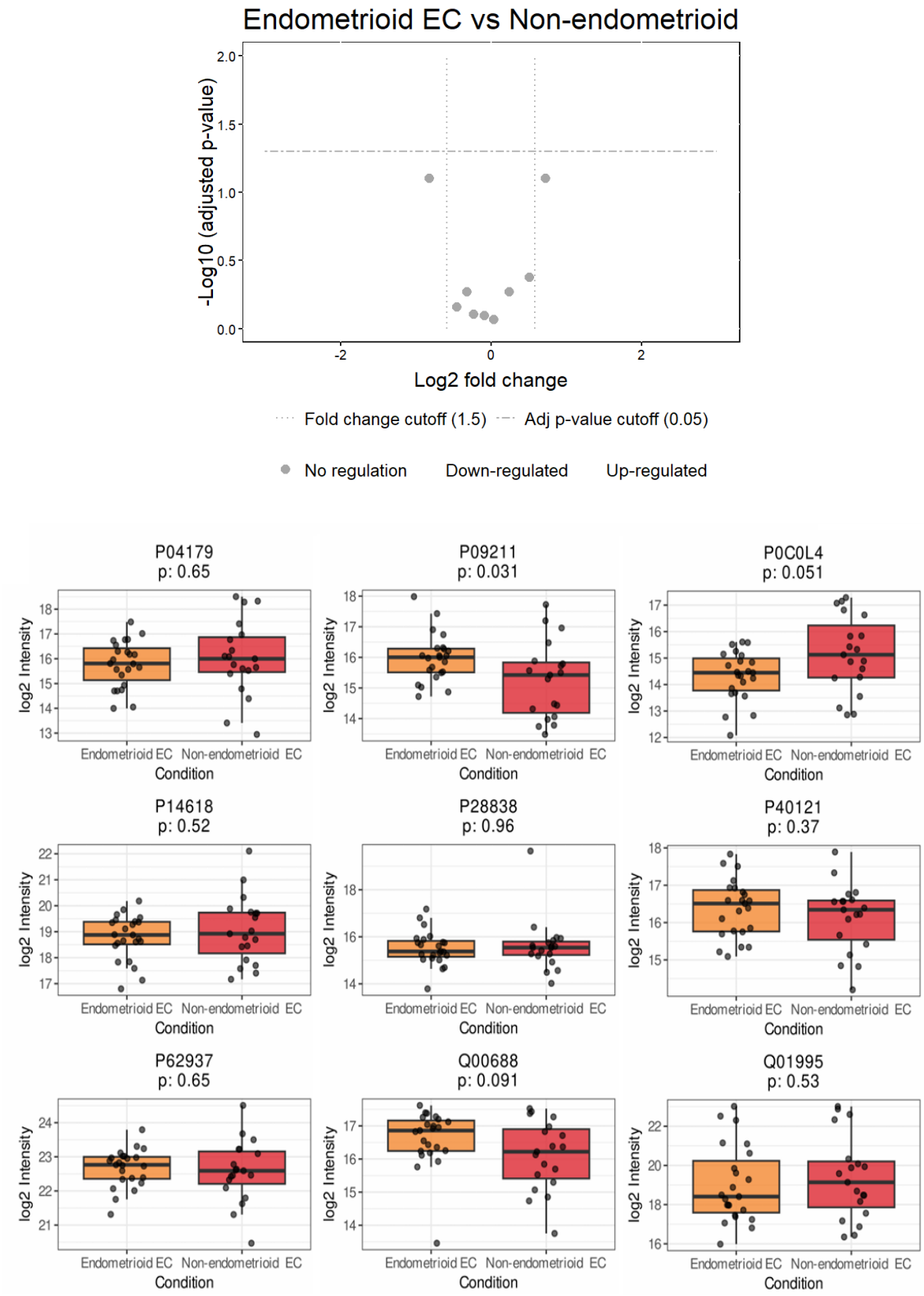

Figure 3.6 (*a) The volcano graphs showing the regulations of candidate biomarkers between EEC and NEC groups. (b) p-values and box plots for each protein, comparing the protein levels between EEC and NEC groups*

Receiver operating characteristic curve (ROC) is a statistical tool that can be used to evaluate the performance of biomarkers. It shows the relationship between the true positive rate (TPR, i.e. sensitivity) and the false positive rate (FPR, i.e. 1-specificity).[125] High sensitivity demonstrates the model's ability to correctly identify true positives (minimizing false negatives), while high specificity indicates accurate identification of true negatives (minimizing false positives). Together, these metrics confirm that the model performs well in both detecting the condition and preventing some cases from misclassification.

In figure 3.7, among nine proteins, seven proteins revealed a discriminatory ability between the EEC and healthy groups.

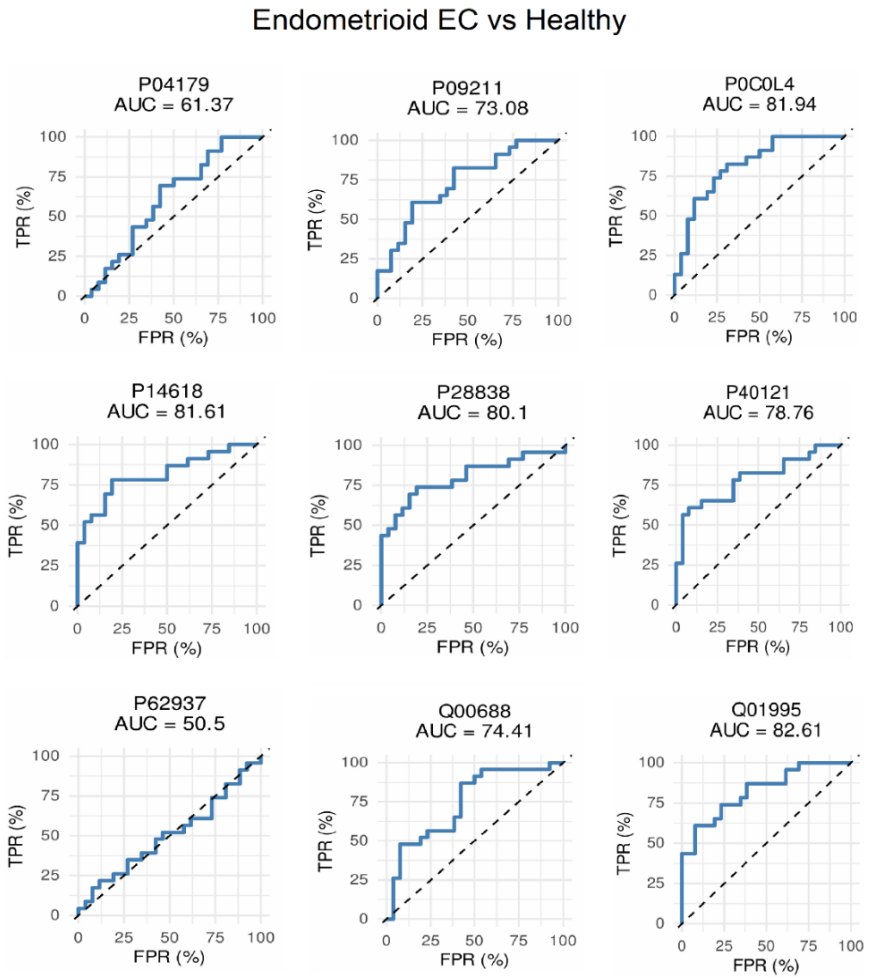

Figure 3.7 *ROCs and AUC values for each protein, indicating the classification performance between EEC and healthy groups*

The AUC values of P0C0L4, P14618, P28838, and Q01995 proteins exceeding 80%, and an AUC of 78.76% for P40121 protein reflected a good classification performance, and those proteins have a potential for clinical applications. P09211 and Q00688 proteins indicated moderate classification performance with AUC values above 70%, meaning that they have a discriminative property but limited potential for clinical applications.

Figure 3.8 indicated the classification performance of proteins between non-endometrioid and healthy groups.

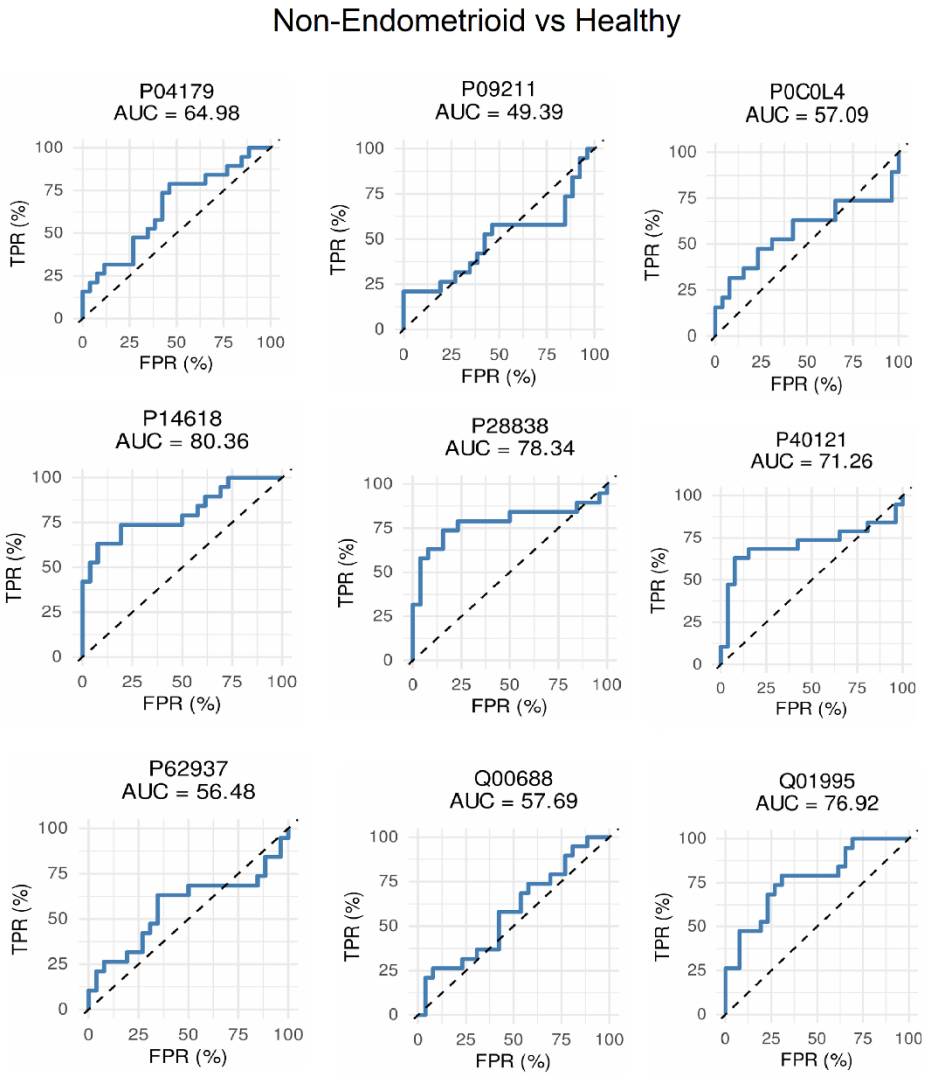

Figure 3.8 *ROCs and AUC values for each protein, indicating the classification performance between NEC and healthy groups*

The AUC values of P14618 and P28838 showed a good discriminative property with 80.36% and 78.34%, respectively. Moderate classification performance was demonstrated by P40121 and Q001995 proteins.

The ROCs of the classification of subtypes of EC illustrated in Figure 3.9, there was no good discriminative protein. Only P09211 protein was close to moderate classification performance with AUC of 69.57% (≈70%). Additionally, P0C0L4 and Q00688 proteins represented low to moderate discriminative ability, which is slightly better than random classification. The other proteins with the performance in 50%-60% range could not distinguish the subtypes.

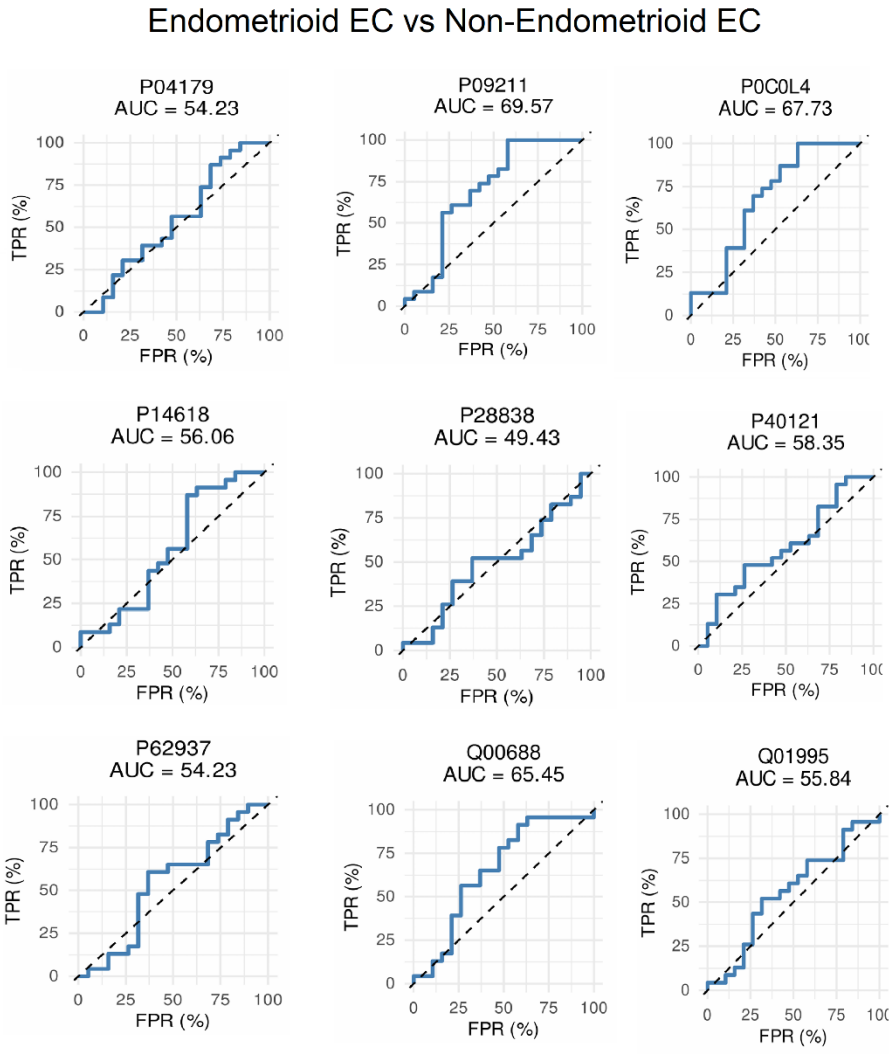

Figure 3.9 *ROCs and AUC values for each protein, indicating the classification performance between EEC and NEC groups*

3.2 Discussion

- **Down-regulation of Transgelin Protein (Q01995)**

Transgelins exist in three isoforms: transgelin-1 (Q01995/SM22α), transgelin-2 (P37802/SM22β), and transgelin-3 (Q9UI15/SM22γ). They belong to a family of actin-binding proteins that regulate cytoskeletal structure and morphology. These proteins contribute to key cellular processes including proliferation, migration, and apoptosis in a wide range of cancers[132]. Their altered expression is associated with tumorigenesis. Hence, those proteins present potential indicators of cancer progression and targets for therapy[133].

Transgelin protein was detected at low abundance in both endometrioid and non-endometrioid EC groups compared to the control group in this study. The down-regulation of transgelin protein has been reported in the other EC studies[41,44,54]. Transgelin protein has further been associated with down-regulation in breast and colon carcinomas[134] as well as in a lung[135] and prostate cancer[133]. As an actin-binding protein, down-regulation of transgelin protein disrupts cytoskeletal stability, thereby enhancing cellular migration and invasion, which lead to tumor progression and metastasis[136,137]. Transgelin protein also acts as a tumor suppressor[138]. In prostate cancer, transgelin has been reported to inhibit androgen-induced cell growth by blocking the interaction between the androgen receptor and its co-activator, thereby preventing the receptor's translocation to the nucleus[139]. Transgelin has been shown to inhibit the expression of matrix metalloproteinase-9 (MMP-9), a protein involved in tissue remodeling that facilitates cancer cell invasion and migration, and whose expression is elevated in prostate, breast, and colon cancers[140]. Some EC studies also indicated the up-regulation MMP9 protein in the cancer state[141,142]. Thus, reduced transgelin expression may contribute to the emergence of certain cancer cell hallmarks in these tumors. Consequently, transgelin protein may represent a promising target for therapeutic intervention in these common cancers[138].

- **Down-regulation of Complement Component C4A Protein (P0C0L4)**

The complement system constitutes a complex network of proteins within the innate immune response that contributes to antitumor defense by promoting the recruitment of leukocytes to the tumor microenvironment, inducing tumor cell lysis, and facilitating the release of proinflammatory mediators[143]. C4A is an inflammatory mediator that contributes to the formation of immune complexes and helps regulate the binding of immune aggregates[144,145].

Several studies have indicated that abnormal C4A expression is linked to different types of cancer. It has been reported that serum C4A was associated with the development of colorectal cancer[145]. Similarly, serum C4A levels were significantly higher in the chemosensitive group than in the chemoresistant group of epithelial ovarian cancer patients[146]. Elevated serum C4A was correlated with breast cancer[147]. In addition, an up-regulation of serum C4A/B in papillary thyroid carcinoma was found compared to benign thyroid nodules and healthy controls[148].

In contrast, complement component C4A protein was found to be significantly down-regulated in the endometrioid EC group compared to the healthy controls. The role of C4A in the tumorigenesis of EC has not yet been clarified, and further mechanistic studies are warranted to understand its biological significance[149].

- **Up-regulation of Pyruvate Kinase M1/M2 Protein (P14618)**

Pyruvate kinase (PK) is an essential enzyme in glycolysis that drives the conversion of phosphoenolpyruvate into pyruvate while simultaneously producing ATP from ADP. Unlike ATP derived from mitochondrial respiration, this process does not rely on oxygen. Because of this, pyruvate kinase was originally thought to help sustain cells in low-oxygen (hypoxic) environments, a hallmark of many tumors[150].

Pyruvate kinase exists in four tissue-specific isoforms: PKL, PKR, PKM1, and PKM2. The M1 isoform is predominantly found in skeletal muscle and brain,

whereas the M2 isoform is typical of fetal tissues and is also expressed in rapidly proliferating cells such as adult stem cells, early embryonic cells, and cancer cells[151-153]. In cancer cells, PKM2 expression is elevated, while the levels of the tissue-specific isoforms PKM1, PKL, and PKR progressively decrease[154,155]. PKM1 and PKM2 exhibit distinct enzymatic characteristics and are controlled by multiple factors at both transcriptional and post-transcriptional levels. PKM1 functions as a constitutively active enzyme with high affinity for its substrate phosphoenolpyruvate, while PKM2 is regulated through complex allosteric mechanisms, playing a key role in supporting tumor development and growth[156,157].

Similar to our results, PKM2 is markedly overexpressed in malignant endometrial lesions and is linked to poor overall survival, while its expression remains low in normal endometrial tissue[158]. Additionally, in the previous studies on proteomics analysis of EC, increased PKM2 expression levels were observed in both endometrioid and non-endometrioid EC[57,159]. The use of PKM2 as a prognostic marker has been validated in various cancers, and the application of PKM2 activators or inhibitors in cancer treatment can be expected in the near future[160].

- **Up-regulation of Macrophage Capping Protein (P40121)**

Macrophage capping protein, also known as gelsolin-like (CAPG), is a member of the gelsolin protein family, which includes cytoplasmic and nuclear proteins[161]. It controls cell motility by regulating actin filament dynamics, which are essential for cell migration and invasion in various cancers[162].

Previous studies have suggested that some factors such as tyrosine kinase[163], semaphorin 3A[164], and hypoxia-inducible factor-1[165], which are cancer-associated regulators, can lead to the up-regulation of CAPG. Moreover, overexpression of CAPG has been reported to influence cell proliferation and apoptosis through the Caspase 6/Caspase 9/Bcl-2/p-Akt/Akt signaling pathway[166], as well as to promote tumorigenesis and metastasis via the Hippo pathway through YAP activation[167].

The up-regulation of CAPG has been detected in some cancer types such as gastric[168], pancreatic, lung[169,170], ovarian[171] as well as pancreatic[172] and prostate[165]. It has been reported that overexpression of CAPG in pancreatic cancer cells increases cell motility[172]. In another study, it has been revealed that inhibition of CAPG gene expression in prostate cancer cell lines causes an obvious reduction in their proliferation[165].

Similar to the other types of cancer, macrophage capping protein was detected at high abundance in both endometrioid and non-endometrioid cancer groups. A previous study highlighted that overexpression of CAPG was linked to poor prognosis in EC, and silencing CAPG contributes to the inhibition of proliferation and metastasis in EC cell lines[173]. Also, the study emphasized that CAPG and other members of gelsolin protein family are closely related to prognosis and immune response in EC[173].

- **Up-regulation of Peptidyl-prolyl Cis-trans Isomerase FKBP3 Protein (Q00688)**

FKBP3, a member of the FK506-binding protein (FKBP) family, exhibits peptidylprolyl cis-trans isomerase activity, interacts with immunosuppressive drugs, and is involved in various processes, including cancer progression and chemoresistance[174,175].

A study has been reported that overexpression of FKBP3 promotes lung cancer cell proliferation and cell cycle progression through the regulation of Sp1/HDAC2/p27 signaling[176]. Furthermore, elevated FKBP3 expression was linked to poor prognosis in lung adenocarcinoma patients and was found to suppress immune cell infiltration within tumor tissues[177]. Additionally, overexpression of FKBP3 was detected in tumors of colorectal cancer patients[178]. Silencing FKBP3 in colorectal cancer has been shown to diminish oxaliplatin resistance, in which cancer cells prevent from the cytotoxic effects of the drug, by modulating the PTEN/AKT signaling[178].

This study revealed the up-regulation of FKBP3 in the EEC patients. Even though the expression of FKBP3 in EC is unclear in the literature, a study showed that FKBP38, a member of FK506-binding protein family, suppressed the proliferation and metastasis of EC cells through the inhibition of the mammalian target of rapamycin pathway that is a key regulator of cell growth and survival[179]. The mechanistic studies are required to elucidate its biological significance of FKBP3 in EC.

- **Up-regulation of Cytosol Aminopeptidase Protein (P28838)**

Cytosol aminopeptidase, also known as leucine aminopeptidase (LAP3), is a member of the M1 aminopeptidase family, which catalyzes the removal of leucine residues from protein amino termini. LAP3 dysregulation is associated with enhanced tumor cell proliferation, migration, and invasion[180].

The overexpression of LAP3 enhance cell proliferation and migration in glioma tumors[181] and contribute to the malignant progression of human esophageal squamous cell carcinoma[182]. Moreover, another study reported that up-regulation of LAP3 promotes migration and invasion of breast cancer cells by reducing Hsp27 phosphorylation while increasing fascin expression, Akt phosphorylation, and matrix metalloproteinase-2/9 levels. These effects drive greater cancer cell growth, survival, and metastatic potential[183]. It has been revealed that the alteration of LAP3 expression also contributes to the changes of cell cycle progression in gynecologic cancers such as ovarian epithelial malignancy, breast cancer and endometrial carcinoma[184-186]. In this study, the up-regulation of cytosol aminopeptidase protein was reported in both endometrioid and non-endometrioid EC. A study has reported that overexpression of LAP3 is associated with clinicopathological features and prognosis in endometrioid endometrial adenocarcinoma. The potential role of LAP3 in cellular processes such as proliferation and tumor progression should be investigated to develop novel therapeutic strategies for EC[187].

- **Up-regulation of Glutathione S-transferase P Protein (P09211)**

Glutathione S-transferases involve a superfamily of ubiquitous, which are responsible for cellular detoxification, protection of macromolecules against reactive electrophiles such as chemotherapeutic agents, reactive oxygen species, and environmental carcinogens[188]. It has been reported that glutathione-S-transferase-P (GSTP1) play a key role in the resistance of cancer cells against alkylating agents among the glutathione S-transferase isozymes[189].

In various cancers, GSTP1 overexpression has been linked to reduced treatment response and poor survival. In breast cancer, GSTP1 expression is strongly correlated with chemotherapy response and clinical outcome[190-193]. Moreover, it has been revealed that overexpression of GSTP1 is also related to chemosensitivity in osteosarcoma and prostate cancer[194,195]. In bladder transitional cell carcinoma, the mechanism of GSTP1 with c-Jun N-terminal kinase was reported, which are forming complexes that suppress apoptosis[196].

Glutathione S-transferase P was detected at high abundance in the comparison of EEC patients and healthy group. Also, it was the only protein showing significant difference in the comparison of sub-types, which was up-regulated in EEC group compared to NEC group. Studies have revealed the overexpression of GSTP1 in EC mechanism is not common; however, its reduced expression was linked to hypermethylation of the GSTP1 promoter region[197]. Furthermore, a study has been reported that downexpression of GSTP1 has been correlated with more aggressive tumor characteristics, including deeper invasion and higher grade. Thus, GSTP1 may act as a molecular marker for prognosis, reflecting a higher risk of recurrence and poorer outcomes when silenced[197].

CHAPTER 4

CONCLUSION

This study represents the progression of EC biomarker research from the discovery phase to the verification phase. This progression was achieved by developing a high selective and sensitive MRM-MS method for the nine target protein biomarkers. This MRM method monitored twenty three unique peptides representing nine proteins, which is not present in the current literature, and applied to verify the candidate biomarkers of EC for the first time.

Method performance was evaluated with MS-QC sample and its CV% values, ranging from 0.3% to 15.8%, indicated instrument stability through reproducible results. Reproducibility of protein digestion was tested using three different EC-QC samples through parallel tissue sample processing, provided the CV% values of 1.2% - 10.4%. Both met the acceptance criteria according to the EMA guideline. Method performance was assessed through analytical parameters, including linearity with high correlation coefficients (R^2: 0.9796 - 0.9992), and LOD values (9.1×10^{-12} to 3.0×10^{-9} µmol/µL).

A total of 69 fresh-frozen tissue samples were collected from the patients with endometrioid EC (n=23), non-endometrioid EC (n=20), and healthy group (n=26). The developed method was effectively implemented to measure the candidate proteins in clinical tissue samples. The pairwise comparisons of control and cancer groups as well as subtypes were performed using Student's t-test, and diagnostic performance of the proteins was evaluated by area under ROCs. The candidate proteins were successfully verified with statistically significant results, and consistency with their biological role.

In conclusion, the developed MRM method offers a reliable and reproducible quantification of clinical samples, serving as a basis for biomarker verification and

validation processes. This approach has a high potential for early diagnosis, and subtype differentiation of endometrioid EC and non-endometrioid EC in the clinical studies. High diagnostic performance of four proteins with area under ROC values above 80%, demonstrated the potential for clinical validation of these candidates.

In summary, this study presents first MRM–MS method for verifying EC-associated proteins. Method achieved robust analytical performance and reproducibility. These findings highlight that combining multiple protein candidates could further improve EC diagnostic accuracy. Thus, future studies could improve classification performance by panel-based biomarker approaches. In order to advance toward clinical application, the next phases of the biomarker pipeline, such as validation in larger and more diverse cohorts, should be followed for the verified proteins. Also, clinical trials will be performed with non-invasive samples. Their mechanisms will be discovered in EC and treatment strategies will be improved.

REFERENCES

(1) Morice, P., Leary, A., Creutzberg, C., Abu-Rustum, N., & Darai, E. (2016). Endometrial cancer. Lancet (London, England), 387(10023), 1094–1108.

(2) Bray, F., Laversanne, M., Sung, H., Ferlay, J., Siegel, R. L., Soerjomataram, I., & Jemal, A. (2024). Global cancer statistics 2022: GLOBOCAN estimates of incidence and mortality worldwide for 36 cancers in 185 countries. CA: A Cancer Journal for Clinicians, 74(3), 229–263.

(3) Siegel, R. L., Kratzer, T. B., Giaquinto, A. N., Sung, H., & Jemal, A. (2025). Cancer statistics, 2025. CA: A Cancer Journal for Clinicians, 75(1), 10–45.

(4) Makker, V., MacKay, H., Ray-Coquard, I., Levine, D. A., Westin, S. N., Aoki, D., & Oaknin, A. (2021). Endometrial cancer. Nature Reviews Disease Primers, 7(1).

(5) Terzic, M., Aimagambetova, G., Kunz, J., Bapayeva, G., Aitbayeva, B., Terzic, S., & Laganà, A. S. (2021). Molecular Basis of Endometriosis and Endometrial Cancer: Current Knowledge and Future Perspectives. International Journal of Molecular Sciences, 22(17), Article 17.

(6) Onstad, M. A., Schmandt, R. E., & Lu, K. H. (2016). Addressing the role of obesity in endometrial cancer risk, prevention, and treatment. Journal of Clinical Oncology, 34(35), 4225–4230.

(7) Clarke M. A., Long B. J., Del Mar Morillo A., Arbyn M., Bakkum-Gamez J. N., Wentzensen N. (2018). Association of Endometrial Cancer Risk with Postmenopausal Bleeding in Women: A Systematic Review and Meta-analysis. JAMA Intern Med., 178(9):1210–1222.

(8) Njoku, K., Pierce, A., Chiasserini, D., Geary, B., Campbell, A. E., Kelsall, J., Reed, R., Geifman, N., Whetton, A. D., & Crosbie, E. J. (2024). Detection of endometrial cancer in cervico-vaginal fluid and blood plasma: leveraging proteomics and machine learning for biomarker discovery. Ebiomedicine, 102, 105064.

(9) Martinez-Garcia, E., Coll-de la Rubia, E., Lesur, A., Dittmar, G., Gil-Moreno, A., Cabrera, S., & Colas, E. (2023). Cervical fluids are a source of protein biomarkers for early, non-invasive endometrial cancer diagnosis. Cancers, 15(3), 911.

(10) Salvesen, H. B., Carter, S. L., Mannelqvist, M., Dutt, A., Getz, G., Stefansson, I. M., Raeder, M. B., Sos, M. L., Engelsen, I. B., Trovik, J., Wik, E., Greulich, H., Bø, T. H., Jonassen, I., Thomas, R. K., Zander, T., Garraway, L. A., Øyan, A. M., Sellers, W. R., … Beroukhim, R. (2009). Integrated genomic profiling of endometrial carcinoma associates aggressive tumors with indicators of PI3 kinase activation. Proceedings of the National Academy of Sciences, 106(12), 4834–4839.

(11) Yildirim, O. S., Yildiz, P., Karaer, A., Calleja-Agius, J., & Ozcan, S. (2025). Exploring the protein signature of endometrial cancer: A comprehensive review through diverse samples and mass spectrometry-based proteomics. European Journal of Surgical Oncology, 51(4), 108783.

(12) FDA-NIH Biomarker Working Group. (2016). BEST (Biomarkers, EndpointS, and other Tools) Resource. Silver Spring (MD): Food and Drug Administration (US).

(13) Passaro, A., Al Bakir, M., Hamilton, E. G., Diehn, M., André, F., Roy-Chowdhuri, S., Mountzios, G., Wistuba, I. I., Swanton, C., & Peters, S. (2024). Cancer biomarkers: Emerging trends and clinical implications for personalized treatment. Cell, 187(7), 1617–1635.

(14) Sarhadi, V. K., & Armengol, G. (2022). Molecular biomarkers in cancer. Biomolecules, 12(8), 1021.

(15) Jain, K. K. (2017). The Handbook of Biomarkers. Humana Press.

(16) Ahmad, A., Imran, M., & Ahsan, H. (2023). Biomarkers as biomedical bioindicators: Approaches and techniques for the detection, analysis, and validation of novel biomarkers of diseases. Pharmaceutics, 15(6), 1630.

(17) Edahiro, T., Ureshino, H., Yoshida, T., Fukushima, N., & Ichinohe, T. (2023). Challenging diagnosis of lytic bone lesions between multiple myeloma and bone metastasis of primary breast cancer. Cureus.

(18) Imoto, M., Nakatani, Y., Watanabe, K., & Kamisako, T. (2025). Proposed method using the urinary albumin-to-total protein ratio for detection of urinary Bence Jones protein. Clinical Laboratory, 71(05/2025).

(19) Sun, H., Liu, J., Zhang, Q., Yang, L., Zhou, M., & Song, D. (2025). Advances in carcinoembryonic antigen detection: A review of Clinical Applications and Standardization. Analytical and Bioanalytical Chemistry, 417(9), 1751–1764.

(20) Sato, R., Oikawa, M., Kakita, T., Abe, T., Akazawa, N., Okano, H., Ito, K., & Tsuchiya, T. (2024). Prognostic value of carcinoembryonic antigen (CEA) and ca 19-9 levels in patients with obstructive colorectal cancer treated with a self-expandable metallic stent and curative surgery. Surgery Today, 55(5), 618–626.

(21) Füzéry, A. K., Levin, J., Chan, M. M., & Chan, D. W. (2013). Translation of proteomic biomarkers into FDA approved cancer diagnostics: Issues and challenges. Clinical Proteomics, 10(1).

(22) Stastna, M., & Van Eyk, J. E. (2012). Secreted proteins as a fundamental source for biomarker discovery. Proteomics, 12(4–5), 722–735.

(23) Kumar, R. R., Kumar, A., Chuang, C.-H., & Shaikh, M. O. (2023). Recent advances and emerging trends in Cancer Biomarker Detection Technologies. Industrial & Engineering Chemistry Research, 62(14), 5691–5713.

(24) Drabovich, A. P., Pavlou, M. P., Batruch, I., & Diamandis, E. P. (2013). Proteomic and mass spectrometry technologies for Biomarker Discovery. Proteomic and Metabolomic Approaches to Biomarker Discovery, 17–37.

(25) Nakayasu, E. S., Gritsenko, M., Piehowski, P. D., Gao, Y., Orton, D. J., Schepmoes, A. A., Fillmore, T. L., Frohnert, B. I., Rewers, M., Krischer, J. P., Ansong, C., Suchy-Dicey, A. M., Evans-Molina, C., Qian, W.-J., Webb-Robertson, B.-J. M., & Metz, T. O. (2021). Tutorial: Best practices and considerations for mass-spectrometry-based protein biomarker discovery and validation. Nature Protocols, 16(8), 3737–3760.

(26) Surinova, S., Schiess, R., Hüttenhain, R., Cerciello, F., Wollscheid, B., & Aebersold, R. (2011). On the development of plasma protein biomarkers. Journal of Proteome Research, 10(1), 5–16.

(27) Rifai, N., Gillette, M. A., & Carr, S. A. (2006). Protein biomarker discovery and validation: The long and uncertain path to clinical utility. Nature Biotechnology, 24(8), 971–983.

(28) Ono, K., Tanaka, T., Tsunoda, T., Kitahara, O., Kihara, C., Okamoto, A., Ochiai, K., Takagi, T., & Nakamura, Y. (2000). Identification by cDNA microarray of genes involved in ovarian carcinogenesis. Cancer research, 60(18), 5007–5011.

(29) Anastasi, E., Marchei, G. G., Viggiani, V., Gennarini, G., Frati, L., & Reale, M. G. (2010). HE4: a new potential early biomarker for the recurrence of ovarian cancer. Tumour biology: the journal of the International Society for Oncodevelopmental Biology and Medicine, 31(2), 113–119.

(30) Zhang, Y., Fonslow, B. R., Shan, B., Baek, M.-C., & Yates, J. R. (2013). Protein analysis by Shotgun/bottom-up proteomics. Chemical Reviews, 113(4), 2343–2394.

(31) Han, X., Aslanian, A., & Yates, J. R. (2008). Mass spectrometry for proteomics. Current Opinion in Chemical Biology, 12(5), 483–490.

(32) Parker, C. E., & Borchers, C. H. (2014). Mass spectrometry based Biomarker Discovery, verification, and validation — quality assurance and control of protein biomarker assays. Molecular Oncology, 8(4), 840–858.

(33) Ross, P. L., Huang, Y. N., Marchese, J. N., Williamson, B., Parker, K., Hattan, S., Khainovski, N., Pillai, S., Dey, S., Daniels, S., Purkayastha, S., Juhasz, P., Martin, S., Bartlet-Jones, M., He, F., Jacobson, A., & Pappin, D. J. (2004). Multiplexed protein quantitation in saccharomyces cerevisiae using amine-reactive isobaric tagging reagents. Molecular & Cellular Proteomics, 3(12), 1154–1169.

(34) Njoku, K., Pierce, A., Chiasserini, D., Geary, B., Campbell, A. E., Kelsall, J., Reed, R., Geifman, N., Whetton, A. D., & Crosbie, E. J. (2024). Detection of endometrial cancer in Cervico-vaginal fluid and blood plasma: Leveraging Proteomics and Machine Learning for Biomarker Discovery. eBioMedicine, 102, 105064.

(35) Mujammami, M., Rafiullah, M., Akkour, K., Alfadda, A. A., Masood, A., Joy, S. S., Alhalal, H., Arafah, M., Alshehri, E., Alanazi, I. O., & Benabdelkamel, H. (2024). Plasma proteomic signature of endometrial cancer in patients with diabetes. ACS Omega, 9(4), 4721–4732.

(36) Sommella, E., Capaci, V., Aloisio, M., Salviati, E., Campiglia, P., Molinario, G., Licastro, D., Di Lorenzo, G., Romano, F., Ricci, G., Monasta, L., & Ura, B. (2022). A label-free proteomic approach for the identification of biomarkers in the exosome of endometrial cancer serum. Cancers, 14(24), 6262.

(37) Akkour, K., Alanazi, I. O., Alfadda, A. A., Masood, A., Alhalal, H., Joy, S. S., Bassi, A., Alshehri, E., Alwehaibi, M. A., Arafah, M., & Benabdelkamel, H. (2024). Plasma-based proteomic profiling identifies the distinct regulation of proteins in hyperplasia and endometrial cancer. BMC Cancer, 24(1).

(38) Pietkiewicz, D., Zaborowski, M. P., Jaz, K., Matuszewska, E., Światły-Błaszkiewicz, A., Kluz, T., Kokot, Z. J., Nowak-Markwitz, E., & Matysiak, J. (2023). Serum proteomic profiles of patients with high and low risk of endometrial cancer recurrence. International Journal of Molecular Sciences, 24(19), 14528.

(39) Tarney, C. M., Wang, G., Bateman, N. W., Conrads, K. A., Zhou, M., Hood, B. L., Loffredo, J., Tian, C., Darcy, K. M., Hamilton, C. A., Casablanca, Y., Lokshin, A., Conrads, T. P., & Maxwell, G. L. (2019). Biomarker panel for early

detection of endometrial cancer in the prostate, Lung, colorectal, and Ovarian Cancer Screening trial. American Journal of Obstetrics and Gynecology, 221(5).

(40) Song, Y., Wang, M., Tong, H., Tan, Y., Hu, X., Wang, K., & Wan, X. (2020). Plasma exosomes from endometrial cancer patients contain LGALS3BP to promote endometrial cancer progression. Oncogene, 40(3), 633–646.

(41) Martinez-Garcia, E., Coll-de la Rubia, E., Lesur, A., Dittmar, G., Gil-Moreno, A., Cabrera, S., & Colas, E. (2023). Cervical fluids are a source of protein biomarkers for early, non-invasive endometrial cancer diagnosis. Cancers, 15(3), 911.

(42) Ura, B., Monasta, L., Arrigoni, G., Franchin, C., Radillo, O., Peterlunger, I., Ricci, G., & Scrimin, F. (2017). A proteomic approach for the identification of biomarkers in endometrial cancer uterine aspirate. Oncotarget, 8(65), 109536–109545.

(43) Artuyants, A., Guo, G., Flinterman, M., Middleditch, M., Jacob, B., Lee, K., Vella, L., Su, H., Wilson, M., Eva, L., Shelling, A. N., & Blenkiron, C. (2024). The tumour-derived extracellular vesicle proteome varies by endometrial cancer histology and is confounded by an obesogenic environment. PROTEOMICS, 24(11).

(44) Akkour, K., Alanazi, I. O., Alfadda, A. A., Alhalal, H., Masood, A., Musambil, M., Rahman, A. M., Alwehaibi, M. A., Arafah, M., Bassi, A., & Benabdelkamel, H. (2022). Tissue-based proteomic profiling in patients with hyperplasia and endometrial cancer. Cells, 11(13), 2119.

(45) Hsu, C.-Y., Hsieh, T.-H., Lin, H.-Y., Lu, C.-Y., Lo, H.-W., Tsai, C.-C., & Tsai, E.-M. (2021). Characterization and proteomic analysis of endometrial

stromal cell–derived small extracellular vesicles. The Journal of Clinical Endocrinology & Metabolism, 106(5), 1516–1529.

(46) Acland, M., Arentz, G., Mussared, M., Whitehead, F., Hoffmann, P., Klingler-Hoffmann, M., & Oehler, M. K. (2020). Proteomic analysis of pre-invasive serous lesions of the endometrium and fallopian tube reveals their metastatic potential. Frontiers in Oncology, 10.

(47) Mittal, P., Klingler-Hoffmann, M., Arentz, G., Winderbaum, L., Kaur, G., Anderson, L., Scurry, J., Leung, Y., Stewart, C. J., Carter, J., Hoffmann, P., & Oehler, M. K. (2017). Annexin A2 and Alpha Actinin 4 expression correlates with metastatic potential of primary endometrial cancer. Biochimica et Biophysica Acta (BBA) - Proteins and Proteomics, 1865(7), 846–857.

(48) Janacova, L., Faktor, J., Capkova, L., Paralova, V., Pospisilova, A., Podhorec, J., Ebhardt, H. A., Hrstka, R., Nenutil, R., Aebersold, R., & Bouchal, P. (2020). Swath-MS analysis of FFPE tissues identifies Stathmin as a potential marker of endometrial cancer in patients exposed to tamoxifen. Journal of Proteome Research, 19(7), 2617–2630.

(49) Capaci, V., Arrigoni, G., Monasta, L., Aloisio, M., Rocca, G., Di Lorenzo, G., Licastro, D., Romano, F., Ricci, G., & Ura, B. (2023). Phospho-dige identified phosphoproteins involved in pathways related to tumour growth in endometrial cancer. International Journal of Molecular Sciences, 24(15), 11987.

(50) Javadian, P., Xu, C., Sjoelund, V., Borden, L. E., Garland, J., & Benbrook, D. M. (2022). Identification of candidate biomarker and drug targets for improving endometrial cancer racial disparities. International Journal of Molecular Sciences, 23(14), 7779.

(51) Hu, Z., Wu, Z., Liu, W., Ning, Y., Liu, J., Ding, W., Fan, J., Cai, S., Li, Q., Li, W., Yang, X., Dou, Y., Wang, W., Peng, W., Lu, F., Zhuang, X., Qin, T., Kang, X., Feng, C., … Sun, C. (2024). Proteogenomic insights into early-onset endometrioid endometrial carcinoma: Predictors for fertility-sparing therapy response. Nature Genetics, 56(4), 637–651.

(52) Kurimchak, A. M., Kumar, V., Herrera-Montávez, C., Johnson, K. J., Srivastava, N., Davarajan, K., Peri, S., Cai, K. Q., Mantia-Smaldone, G. M., & Duncan, J. S. (2020). Kinome profiling of primary endometrial tumors using multiplexed inhibitor beads and mass spectrometry identifies SRPK1 as candidate therapeutic target. Molecular & Cellular Proteomics, 19(12), 2068–2090.

(53) Galazis, N., Pang, Y.-L., Galazi, M., Haoula, Z., Layfield, R., & Atiomo, W. (2013). Proteomic biomarkers of endometrial cancer risk in women with polycystic ovary syndrome: A systematic review and Biomarker Database Integration. Gynecological Endocrinology, 29(7), 638–644.

(54) DeSouza, L., Diehl, G., Rodrigues, M. J., Guo, J., Romaschin, A. D., Colgan, T. J., & Siu, K. W. (2005). Search for cancer markers from endometrial tissues using differentially labeled tags iTraq and CICAT with multidimensional liquid chromatography and Tandem Mass Spectrometry. Journal of Proteome Research, 4(2), 377–386.

(55) Monge, M., Doll, A., Colas, E., Gil-Moreno, A., Castellvi, J., Garcia, A., Colome, N., Perez-Benavente, A., Pedrola, N., Lopez-Lopez, R., Dolcet, X., Ramon y Cajal, S., Xercavins, J., Matias-Guiu, X., Canals, F., Reventos, J., & Abal, M. (2009). Subtractive proteomic approach to the endometrial carcinoma invasion front. Journal of Proteome Research, 8(10), 4676–4684.

(56) Li, Z., Zhao, X., Bai, S., Wang, Z., Chen, L., Wei, Y., & Huang, C. (2008). Proteomics identification of Cyclophilin A as a potential prognostic factor and therapeutic target in endometrial carcinoma. Molecular & Cellular Proteomics, 7(10), 1810–1823.

(57) Negishi, A., Ono, M., Handa, Y., Kato, H., Yamashita, K., Honda, K., Shitashige, M., Satow, R., Sakuma, T., Kuwabara, H., Omura, K., Hirohashi, S., & Yamada, T. (2009). Large-scale quantitative clinical proteomics by Label-Free Liquid Chromatography and mass spectrometry. Cancer Science, 100(3), 514–519.

(58) Ma, X., Fan, L., Meng, Y., Hou, Z., Mao, Y.-D., Wang, W., Ding, W., & Liu, J.-Y. (2007). Proteomic analysis of human ovaries from normal and polycystic ovarian syndrome. MHR: Basic Science of Reproductive Medicine, 13(8), 527–535.

(59) Matharoo-Ball, B., Hughes, C., Lancashire, L., Tooth, D., Ball, G., Creaser, C., Elgasim, M., Rees, R., Layfield, R., & Atiomo, W. (2007). Characterization of biomarkers in polycystic ovary syndrome (PCOS) using multiple distinct proteomic platforms. Journal of Proteome Research, 6(8), 3321–3328.

(60) Borro, M., Gentile, G., Stigliano, A., Misiti, S., Toscano, V., & Simmaco, M. (2007). Proteomic analysis of peripheral T lymphocytes, suitable circulating biosensors of strictly related diseases. Clinical and Experimental Immunology, 150(3), 494–501.

(61) Voisin, S. N., Krakovska, O., Matta, A., DeSouza, L. V., Romaschin, A. D., Colgan, T. J., & Siu, K. W. (2011). Identification of novel molecular targets for endometrial cancer using a drill-down LC-MS/MS approach with itraq. PLoS ONE, 6(1).

(62) Morelli, M., Scumaci, D., Di Cello, A., Venturella, R., Donato, G., Faniello, M. C., Quaresima, B., Cuda, G., Zullo, F., & Costanzo, F. (2014). DJ-1 in endometrial cancer. International Journal of Gynecological Cancer, 24(4), 649–658.

(63) Konje, J., Taylor, A. H., & Ayakannu, T. (2022). Identification of potentially novel molecular targets of endometrial cancer using a non-biased proteomic approach. SSRN Electronic Journal.

(64) Lin, A. V. (2015). Indirect Elisa. Methods in Molecular Biology, 51–59.

(65) Haab, B. B., Paulovich, A. G., Anderson, N. L., Clark, A. M., Downing, G. J., Hermjakob, H., LaBaer, J., & Uhlen, M. (2006). A reagent resource to identify proteins and peptides of interest for the cancer community. Molecular & Cellular Proteomics, 5(10), 1996–2007.

(66) Wang, P., Whiteaker, J. R., & Paulovich, A. G. (2009). The Evolving Role of Mass Spectrometry in Cancer Biomarker Discovery. Cancer Biology & Therapy, 8(12), 1083–1094.

(67) Hoofnagle, A. N., & Wener, M. H. (2009). The fundamental flaws of immunoassays and potential solutions using tandem mass spectrometry. Journal of Immunological Methods, 347(1–2), 3–11.

(68) Krastins, B., Prakash, A., Sarracino, D. A., Nedelkov, D., Niederkofler, E. E., Kiernan, U. A., Nelson, R., Vogelsang, M. S., Vadali, G., Garces, A., Sutton, J. N., Peterman, S., Byram, G., Darbouret, B., Pérusse, J. R., Seidah, N. G., Coulombe, B., Gobom, J., Portelius, E., … Lopez, M. F. (2013). Rapid development of sensitive, high-throughput, quantitative and highly selective

mass spectrometric targeted immunoassays for clinically important proteins in human plasma and serum. Clinical Biochemistry, 46(6), 399–410.

(69) Percy, A. J., Chambers, A. G., Yang, J., Hardie, D. B., & Borchers, C. H. (2014). Advances in multiplexed MRM-based protein biomarker quantitation toward clinical utility. Biochimica et Biophysica Acta (BBA) - Proteins and Proteomics, 1844(5), 917–926.

(70) Luo, Y., Pehrsson, M., Langholm, L., Karsdal, M., Bay-Jensen, A.-C., & Sun, S. (2023). Lot-to-lot variance in immunoassays—causes, consequences, and solutions. Diagnostics, 13(11), 1835.

(71) Picotti, P., & Aebersold, R. (2012). Selected reaction monitoring–based proteomics: Workflows, potential, pitfalls and Future Directions. Nature Methods, 9(6), 555–566.

(72) Fu, Q., Chen, Z., Zhang, S., Parker, S. J., Fu, Z., Tin, A., Liu, X., & Van Eyk, J. E. (2016). Multiple and selective reaction monitoring using triple quadrupole mass spectrometer: Preclinical large cohort analysis. Methods in Molecular Biology, 249–264.

(73) Kondrat, R. W., McClusky, G. A., & Cooks, R. G. (1978). Multiple reaction monitoring in mass spectrometry/mass spectrometry for direct analysis of complex mixtures. Analytical Chemistry, 50(14), 2017–2021.

(74) Lange, V., Picotti, P., Domon, B., & Aebersold, R. (2008). Selected reaction monitoring for quantitative proteomics: A tutorial. Molecular Systems Biology, 4(1).

(75) Ong, S.-E., & Mann, M. (2005). Mass spectrometry–based proteomics turns quantitative. Nature Chemical Biology, 1(5), 252–262.

(76) Mermelekas, G., Vlahou, A., & Zoidakis, J. (2015). SRM/MRM Targeted Proteomics as a tool for biomarker validation and absolute quantification in human urine. Expert Review of Molecular Diagnostics, 15(11), 1441–1454.

(77) Gutman, S., & Kessler, L. G. (2006). The US Food and Drug Administration perspective on Cancer Biomarker Development. Nature Reviews Cancer, 6(7), 565–571.

(78) Draft guidance for Industry, Clinical Laboratories, and FDA staff: In vitro diagnostic multivariate index assays. (2007). Biotechnology Law Report, 26(2), 151–154

(79) Paulovich, A. G., Whiteaker, J. R., Hoofnagle, A. N., & Wang, P. (2008). The interface between Biomarker Discovery and clinical validation: The tar pit of the protein biomarker pipeline. PROTEOMICS – Clinical Applications, 2(10–11), 1386–1402

(80) Meng, Z., & Veenstra, T. D. (2011). Targeted mass spectrometry approaches for protein biomarker verification. Journal of Proteomics, 74(12), 2650–2659.

(81) Institute of Environmental Science and Research. (2012, April). Guidelines for the Investigation and Control of Disease Outbreaks. Retrieved from July 16, 2025, from https://www.esr.cri.nz/media/elyets2m/guidelinesforinvestigating commdiseaseobs.pdf

(82) Liechti, T., Van Gassen, S., Beddall, M., Ballard, R., Iftikhar, Y., Du, R., Venkataraman, T., Novak, D., Mangino, M., Perfetto, S., Larman, H. B., Spector,

T., Saeys, Y., & Roederer, M. (2023). A robust pipeline for high-content, high-throughput immunophenotyping reveals age- and genetics-dependent changes in blood leukocytes. Cell Reports Methods, 3(10), 100619.

(83) Aslam, B., Basit, M., Nisar, M. A., Khurshid, M., & Rasool, M. H. (2016). Proteomics: Technologies and Their Applications. Journal of Chromatographic Science, 55(2), 182–196.

(84) Kolsrud, H., Malerod, H., Ray, S., Reubsaet, L., Lundanes, E., & Greibrokk, T. (2012). A Critical Review of Trypsin Digestion for LC-MS Based Proteomics. Integrative Proteomics.

(85) Duong, V.-A., & Lee, H. (2023). Bottom-up proteomics: Advancements in sample preparation. International Journal of Molecular Sciences, 24(6), 5350.

(86) Dupree, E. J., Jayathirtha, M., Yorkey, H., Mihasan, M., Petre, B. A., & Darie, C. C. (2020). A critical review of bottom-up proteomics: The good, the bad, and the future of this field. Proteomes, 8(3), 14.

(87) Oswald, E. S., Brown, L. M., Bulinski, J. C., & Hung, C. T. (2011). Label-free protein profiling of adipose-derived human stem cells under hyperosmotic treatment. Journal of Proteome Research, 10(7), 3050–3059.

(88) Bladergroen, M. R., & van der Burgt, Y. E. (2015). Solid-phase extraction strategies to surmount body fluid sample complexity in high-throughput mass spectrometry-based proteomics. Journal of Analytical Methods in Chemistry, 2015, 1–8.

(89) Doerr, A. (2010). Targeted proteomics. Nature Methods, 8(1), 43–43.

(90) Kontostathi, G., Makridakis, M., Bitsika, V., Tsolakos, N., Vlahou, A., & Zoidakis, J. (2019). Development and validation of multiple reaction monitoring (MRM) assays for clinical applications. Methods in Molecular Biology, 205–223.

(91) Picotti, P., Aebersold, R., & Domon, B. (2007). The implications of proteolytic background for shotgun proteomics. Molecular & Cellular Proteomics, 6(9), 1589–1598.

(92) Olsen, J. V., Ong, S.-E., & Mann, M. (2004). Trypsin Cleaves exclusively C-terminal to arginine and lysine residues. Molecular & Cellular Proteomics, 3(6), 608–614.

(93) Wang, X., Codreanu, S. G., Wen, B., Li, K., Chambers, M. C., Liebler, D. C., & Zhang, B. (2018). Detection of proteome diversity resulted from alternative splicing is limited by trypsin cleavage specificity. Molecular & Cellular Proteomics, 17(3), 422–430.

(94) Stergachis, A. B., MacLean, B., Lee, K., Stamatoyannopoulos, J. A., & MacCoss, M. J. (2011). Rapid empirical discovery of optimal peptides for targeted proteomics. Nature Methods, 8(12), 1041–1043.

(95) Kuzyk, M. A., Parker, C. E., Domanski, D., & Borchers, C. H. (2013). Development of MRM-based assays for the absolute quantitation of plasma proteins. Methods in Molecular Biology, 53–82.

(96) Ludwig, C. (2016, March 1). The ABC of SRM - Tina Ludwig - Targeted Proteomics Course - ETHZ 2016. YouTube. Retrieved July 17, 2025, from https://www.youtube.com/watch?v=qloNeHVw95E&t=796s

(97) van Duijl, T. T., Ruhaak, L. R., Smit, N. P., Pieterse, M. M., Romijn, F. P., Dolezal, N., Drijfhout, J. W., de Fijter, J. W., & Cobbaert, C. M. (2021). Development and provisional validation of a multiplex LC-MRM-MS test for timely kidney injury detection in urine. Journal of Proteome Research, 20(12), 5304–5314.

(98) Kusebauch, U., Hernández-Castellano, L. E., Bislev, S. L., Moritz, R. L., Røntved, C. M., & Bendixen, E. (2018). Selected reaction monitoring mass spectrometry of mastitis milk reveals pathogen-specific regulation of bovine host response proteins. Journal of Dairy Science, 101(7), 6532–6541.

(99) Kettenbach, A. N., Rush, J., & Gerber, S. A. (2011). Absolute quantification of protein and post-translational modification abundance with stable isotope–labeled synthetic peptides. Nature Protocols, 6(2), 175–186.

(100) Kim, Y. J., Sertamo, K., Pierrard, M. A., Mesmin, C., Kim, S. Y., Schlesser, M., Berchem, G., & Domon, B. (2015). Verification of the biomarker candidates for non-small-cell lung cancer using a targeted proteomics approach. Journal of proteome research, 14(3), 1412–1419.

(101) Wang, Q., Zhang, M., Tomita, T., Vogelstein, J. T., Zhou, S., Papadopoulos, N., Kinzler, K. W., & Vogelstein, B. (2017). Selected reaction monitoring approach for validating peptide biomarkers. Proceedings of the National Academy of Sciences of the United States of America, 114(51), 13519–13524.

(102) Rezeli, M., Végvári, A., Ottervald, J., Olsson, T., Laurell, T., & Marko-Varga, G. (2011). MRM assay for quantitation of complement components in human blood plasma - a feasibility study on multiple sclerosis. Journal of proteomics, 75(1), 211–220.

(103) Schnatbaum, K., Zerweck, J., Nehmer, J., Wenschuh, H., Schutkowski, M., & Reimer, U. (2011a). SpikeTides^{TM}—proteotypic peptides for large-scale MS-based proteomics. Nature Methods, 8(3), i–ii.

(104) Brönstrup, M. (2004). Absolute quantification strategies in proteomics based on mass spectrometry. Expert Review of Proteomics, 1(4), 503–512.

(105) Ludwig, C. (2017, July 5). General Principles of Quantitative Proteomics - Tina Ludwig - DIA/SWATH Course 2017 - ETH Zurich. YouTube. Retrieved July 17, 2025, from https://www.youtube.com/watch?v=YJVgIDp6q2U

(106) Loo, J. A., Loo, R. R., Light, K. J., Edmonds, C. G., & Smith, R. D. (1992). Multiply charged negative ions by electrospray ionization of polypeptides and proteins. Analytical Chemistry, 64(1), 81–88.

(107) McLuckey, S. A., & Mentinova, M. (2011). Ion/neutral, ion/electron, ion/photon, and ion/ion interactions in tandem mass spectrometry: Do we need them all? are they enough? Journal of the American Society for Mass Spectrometry, 22(1), 3–12.

(108) Roth, K. D., Huang, Z.-H., Sadagopan, N., & Watson, J. T. (1998). Charge derivatization of peptides for analysis by mass spectrometry. Mass Spectrometry Reviews, 17(4), 255–274.

(109) Johnson, R. S., Martin, S. A., & Biemann, K. (1988). Collision-induced fragmentation of $(M+H)^+$ ions of peptides. side chain specific sequence ions. International Journal of Mass Spectrometry and Ion Processes, 86, 137–154.

(110) Holstein (Sherwood), C. A., Gafken, P. R., & Martin, D. B. (2011). Collision energy optimization of B- and Y-ions for multiple reaction monitoring mass spectrometry. Journal of Proteome Research, 10(1), 231–240.

(111) Szabó, D., Schlosser, G., Vékey, K., Drahos, L., & Révész, Á. (2020). Collision energies on QTof and Orbitrap Instruments: How to make proteomics measurements comparable? Journal of Mass Spectrometry, 56(1).

(112) Yocum, A. K., & Chinnaiyan, A. M. (2009). Current Affairs in Quantitative Targeted Proteomics: Multiple Reaction Monitoring-mass spectrometry. Briefings in Functional Genomics and Proteomics, 8(2), 145–157.

(113) Chambers, A. G., Percy, A. J., Yang, J., Camenzind, A. G., & Borchers, C. H. (2013). Multiplexed quantitation of endogenous proteins in dried blood spots by multiple reaction monitoring - mass spectrometry. Molecular & Cellular Proteomics, 12(3), 781–791.

(114) Ozcan, S., Cooper, J. D., Lago, S. G., Kenny, D., Rustogi, N., Stocki, P., & Bahn, S. (2017). Towards reproducible MRM based biomarker discovery using dried blood spots. Scientific Reports, 7(1).

(115) European Medicines Agency. (2011, July 21). Guideline on bioanalytical method validation | EMA. Retrieved from July 2025, https://www.ema.europa.eu/en/documents/scientific-guideline/guideline-bioanalytical-method-validation_en.pdf

(116) U.S. Food and Drug Administration. (2018, May). Bioanalytical method validation guidance for industry. Retrieved from July 2025, https://www.fda.gov/files/drugs/published/Bioanalytical-Method-Validation-Guidance-for-Industry.pdf

(117) Lundeen, R. A., Kennedy, J. J., Murillo, O. D., Ivey, R. G., Zhao, L., Schoenherr, R. M., Hoofnagle, A. N., Wang, P., Whiteaker, J. R., & Paulovich, A. G. (2023). Monitoring both extended and tryptic forms of stable isotope-labeled standard peptides provides an internal quality control of proteolytic digestion in targeted mass spectrometry-based assays. Molecular & Cellular Proteomics, 22(9), 100621.

(118) Anderson, N. L., & Anderson, N. G. (2003). The human plasma proteome: History, character, and diagnostic prospects. Molecular & Cellular Proteomics, 2(1), 50.

(119) Anderson, L., & Hunter, C. L. (2006). Quantitative mass spectrometric multiple reaction monitoring assays for major plasma proteins. Molecular & Cellular Proteomics, 5(4), 573–588.

(120) MacLean, B., Tomazela, D. M., Shulman, N., Chambers, M., Finney, G. L., Frewen, B., Kern, R., Tabb, D. L., Liebler, D. C., & MacCoss, M. J. (2010). Skyline: An open source document editor for creating and analyzing targeted proteomics experiments. Bioinformatics, 26(7), 966–968.

(121) Kawahara, R., Bollinger, J. G., Rivera, C., Ribeiro, A. C., Brandão, T. B., Leme, A. F., & MacCoss, M. J. (2015). A targeted proteomic strategy for the measurement of oral cancer candidate biomarkers in human saliva. PROTEOMICS, 16(1), 159–173.

(122) Kuzyk, M. A., Smith, D., Yang, J., Cross, T. J., Jackson, A. M., Hardie, D. B., Anderson, N. L., & Borchers, C. H. (2009). Multiple reaction monitoring-based, multiplexed, absolute quantitation of 45 proteins in human plasma. Molecular & Cellular Proteomics, 8(8), 1860–1877.

(123) Sullivan, M. P. (2016). LC/MS methods for small molecule biomarkers. AAPS Advances in the Pharmaceutical Sciences Series, 99–113.

(124) Mishra, P., Singh, U., Pandey, C. M., Mishra, P., & Pandey, G. (2019). Application of student's t-test, analysis of variance, and covariance. Annals of Cardiac Anaesthesia, 22(4), 407–411.

(125) Ray, P., Manach, Y. L., Riou, B., Houle, T. T., & Warner, D. S. (2010). Statistical evaluation of a biomarker. Anesthesiology, 112(4), 1023–1040.

(126) Mandrekar, J. N. (2010). Receiver operating characteristic curve in diagnostic test assessment. Journal of Thoracic Oncology, 5(9), 1315–1316.

(127) Nelson, D. L., Cox, M. M., & Lehninger, A. L. (2017). Lehninger Principles of biochemistry. W.H. Freeman.

(128) Wiśniewski, J. R., Zougman, A., Nagaraj, N., & Mann, M. (2009a). Universal Sample Preparation Method for Proteome Analysis. Nature Methods, 6(5), 359–362.

(129) Choi, M., Chang, C.-Y., Clough, T., Broudy, D., Killeen, T., MacLean, B., & Vitek, O. (2014). MSstats: An R package for statistical analysis of quantitative mass spectrometry-based proteomic experiments. Bioinformatics, 30(17), 2524–2526.

(130) Surinova, S., Hüttenhain, R., Chang, C.-Y., Espona, L., Vitek, O., & Aebersold, R. (2013). Automated selected reaction monitoring data analysis workflow for large-scale targeted Proteomic Studies. Nature Protocols, 8(8), 1602–1619.

(131) Vogel, C., & Marcotte, E. M. (2012). Insights into the regulation of protein abundance from proteomic and transcriptomic analyses. Nature Reviews Genetics, 13(4), 227–232.

(132) Liu, J., Zhang, Y., Li, Q., & Wang, Y. (2020). Transgelins: Cytoskeletal Associated Proteins Implicated in the Metastasis of Colorectal Cancer. Frontiers in cell and developmental biology, 8, 573859.

(133) Prasad, P. D., Stanton, J.-A. L., & Assinder, S. J. (2009). Expression of the actin-associated protein transgelin (SM22) is decreased in prostate cancer. Cell and Tissue Research, 339(2), 337–347.

(134) Shields, J. M., Rogers-Graham, K., & Der, C. J. (2002). Loss of Transgelin in breast and colon tumors and in rie-1 cells by RAS deregulation of gene expression through RAF-independent pathways. Journal of Biological Chemistry, 277(12), 9790–9799.

(135) Chang, J. W., Jeon, H. B., Lee, J. H., Yoo, J. S., Chun, J. S., Kim, J. H., & Yoo, Y. J. (2001). Augmented expression of peroxiredoxin I in lung cancer. Biochemical and Biophysical Research Communications, 289(2), 507–512.

(136) Lawson, D., Harrison, M., & Shapland, C. (1997). Fibroblast transgelin and smooth muscle SM22alpha are the same protein, the expression of which is down-regulated in many cell lines. Cell motility and the cytoskeleton, 38(3), 250–257.

(137) Shapland, C., Hsuan, J. J., Totty, N. F., & Lawson, D. (1993). Purification and properties of transgelin: a transformation and shape change sensitive actin-gelling protein. The Journal of cell biology, 121(5), 1065–1073.

(138) Assinder, S. J., Stanton, J.-A. L., & Prasad, P. D. (2009). Transgelin: An actin-binding protein and tumour suppressor. The International Journal of Biochemistry & Cell Biology, 41(3), 482–486.

(139) Yang, Z., Chang, Y.-J., Miyamoto, H., Ni, J., Niu, Y. J., Chen, Z. D., et al. (2007). Transgelin functions as a suppressor via inhibition of ARA54-enhanced androgen receptor transactivation and prostate cancer cell growth. Mol. Endocrinol., 21, 343–358.

(140) Nair, R. J., Solway, J., & Boyd, D. D. (2006). Expression cloning identifies transgelin (SM22) as a novel repressor of 92-kDa type IV collagenase (MMP-9) expression. J. Biol. Chem., 281, 26424–26436.

(141) Amalinei, C., Cianga, C., Balan, R., Cianga, P., Giusca, S., & Caruntu, I.-D. (2011). Immunohistochemical analysis of steroid receptors, proliferation markers, apoptosis related molecules, and gelatinases in non-neoplastic and neoplastic endometrium. Annals of Anatomy - Anatomischer Anzeiger, 193(1), 43–55.

(142) Martinez-Garcia E., Lesur A., Devis L., Campos A., Cabrera S., Oostrum J. van, Matias-Guiu X., Gil-Moreno A., Reventos J., Colas E., Domon B. Development of a sequential workflow based on LC-PRM for the verification of endometrial cancer protein biomarkers in uterine aspirate samples. Oncotarget. 2016; 7: 53102-53115.

(143) Rogers, L. M., Veeramani, S., & Weiner, G. J. (2014). Complement in monoclonal antibody therapy of cancer. Immunologic Research, 59(1–3), 203–210.

(144) Fredslund, F., Jenner, L., Husted, L. B., Nyborg, J., Andersen, G. R., & Sottrup-Jensen, L. (2006). The structure of bovine complement component 3 reveals the basis for thioester function. Journal of molecular biology, 361(1), 115–127.

(145) Tikhonov, D., Kulikova, L., Kopylov, A., Malsagova, K., Stepanov, A., Rudnev, V., & Kaysheva, A. (2020). Super Secondary Structures of Proteins with Post-Translational Modifications in Colon Cancer. Molecules (Basel, Switzerland), 25(14), 3144.

(146) Zhang, Z., Qin, K., Zhang, W., Yang, B., Zhao, C., Zhang, X., Zhang, F., Zhao, L., & Shan, B. (2019). Postoperative recurrence of epithelial ovarian cancer patients and chemoresistance related protein analyses. Journal of ovarian research, 12(1), 29.

(147) van den Broek, I., Sparidans, R. W., Schellens, J. H., & Beijnen, J. H. (2010). Quantitative assay for six potential breast cancer biomarker peptides in human serum by liquid chromatography coupled to tandem mass spectrometry. Journal of chromatography. B, Analytical technologies in the biomedical and life sciences, 878(5-6), 590–602.

(148) Lu, Z. L., Chen, Y. J., Jing, X. Y., Wang, N. N., Zhang, T., & Hu, C. J. (2018). Detection and Identification of Serum Peptides Biomarker in Papillary Thyroid Cancer. Medical science monitor: international medical journal of experimental and clinical research, 24, 1581–1587.

(149) Wang, Y., Zhou, S., Wang, D., Wei, T., Zhu, J., & Li, Z. (2021). Complement C4-A and Plasminogen as Potential Biomarkers for Prediction of Papillary Thyroid Carcinoma. Frontiers in endocrinology, 12, 737638.

(150) Mazurek, S., Boschek, C. B., Hugo, F., & Eigenbrodt, E. (2005). Pyruvate kinase type M2 and its role in tumor growth and spreading. Seminars in cancer biology, 15(4), 300–308.

(151) Mazurek, S., Boschek, C. B., Hugo, F., & Eigenbrodt, E. (2005). Pyruvate kinase type M2 and its role in tumor growth and spreading. Seminars in cancer biology, 15(4), 300–308.

(152) Ugurel, S., Bell, N., Sucker, A., Zimpfer, A., Rittgen, W., & Schadendorf, D. (2005). Tumor type M2 pyruvate kinase (TuM2-PK) as a novel plasma tumor marker in melanoma. International journal of cancer, 117(5), 825–830.

(153) Christofk, H. R., Vander Heiden, M. G., Harris, M. H., Ramanathan, A., Gerszten, R. E., Wei, R., Fleming, M. D., Schreiber, S. L., & Cantley, L. C. (2008). The M2 splice isoform of pyruvate kinase is important for cancer metabolism and tumour growth. Nature, 452(7184), 230–233.

(154) Mazurek S. (2011). Pyruvate kinase type M2: a key regulator of the metabolic budget system in tumor cells. The international journal of biochemistry & cell biology, 43(7), 969–980.

(155) Mazurek S. (2007). Pyruvate kinase type M2: a key regulator within the tumour metabolome and a tool for metabolic profiling of tumours. Ernst Schering Foundation symposium proceedings, (4), 99–124.

(156) Wong, N., De Melo, J., & Tang, D. (2013). PKM2, a Central Point of Regulation in Cancer Metabolism. International journal of cell biology, 2013, 242513.

(157) Gui, D. Y., Lewis, C. A., & Vander Heiden, M. G. (2013). Allosteric regulation of PKM2 allows cellular adaptation to different physiological states. Science signaling, 6(263), pe7.

(158) Lai, Y. J., Chou, Y. C., Lin, Y. J., Yu, M. H., Ou, Y. C., Chu, P. W., Wu, C. C., Wang, Y. C., & Chao, T. K. (2019). Pyruvate Kinase M2 Expression: A Potential Metabolic Biomarker to Differentiate Endometrial Precancer and Cancer That Is Associated with Poor Outcomes in Endometrial Carcinoma. International journal of environmental research and public health, 16(23), 4589.

(159) Wahl, H., Daudi, S., Kshirsagar, M., Griffith, K., Tan, L., Rhode, J., & Liu, J. R. (2010). Expression of metabolically targeted biomarkers in endometrial carcinoma. Gynecologic oncology, 116(1), 21–27.

(160) Hsu, M. C., & Hung, W. C. (2018). Pyruvate kinase M2 fuels multiple aspects of cancer cells: from cellular metabolism, transcriptional regulation to extracellular signaling. Molecular cancer, 17(1), 35.

(161) Onoda, K., Yu, F. X., & Yin, H. L. (1993). gCap39 is a nuclear and cytoplasmic protein. Cell motility and the cytoskeleton, 26(3), 227–238.

(162) Glaser, J., Neumann, M. H., Mei, Q., Betz, B., Seier, N., Beyer, I., Fehm, T., Neubauer, H., Niederacher, D., & Fleisch, M. C. (2014). Macrophage capping protein CapG is a putative oncogene involved in migration and invasiveness in ovarian carcinoma. BioMed research international, 2014, 379847.

(163) Pierce, A., Unwin, R. D., Evans, C. A., Griffiths, S., Carney, L., Zhang, L., Jaworska, E., Lee, C. F., Blinco, D., Okoniewski, M. J., Miller, C. J., Bitton, D. A., Spooncer, E., & Whetton, A. D. (2008). Eight-channel iTRAQ enables

comparison of the activity of six leukemogenic tyrosine kinases. Molecular & cellular proteomics: MCP, 7(5), 853–863.

(164) Li, X., Chen, Q., Yin, D., Shi, S., Yu, L., Zhou, S., Chen, E., Zhou, Z., Shi, Y., Fan, J., Zhou, J., & Dai, Z. (2017). Novel role of semaphorin 3A in the growth and progression of hepatocellular carcinoma. Oncology reports, 37(6), 3313–3320.

(165) Liao, S. H., Zhao, X. Y., Han, Y. H., Zhang, J., Wang, L. S., Xia, L., Zhao, K. W., Zheng, Y., Guo, M., & Chen, G. Q. (2009). Proteomics-based identification of two novel direct targets of hypoxia-inducible factor-1 and their potential roles in migration/invasion of cancer cells. Proteomics, 9(15), 3901–3912.

(166) Li, T., Hong, X., Zhao, J., Teng, Y., Zheng, J., Chen, H., Chen, H., & Li, H. (2016). Gelsolin-like actin-capping protein is associated with patient prognosis, cellular apoptosis and proliferation in prostate cancer. Biomarkers in medicine, 10(12), 1251–1260.

(167) Zhaojie, L., Yuchen, L., Miao, C., Yacun, C., Shayi, W., Anbang, H., Xinhui, L., Meng, Z., Peipei, W., Hongbing, M., Feng, W., Zhiming, C., & Xinyuan, G. (2019). Gelsolin-like actin-capping protein has prognostic value and promotes tumorigenesis and epithelial-mesenchymal transition via the Hippo signaling pathway in human bladder cancer. Therapeutic advances in medical oncology, 11, 1758835919841235.

(168) Ichikawa, H., Kanda, T., Kosugi, S., Kawachi, Y., Sasaki, H., Wakai, T., & Kondo, T. (2013). Laser microdissection and two-dimensional difference gel electrophoresis reveal the role of a novel macrophage-capping protein in lymph

node metastasis in gastric cancer. Journal of proteome research, 12(8), 3780–3791.

(169) Shao, F., Zhang, R., Don, L., & Ying, K. (2011). Overexpression of gelsolin-like actin-capping protein is associated with progression of lung adenocarcinoma. The Tohoku journal of experimental medicine, 225(2), 95–101.

(170) Zhu, W. Y., Hunag, Y. Y., Liu, X. G., He, J. Y., Chen, D. D., Zeng, F., Zhou, J. H., & Zhang, Y. K. (2012). Prognostic evaluation of CapG, gelsolin, P-gp, GSTP1, and Topo-II proteins in non-small cell lung cancer. Anatomical record (Hoboken, N.J.: 2007), 295(2), 208–214.

(171) Partheen, K., Levan, K., Osterberg, L., Claesson, I., Fallenius, G., Sundfeldt, K., & Horvath, G. (2008). Four potential biomarkers as prognostic factors in stage III serous ovarian adenocarcinomas. International journal of cancer, 123(9), 2130–2137.

(172) Tonack, S., Patel, S., Jalali, M., Nedjadi, T., Jenkins, R. E., Goldring, C., Neoptolemos, J., & Costello, E. (2011). Tetracycline-inducible protein expression in pancreatic cancer cells: effects of CapG overexpression. World journal of gastroenterology, 17(15), 1947–1960.

(173) Jiang, S., Ye, M., Wan, J., Ye, Q., Qiu, S., Yang, Y., & Li, X. (2025). Significance of gelsolin superfamily genes in diagnosis, prognosis and immune microenvironment regulation for endometrial cancer. Cancer Medicine, 14(4).

(174) Jin, Y. J., Burakoff, S. J., & Bierer, B. E. (1992). Molecular cloning of a 25-kDa high affinity rapamycin binding protein, FKBP25. The Journal of biological chemistry, 267(16), 10942–10945.

(175) Luo, K., Li, Y., Yin, Y., Li, L., Wu, C., Chen, Y., Nowsheen, S., Hu, Q., Zhang, L., Lou, Z., & Yuan, J. (2017). USP49 negatively regulates tumorigenesis and chemoresistance through FKBP51-AKT signaling. The EMBO journal, 36(10), 1434–1446.

(176) Zhu, W., Li, Z., Xiong, L., Yu, X., Chen, X., & Lin, Q. (2017). FKBP3 Promotes Proliferation of Non-Small Cell Lung Cancer Cells through Regulating Sp1/HDAC2/p27. Theranostics, 7(12), 3078–3089.

(177) Li, S., Yang, L., & Li, J. (2024). FKBP3, a poor prognostic indicator, promotes the progression of LUAD via regulating ferroptosis and immune infiltration. Medicine, 103(26), e38606.

(178) Tong, J., Shen, Y., Chen, X., Wang, R., Hu, Y., Zhang, X., Zhang, Z., & Han, L. (2019). FKBP3 mediates oxaliplatin resistance in colorectal cancer cells by regulating HDAC2 expression. Oncology reports, 42(4), 1404–1412.

(179) Yan, Y., Wang, S., Zhang, Z., Tang, M., Zhao, A. Z., Li, Z., Wu, X., & Li, F. (2024). FKBP38 suppresses endometrial cancer cell proliferation and metastasis by inhibiting the mTOR pathway. Archives of biochemistry and biophysics, 752, 109891

(180) Huang, H., Tanaka, H., Hammock, B. D., & Morisseau, C. (2009). Novel and highly sensitive fluorescent assay for leucine aminopeptidases. Analytical biochemistry, 391(1), 11–16.

(181) He, X., Huang, Q., Qiu, X., Liu, X., Sun, G., Guo, J., Ding, Z., Yang, L., Ban, N., Tao, T., & Wang, D. (2015). LAP3 promotes glioma progression by regulating proliferation, migration and invasion of glioma cells. International journal of biological macromolecules, 72, 1081–1089.

(182) Zhang, S., Yang, X., Shi, H., Li, M., Xue, Q., Ren, H., Yao, L., Chen, X., Zhang, J., & Wang, H. (2014). Overexpression of leucine aminopeptidase 3 contributes to malignant development of human esophageal squamous cell carcinoma. Journal of molecular histology, 45(3), 283–292.

(183) Fang, C., Zhang, J., Yang, H., Peng, L., Wang, K., Wang, Y., Zhao, X., Liu, H., Dou, C., Shi, L., Zhao, C., Liang, S., Li, D., & Wang, X. (2019). Leucine aminopeptidase 3 promotes migration and invasion of breast cancer cells through upregulation of fascin and matrix metalloproteinases-2/9 expression. Journal of cellular biochemistry, 120(3), 3611–3620.

(184) Mizutani, S., Shibata, K., Kikkawa, F., Hattori, A., Tsujimoto, M., Ishii, M., & Kobayashi, H. (2007). Essential role of placental leucine aminopeptidase in gynecologic malignancy. Expert opinion on therapeutic targets, 11(4), 453–461.

(185) Shibata, K., Kikkawa, F., Mizokami, Y., Kajiyama, H., Ino, K., Nomura, S., & Mizutani, S. (2005). Possible involvement of adipocyte-derived leucine aminopeptidase via angiotensin II in endometrial carcinoma. Tumour biology: the journal of the International Society for Oncodevelopmental Biology and Medicine, 26(1), 9–16.

(186) Pilar Carrera M, Ramirez-Exposito MJ, Duenas B, Dolores Mayas M, Jesus Garcia M, De la Chica S, Cortes P, Ruiz-Sanjuan M and Martinez-Martos JM. Insulin-regulated aminopeptidase/placental leucil Aminopeptidase (IRAP/P-lAP) and angiotensin IV-forming activities are modified in serum of rats with breast cancer induced by N-methyl-nitrosourea. Anticancer Res 2006; 26: 1011-1014.

(187) Shibata, K., Kikkawa, F., Mizokami, Y., Kajiyama, H., Ino, K., Nomura, S., & Mizutani, S. (2005). Possible involvement of adipocyte-derived leucine aminopeptidase via angiotensin II in endometrial carcinoma. Tumour biology: the journal of the International Society for Oncodevelopmental Biology and Medicine, 26(1), 9–16.

(188) Strange, R. C., Jones, P. W., & Fryer, A. A. (2000). Glutathione S-transferase: genetics and role in toxicology. Toxicology letters, 112-113, 357–363.

(189) Traverso, N., Ricciarelli, R., Nitti, M., Marengo, B., Furfaro, A. L., Pronzato, M. A., Marinari, U. M., & Domenicotti, C. (2013). Role of glutathione in cancer progression and chemoresistance. Oxidative medicine and cellular longevity, 2013, 972913.

(190) Jin, P., Xie, J., Zhu, X., Zhou, C., Ding, X., & Yang, L. (2014). shRNA-mediated GSTP1 gene silencing enhances androgen-independent cell line DU145 chemosensitivity. International urology and nephrology, 46(6), 1115–1121.

(191) Miyake, T., Nakayama, T., Naoi, Y., Yamamoto, N., Otani, Y., Kim, S. J., Shimazu, K., Shimomura, A., Maruyama, N., Tamaki, Y., & Noguchi, S. (2012). GSTP1 expression predicts poor pathological complete response to neoadjuvant chemotherapy in ER-negative breast cancer. Cancer science, 103(5), 913–920.

(192) Pasello, M., Michelacci, F., Scionti, I., Hattinger, C. M., Zuntini, M., Caccuri, A. M., Scotlandi, K., Picci, P., & Serra, M. (2008). Overcoming glutathione S-transferase P1-related cisplatin resistance in osteosarcoma. Cancer research, 68(16), 6661–6668.

(193) Chen, S. Y., Hu, S. S., Dong, Q., Cai, J. X., Zhang, W. P., Sun, J. Y., Wang, T. T., Xie, J., He, H. R., Xing, J. F., Lu, J., & Dong, Y. L. (2013). Establishment of paclitaxel-resistant breast cancer cell line and nude mice models, and underlying multidrug resistance mechanisms in vitro and in vivo. Asian Pacific journal of cancer prevention: APJCP, 14(10), 6135–6140.

(194) Franco, R. L., Schenka, N. G., Schenka, A. A., Rezende, L. F., & Gurgel, M. S. (2012). Glutathione S-transferase Pi expression in invasive breast cancer and its relation with the clinical outcome. Journal of B.U.ON. : official journal of the Balkan Union of Oncology, 17(2), 259–264.

(195) Batist, G., Tulpule, A., Sinha, B. K., Katki, A. G., Myers, C. E., & Cowan, K. H. (1986). Overexpression of a novel anionic glutathione transferase in multidrug-resistant human breast cancer cells. The Journal of biological chemistry, 261(33), 15544–15549.

(196) Pljesa-Ercegovac, M., Savic-Radojevic, A., Kravic-Stevovic, T., Bumbasirevic, V., Mimic-Oka, J., & Simic, T. (2010). Co-localization of GSTP1 and JNK in transitional cell carcinoma of urinary bladder. Genetics and molecular biology, 33(3), 460–462.

(197) Chan, Q. K., Khoo, U. S., Chan, K. Y., Ngan, H. Y., Li, S. S., Chiu, P. M., Man, L. S., Ip, P. P., Xue, W. C., & Cheung, A. N. (2005). Promoter methylation and differential expression of pi-class glutathione S-transferase in endometrial carcinoma. The Journal of molecular diagnostics: JMD, 7(1), 8–16.

APPENDICES

A. HPLC-MS Results of SIL Peptides for the Determination of Purity

The chromatograms and MS spectra of four SIL peptide standards among twenty three synthesized by JPT Peptide Technologies were presented in this section.

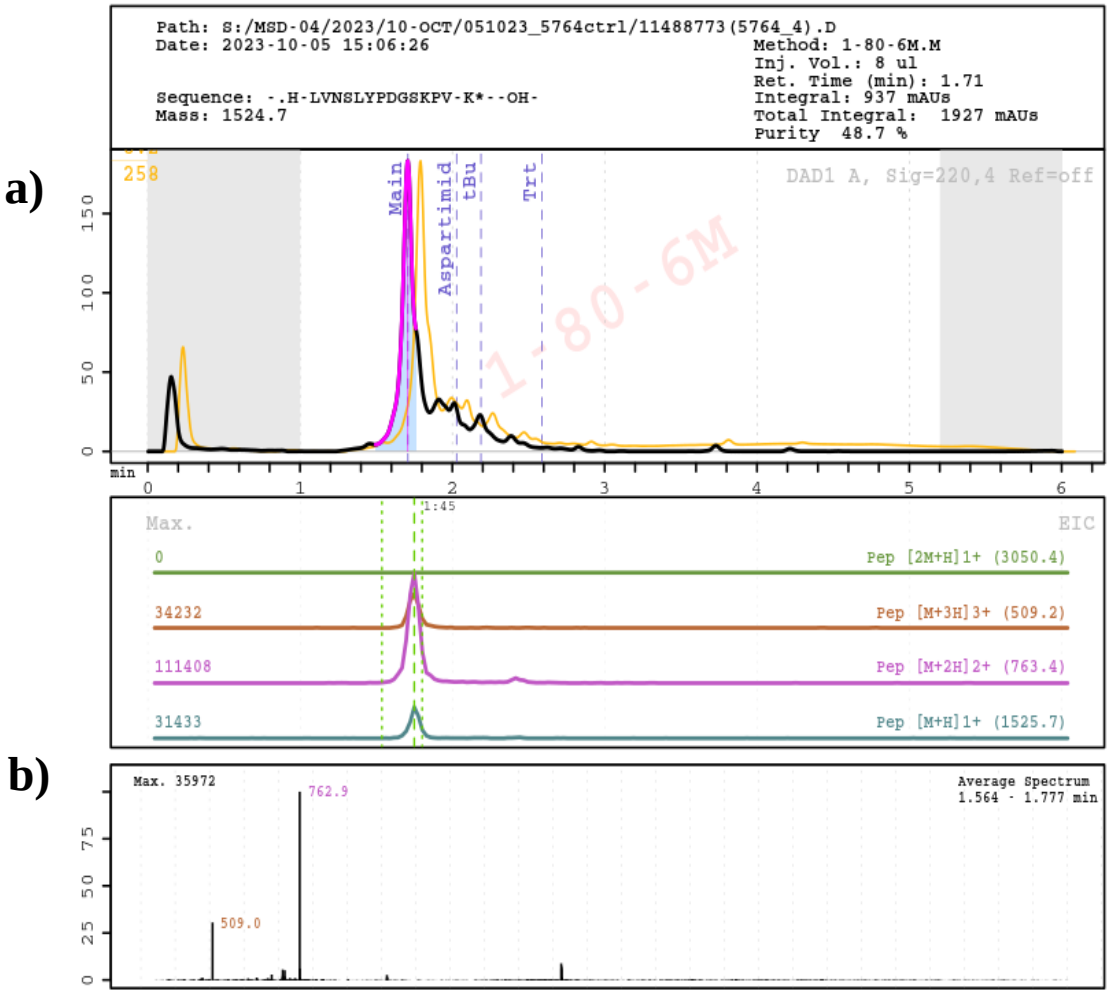

Figure 4.1 *(a) Chromatogram and (b) mass spectrum of LVNSLYPDGSKPVK**

a)

b)

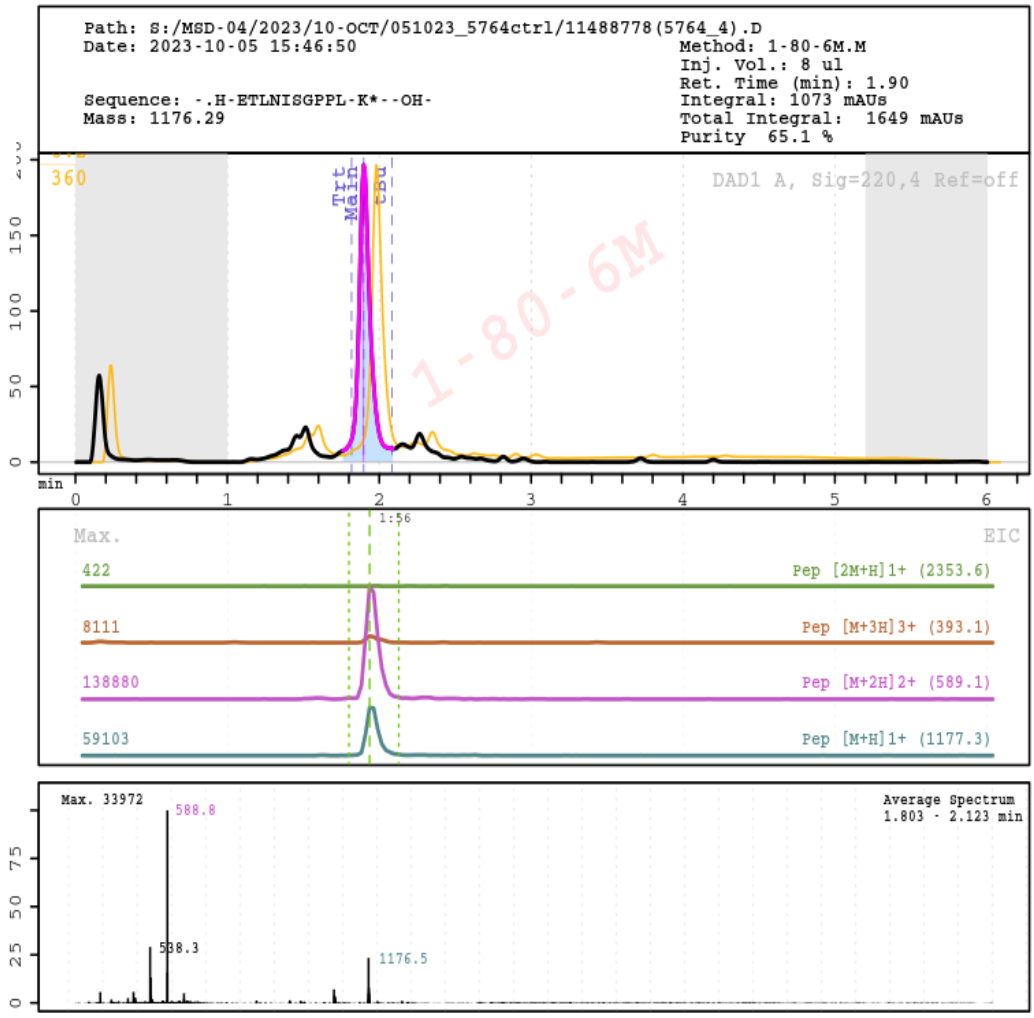

Figure 4.2 *(a) Chromatogram and (b) mass spectrum of ETLNISGPPLK**

a)

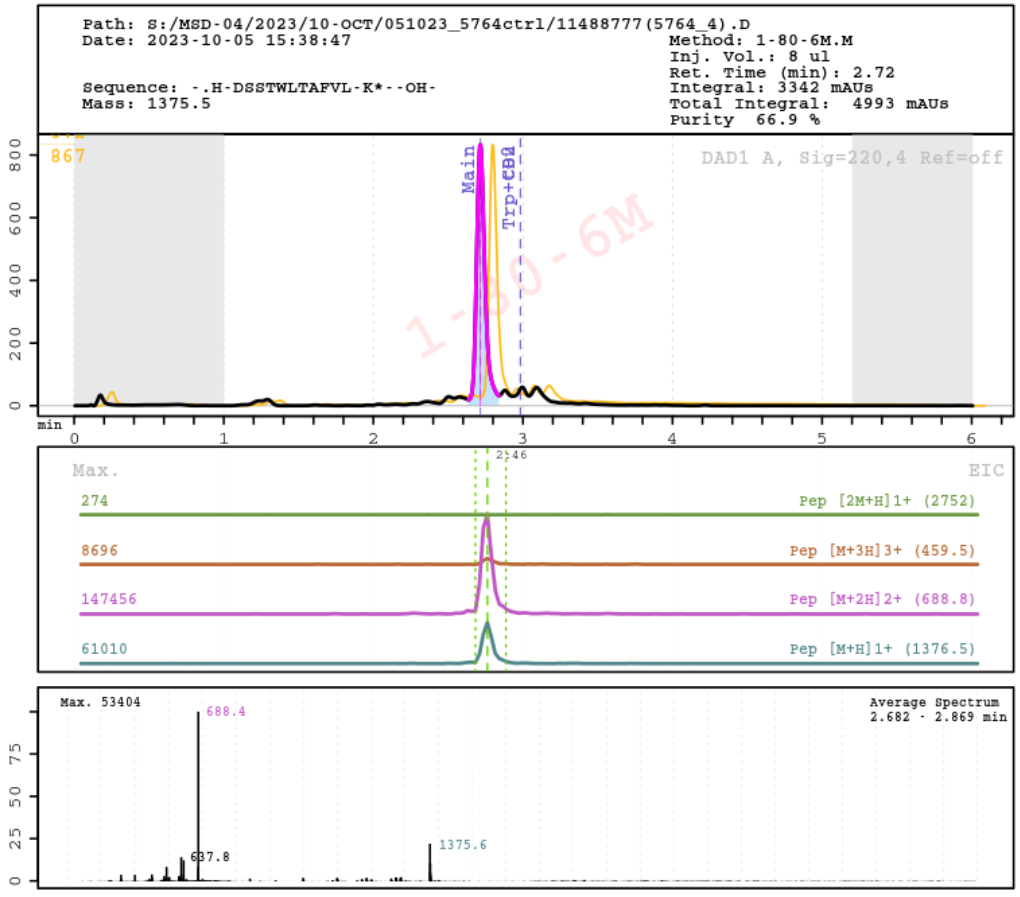

b)

Figure 4.3 *(a) Chromatogram and (b) mass spectrum of DSSTWLTAFVLK**

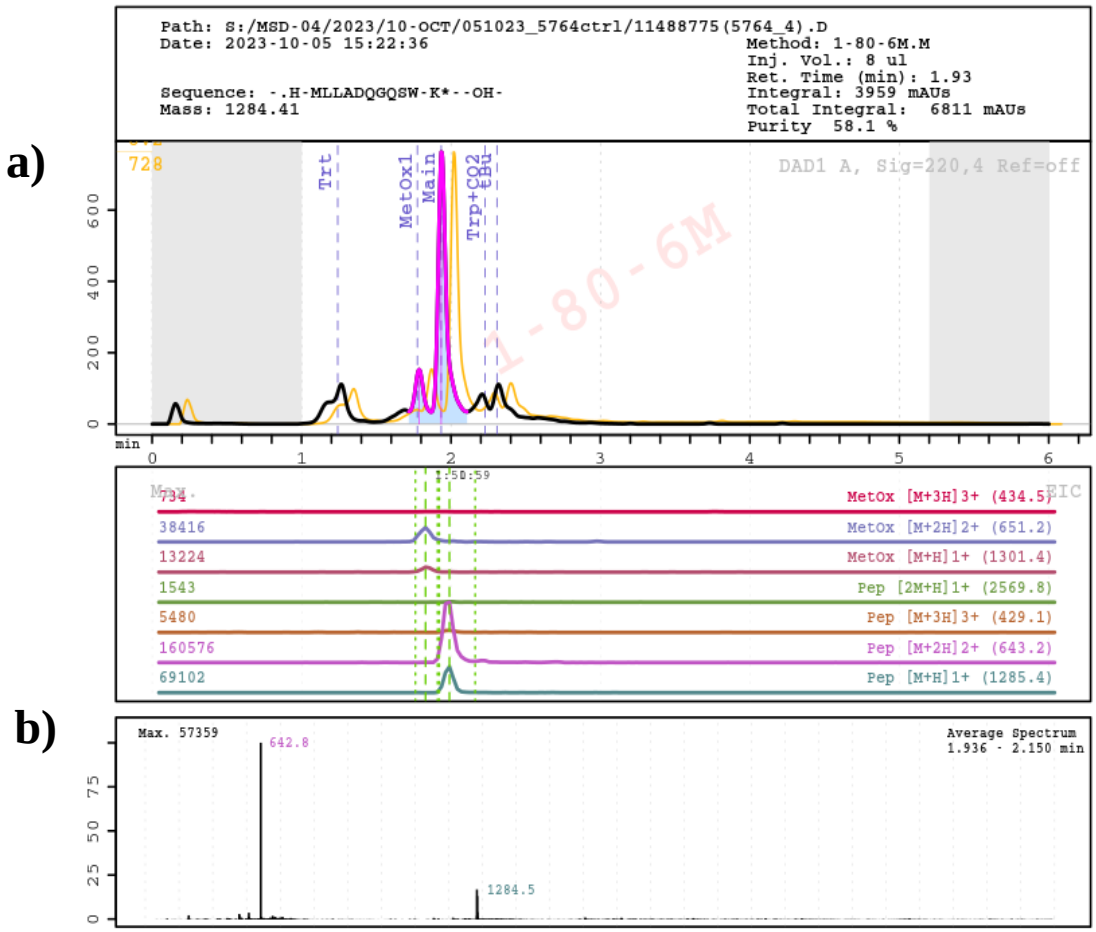

Figure 4.4 *(a) Chromatogram and (b) mass spectrum of MLLADQGQSWK**

B. Ethical Committee Approval

ATATÜRK ÜNİVERSİTESİ TIP FAKÜLTESİ KLİNİK ARAŞTIRMALAR ETİK KURULU

Bölümü : Dekanlık
Servisi : Klinik Araştırmalar Etik Kurulu
Sayı : B.30.2.ATA.0.01.00/2
Konu : Etik Kurul Kararı

29.12.2022

[redacted]
Kadın Hastalıkları ve Doğum Anabilim Dalı
Öğretim Üyesi

Değerlendirilmek üzere Klinik Araştırmalar Etik Kurulu'na başvuruda bulunduğunuz **"Polikistik over sendromunun alt tiplerinde nadir görülen endometriyum kanseri riskini belirlemek için biyobelirteç çalışması"** isimli bilimsel çalışmasına ait Kurul Kararı ekte sunulmuştur.

Bilgilerinizi ve gereğini rica ederim.

[redacted]

Eki :
1 Adet Etik Kurul Kararı

Sorumlu Araştırmacı :
1. [redacted]

Yardımcı Araştırmacı :
1. [redacted]
2. [redacted]
3. [redacted]
4. [redacted]
5. [redacted]
6.

ATATÜRK ÜNİVERSİTESİ TIP FAKÜLTESİ KLİNİK ARAŞTIRMALAR ETİK KURULU